

**Planning Support System Development
for analyzing environmental performance
of form-based design decisions:
*Case Study of Enschede***

ARADHANA TRIPATHY

July 2024

SUPERVISORS:

Dr. M.N. Koeva (Mila)

Dr. P. Nourian (Pirouz)

Advisor: I. Cardenas (Ivan)

THESIS ASSESSMENT BOARD:

Dr. J. A. Martinez (Chair)

Dr. G. Dane (External Examiner, TU Eindhoven)



Planning Support System Development for analyzing environmental performance of form-based design decisions:

Case Study of Enschede

ARADHANA TRIPATHY

Enschede, The Netherlands, July 2024

Thesis submitted to the Faculty of Geo-Information Science and Earth Observation of the University of Twente in partial fulfilment of the requirements for the degree of Master of Science in Geo-information Science and Earth Observation.

Specialization: Urban Planning and Management

SUPERVISORS:

Dr. M.N. Koeva (Mila)

Dr. P. Nourian (Pirouz)

Advisor: I. Cardenas (Iván)

THESIS ASSESSMENT BOARD:

Dr. J. A. Martinez (Chair)

Dr. G. Dane (External Examiner, TU Eindhoven)

DISCLAIMER

This document describes work undertaken as part of a programme of study at the Faculty of Geo-Information Science and Earth Observation of the University of Twente. All views and opinions expressed therein remain the sole responsibility of the author, and do not necessarily represent those of the Faculty.

ABSTRACT

The environmental performance of urban neighbourhoods is a crucial indicator to measure the sustainability of the built urban form, especially as cities face increased urbanisation and densified development. With new construction contributing significantly to global carbon emissions, there is a need to understand how introducing modifications in the urban form of a neighbourhood can affect its environmental performance. This research addresses this need by developing a Planning Support System workflow to aid decision-making in urban planning problems, by analysing and visualising environmental performance at the scale of a neighbourhood, specifically the performance of thermal comfort and solar energy potential indicators. It explores the relationship of urban form and the selected indicators of Annual Solar Potential per rooftop and Physiological Equivalent Temperature while utilising freely available 3D geoinformation data of the Netherlands. It develops simplified workflows using established plug-ins and open-source 3D software that can be utilised by smaller municipalities with resource constraints, thus removing barriers to 3D-data based, data-driven decision-making for sustainable and informed urban planning.

The first workflow utilises CloudCompare to use AHN point clouds to create DEMs of the selected site. Using the developed QGIS toolbox for solar potential estimation, different built form configurations are tested on different dates for estimating the variation in rooftop solar potential. In line with the literature review, the results demonstrate that shadowing due to tall buildings reduces the solar irradiance of rooftops immediately adjacent to the newly introduced tall building(s). However, the estimated solar potential of the neighbourhood increases due to the addition of the new roof plates. Similarly using the developed PET estimation model in QGIS, the wind flow intensities are modelled as well as the mean radiant temperature. The results for the PET analysis demonstrate the contribution of blocking of airflow to increasing the estimated PET while urban shadowing is seen to decrease PET. In line with literature, the effects of building orientation, shadowing and obstructing wind flow are visible in the results.

Analysing the results further shows the nature of changes in the predicted environmental performance at the neighbourhood. While some rooftops are noted to lose the solar potential of their rooftops, the neighbourhood reports an increased mean value of annual yield, reinforcing the benefits of energy sharing using a hyper-local grid to counter the negative effects brought in by introducing tall buildings. While PET reports an increase due to blocking of airflow, the same buildings cause shadowing that increase thermal comfort in another area. Thus, introducing tall buildings is seen to have not only have negative repercussions and can benefit a neighbourhood when planned thoughtfully and in addition with other supporting plans. The final workflow is to view the results of the analysis in a Cesium-based web environment, allowing for sharing of the model to potential stakeholders with the expectation that it will spur more interest in citizen engagement and comprehension of the results.

Keywords: Environmental Performance, Urban Form, LIDAR, Solar Potential, Thermal Comfort, Open Source software, the Netherlands

ACKNOWLEDGEMENTS

A thesis is certainly no one-man job. First and foremost, I would like to extend my sincere gratitude to my supervisor Dr. Mila Koeva, for her constant support, guidance, and positive encouragement through the last year. Her insights into developing the research while also allowing me the freedom to experiment has been instrumental in shaping this research.

I would also like to thank Dr. Pirouz Nourian for his insights on defining the narrative around this research. Our discussions on understanding the ‘why’ rather than the ‘how’ behind any research changed my viewpoint on how I approach problems. I thank my PhD advisor Ivan Cardenas for painstakingly working through many practical problems with me. Those working sessions helped in developing many of the workflows in the research. My sincere appreciation to the comments given by Dr. Zevenbergen in the previous assessments, which also helped shape the communication of the results.

A sincere thanks to the faculty at the PGM department that allowed me to experiment all through the first year and gave me the exposure to the possibilities in the world of technical urban planning. I also thoroughly appreciate friends and acquaintances Rifqi and Marcello for their help in navigating 3D web visualisation.

My colleagues and seniors at het Kadaster have proven invaluable in their meaningful input. My thanks to Peter de Jong and Alma Korteweg for helping me resolve some of my doubts about the Omgevingswet and Dutch laws, and to Dr. Bhavya Kausika for meaningful discussions over the results.

I am grateful for the mental support that my friends here have lent me. UPM has become a family away from home. The special camaraderie that we have developed has given tremendous mental support over the last year. Thanks to Wibi, Amir, Majedeh and Pritam for withstanding my ranting. Thanks to Anchal for the study sessions, for cooking dinners when I was exhausted, for practising spoken Dutch with me and for keeping me motivated throughout. In addition, my deepest regards for the Gods and the psychologist(s) for giving me courage this year.

I have always been grateful for having an incredibly supportive family. Their constant encouragement, even from a distance, proved to be invaluable through the good times as well as the difficult ones. My deepest thanks to my mother for her daily phone calls, to my brother for his monthly phone calls, and my father for arranging bi-annual visits to see each other. Aside from the humour, this thesis and degree would not have been possible without them. Last but certainly not least, a special acknowledgment of my partner Timo and his unfaltering patience with my lists of drafts. He has been my proofreader in both English and Dutch for years, the first audience of all my draft presentations, my tech support, and a truly supportive partner.

TABLE OF CONTENTS

1.	Introduction.....	1
1.1.	Background.....	1
1.2.	Relevance of research	2
1.3.	Objective.....	2
1.4.	Research Gap	3
1.5.	Conceptual Framework.....	4
1.6.	Thesis Structure	4
2.	Literature review	5
2.1.	Effect of Urban Form on Environmental Indicators	5
2.2.	National and local policies in effect in the study area.....	8
2.3.	Energy Modelling for cities and City Modelling in 3D.....	10
2.4.	Summary and Conclusion	10
3.	Study area	12
3.1.	Rationale.....	12
3.2.	Characteristics	12
4.	Research Methodology.....	14
4.1.	Selection of open-source data sources and processing software	14
4.2.	Phasing	14
4.3.	Operationalisation of sub-objectives – Research Matrix.....	21
4.4.	Ethical considerations, risks and contingencies	22
4.5.	Summary	22
5.	Results.....	24
5.1.	Visualising the site in 3D.....	24
5.2.	Analysing environmental performance of original and modified scenarios	24
5.3.	Visualising results in 3D.....	43
5.4.	Summary	45
6.	Discussion.....	46
6.1.	Analysis of results from Solar Workflow	46
6.2.	Analysis of results from PET estimation	50
6.3.	Comparison of results and analysis with literature study	54
6.4.	Selection of plugins	55
7.	Conclusions and Recommendations	56
7.1.	Limitations of study	57
7.2.	Avenues for future research and development	58
7.3.	Policy recommendations	58
8.	Appendix.....	67
8.1.	Organising and documenting research data.....	67

8.2.	Detailed step-by-step workflow – Pre-processing on CloudCompare	67
8.3.	Detailed step-by-step workflow – Estimating Solar potential and savings per rooftop	72
8.4.	Model for PET estimation.....	92
8.5.	Detailed step-by-step workflow – Using 3DBAG to modify urban form in Blender	97
8.6.	Joining Solar Radiation final shp values to 3D model	98
8.7.	Script to view 3d Model and 2D raster using Cesium JS	99
8.8.	Code to analyse the results.....	101

LIST OF FIGURES

Figure 1 - Research Gap of the project.....	3
Figure 2 - Conceptual Framework of the project.....	4
Figure 3 - Municipal Goal for transition of energy demand to renewable energy.....	9
Figure 4 - Municipal Vision for Energy in Enschede.....	9
Figure 5 - 3D textured model made in CityEngine using LIDAR and rule packages. Source: author.....	13
Figure 6 - There is only one tall building in the extended neighbourhood beyond the study area. Source: Google Street View	13
Figure 7 - Phasing of the project.....	14
Figure 8 - Research Methodology.....	15
Figure 9 - Input variables to make the meteorological text file for UMEP calculations.	17
Figure 10 - Simplified open-source methodology for determining approximate solar potential per rooftop.	18
Figure 11 - Variables used to estimate PET. Bowen’s ratio is not included.	19
Figure 12 - Variables used to estimate Tmrt.	19
Figure 13 - Simplified open-source methodology for approximating thermal comfort.	20
Figure 14 - Methodology used for modifying built form in 3D and related data processing.	20
Figure 15 - Summary of the sub-workflows in the proposed PSS	23
Figure 16 - 3D built-form scenarios.	24
Figure 17 - An extract from PVGIS showing the best-case solar irradiance estimate for the given study area. Source:(EU-JRC, n.d.).....	28
Figure 18 - Simplified workflow of the automation as a part of the whole process.....	30
Figure 19 - Interface of the Solar Potential analysis Model.....	31
Figure 20 - Suitable v/s unsuitable roof area for harvesting solar energy in each of the built form cases. .	34
Figure 21 - Summarising the automated workflow for estimating PET using only built form variables.....	41
Figure 22 - Interface for data input for the calculation for PET	42
Figure 23 - A map extract of the site area from Klimaateffectatlas, showing the potential UHI effect. Source:(Stichting Climate Adaptation Services, 2023).....	43
Figure 24 - data from the analysis is joined to the 3D model in Blender.....	43
Figure 25 - Visualising on local system using Blender.....	44
Figure 26 - Visualising the results on the analysis using Cesium – Case A.....	44
Figure 27 - Visualising the results on the analysis using Cesium – Case B.....	45
Figure 28 - Visualising the results on the analysis using Cesium – Case C.....	45
Figure 29 - number of housing rooftop polygons that have an energy estimate.	46
Figure 30 - Distribution of Energy Estimate values per rooftop in each of the built form cases.....	46
Figure 31 - Probability of Energy Estimate of a given rooftop in the neighbourhood. Maximum probability is of generating Energy below 5000kWh.	47
Figure 32 - The average EE probability also rises. Thus, a singular average household can get approx. 300kWh more per year	50

Figure 33 - Distributions with the mean range from 2.5-97.5 percentile range to remove extreme outliers.	50
Figure 34 - Overlaid frequencies of temperature estimates of the three built cases.	53
Figure 35 - Some key trade-offs noticed in this simulation and analysis.....	57
Figure 36 - Folder Structure	67
Figure 37 - Tile selection on Geotiles website.....	68
Figure 38 - Visualising point cloud tile on CloudCompare.....	69
Figure 39 - Zooming into model on CloudCompare.....	69
Figure 40 - Convert to .las format and retain scale.....	70
Figure 41 - Selecting part of point cloud for further modelling.....	70
Figure 42 - Filtering by Scalar Value of layers in CC – this is for the layer which only contains the ground and unclassified points.....	71
Figure 43 - Visualising scalar fields in CC.....	71
Figure 44 - Separating and only visualising building data points.....	72
Figure 45 - Install necessary modules	74
Figure 46 - Converting contiguous patches to vector.....	77
Figure 47 - IRR value of suitable cells	77
Figure 48 - Estimating Energy production per rooftop - in kWh.....	78
Figure 49 - Estimating Euro value of the estimated energy (legend in Euros).....	79
Figure 50 - The suitability filtering is made replicable and time-efficient using Graphic Modeller.....	81
Figure 51 - Graphic modeller diagram of the PET model	92

LIST OF TABLES

Table 1 - Morphological and non-morphological factors affecting solar potential and harvest.....	6
Table 2 - Estimated ranges of PET, its thermal perception, and the Grade of Physiological Stress.....	7
Table 3 - Summary of literature review of the effect of morphology on UHI/Thermal comfort.....	7
Table 4 - Morphological parameters affecting solar potential and UHI, derived from literature review.....	11
Table 5 - Datasets used in developing the workflow.....	14
Table 6 - Proposed Research Matrix of the project.....	21
Table 7 - Summary of suitable pixels, average irradiation per suitable pixel and energy estimates in the three built form scenarios.....	34
Table 8 - Comparison of literature with the results and analysis – Solar Potential estimation and analysis	54
Table 9 - Comparison of literature with the results and analysis - PET estimation and analysis	55
Table 10 - Characteristics of different platforms for viewing results.....	58

LIST OF MAPS

Map 1 - location of selected neighbourhood as study area	12
Map 2 - Shadow Pattern of the built-form scenarios, on 3 selected dates of Spring Equinox, Summer Solstice, and Autumn Equinox	25
Map 3 - Estimation of Annualised Solar Irradiation values of the original scenario – in kWh/m ²	26
Map 4 - Estimation of Annualised Solar Irradiation values of the Modified scenario with a Single tall building – in kWh/m ²	27
Map 5 - Estimation of Annualised Solar Irradiation values of the modified scenario with a cluster of Multiple Tall buildings – in kWh/m ²	27
Map 6 - Shadow x Irradiance X contiguous cells - Suitable cell identification.....	29
Map 7 - Energy production potential estimates made from suitable cells	32
Map 8 - Usable roof area in percentage in each built case and season.....	33
Map 9 - Wind flow speed in m/s calculated for Case A using the on-ground wind conditions in the EPW file for WS10m.....	35
Map 10 - Wind Flow intensities on ground for Case A. The buildings are seen to reduce wind flow intensity at 2m above ground and block the wind flow.	35
Map 11 - Wind flow speed in m/s calculated for Case B using the on-ground wind conditions in the EPW file for WS10m.....	36
Map 12 - Wind Flow intensities on ground for Case B. Wind pattern is seen to be changing around the introduced tall building.....	36
Map 13 - Wind flow speeds in m/s calculated for Case C using the on-ground wind conditions in the EPW file for WS10m.....	37
Map 14 - Wind Flow intensities on ground for Case C. There is considerable change in wind pattern observed due to introducing the tall building aligned E-W, which blocks wind effectively.	37
Map 15 - Sky View factor estimations for all 3 built form scenarios.....	38
Map 16 - Tmrt - Mean radiant temperature estimate using SOLWEIG for Case A.....	38
Map 17 - Tmrt - Mean radiant temperature estimate using SOLWEIG for Case B.....	39
Map 18 - Tmrt - Mean radiant temperature estimate using SOLWEIG for Case C.....	39
Map 19 - PET estimate at 1pm, 22nd June 2017 – case A.....	40
Map 20 - PET estimate at 1pm, 22nd June 2017 – Case B	40
Map 21 - PET estimate at 1pm, 22nd June 2017 - Case C.....	41
Map 22 - Rooftops showing loss of suitability in the built-form scenario of Case B- One Single Tall Building	47
Map 23 - Rooftops showing loss of suitability in the built-form scenario of Case C - Multiple Tall Buildings	48
Map 24 - Roof Area utilization (in percentage) in March/Sep	48
Map 25 - reduction in usable roof area (in percentage) on introducing new buildings.	49
Map 26 - PET values over 40 °C in Case A.....	51
Map 27 - PET values over 40 °C in Case B.....	51
Map 28 - PET values over 40 °C in Case C.....	52

Map 29 - PET values (Case B-CaseA).....	52
Map 30 - PET values (Case C- Case A)	53
Map 31 - Suitable cell filtration using Raster Calculator	76
Map 32 - identifying contiguous clusters of suitable cells.....	76

ABBREVIATIONS

AHN	Actueel Hogebestand Nederland
BAG	Basisregistratie Adressen en Gebouwen
CDC	Center for Disease Control and Prevention (US)
DEM	Digital Elevation Model
DSM	Digital Surface Model
DTM	Digital Terrain Model
EPW	Energy Plus Weather data file
LIDAR	Light Detection and Ranging
LOD	Level of Detail
MEMI	Munich Energy-balance Model for Individuals
PET	Physiological Equivalent Temperature
PSS	Planning Support System
PV	Photo-Voltaic
SDG	Sustainable Development Goals
SEP	Solar Energy Potential
UBEM	Urban Building Energy Modelling
UHI	Urban Heat Island
UHIP	Urban Heat Island Potential
UTCI	Universal Thermal Climate Index

1. INTRODUCTION

1.1. Background

The built form and pattern of urban areas have significant part to play in the environmental performance of the neighbourhood (Mussawar et al., 2023). Given that the construction industry contributes over a third of the total global carbon emissions (van Oostrom, 2022), and urbanisation and densification of cities continue unabated, it is necessary to understand the effect of modifying urban forms in a neighbourhood on its environmental performance. As the scale of action shifts from policy at global level to action at a local level, municipalities are now charged with creating action plans within the realms of the national and international policy (Salter et al., 2020). Acknowledging the critical role of early-stage decision-making in influencing urban form (Méndez Echenagucia et al., 2015), and consequently on its environmental performance, there is a need for a Planning Support System Workflow that facilitates informed decision-making in planning projects with the objective of analysing environmental performance of the built form decisions as a contribution to sustainability at a local scale.

To address the ongoing housing crisis and meet the growing demand for housing stock in the Netherlands, it is essential to build more houses (Geis, 2023). As cities do not wish to expand beyond their limits into agricultural areas, densification within city limits is an alternative option for accommodating new housing stock (Broitman & Koomen, 2015). With this context of the need of new residential spaces to be built, preferably as urban densification, there arises a need to ensure that introducing or regulating (Shach-Pinsly & Capeluto, 2020) new and different built morphology does not severely impair the environmental performance of the existing neighbourhood.

The causal effect of urban form on environmental performance in terms of Thermal Comfort and Solar Energy Potential, amongst other indicators, have been widely studied in the past few decades (Boccalatte et al., 2020; Li et al., 2020; Poon et al., 2020; Siu et al., 2021; Zhou et al., 2017). Studies focusing on analysing block types for solar potential consistently show that parameters such as Floor-Area Ratio, building height and spacing between adjacent buildings (built density) influence solar potential in residential zones (Liu et al., 2023). Similarly, the relationship between urban built form and thermal comfort has been studied using different indicators such as Physiological Equivalent Temperature (PET) and Universal Thermal Climate index (UTCI), and other numerical models (Karimimoshaver et al., 2021; Li et al., 2020; Xu et al., 2019). Intentionally designing urban block morphology in early design stages is essential to improving its environmental performance (Sheng et al., 2021). The environmental performance of buildings and neighbourhoods together contribute to urban liveability as the immediate outdoors are seen as an extension of the living space (Lau et al., 2018).

While multiple performance parameters exist, such as thermal performance, energy consumption, greenery, daylighting, carbon emissions etc., in the context of this project, environmental performance is narrowed down to two performance potentials – the potential of thermal comfort (using Physiological Equivalent Temperature) and the potential of energy transition to solar panels (Solar Energy Potential of individual rooftops). These are selected as both of them are very dependent on location and morphology and have differing morphological requirements for improvement – as is illustrated further in Chapter 2. Thus, this research juxtaposes the effect of modifying morphology at a local scale on the chosen indicators in an attempt to analyse and improve the performance in both indicators in the context of urban form-based decisions. Planning practice involves trade-offs to achieve visions and goals improve and maintain the urban liveability of the city, and this research attempts to analyse a real planning problem and understand the trade-offs that may be involved.

To derive comprehensive insights into the environmental performance of neighbourhood-scale projects, a 3D perspective is important as buildings exist under the influence of their surroundings. It enables understanding spatial relations from a volumetric viewpoint, highlighting the influence of morphology in immediate surroundings. Thus, the project intends to make use of the freely available 3D geoinformation of the Netherlands to model existing and future scenarios to examine *to what manner does change in urban form affect the environmental performance of a neighbourhood.*

1.2. Relevance of research

Urban planners and designers are increasingly tasked with designing sustainable urban environments. While many larger municipalities that lead these tasks have the capacity and funding to carry out individual analyses, this is not always the case with smaller, cash-strapped municipalities (Salter et al., 2020). Thus, this research focuses on developing and testing an open-source workflow that can aid in analysing and visualizing the effect of modifying urban form in a neighbourhood. It also demonstrates multiple further analyses that can be done on the given results, which can help smaller municipalities take an informed decision about the repercussions on the environmental performance of the neighbourhood.

1.3. Objective

The primary objective of this research is to devise a Planning Support System Workflow which can analyse and visualize the environmental performance of existing and modified urban built forms, to aid form-based design decision-making at the neighbourhood scale.

1.3.1. Sub-objectives and Research Questions

1 – To review existing body of literature on the effect of built form on neighborhood environmental performance, and relevant policies guiding urban development in the context of the study area, with a focus on transition to solar energy and improving thermal comfort.

RQ1.1 – What is the current state-of-the-art in analysing environmental performance at neighbourhood-scale using morphological indicators?

RQ1.2 – What are the goals of the local municipality regarding increasing energy transition and improving thermal comfort, and how can that be utilized for designing the PSS?

2 – To investigate and apply appropriate GIS-based methodologies for evaluating Solar Energy Potential of rooftops and Thermal Comfort (via Physiological Equivalent Temperature estimate) of the existing built form in a selected neighbourhood in Enschede.

RQ2.1 – What is the Solar Energy Potential of the rooftops in the existing state of the selected neighbourhood?

RQ2.2 – What is the state of Thermal Comfort in the existing state of the selected neighbourhood?

RQ2.3 – What openly available data on solar potential and thermal comfort can be compared with the results from the workflows used in RQ2.1?

3 – To develop a workflow using 3D geoinformation to model new urban landscapes for scenario analysis, which can work seamlessly with the analysis in Objective2, and simulate the environmental performance of the scenario models.

RQ3.1 – How can 3D geoinformation be visualized and modified by user in an open-source software? Using this workflow, different built scenarios will be created such as introducing one single tall building and a cluster of tall buildings.

RQ3.2 - What is the observed change in the environmental performance of the neighbourhood when the pattern of urban form is modified?

4 – To visualise the results of the simulations in a 3D environment and compare results with literature review.

RQ4.1 – How can the results of the scenarios be visualized 3D model-based environment?

RQ4.2 – How do the results compare to the conclusions of the literature review? What further recommendations can be made for form-based planning in the selected neighbourhood?

1.4. Research Gap

In conducting the literature review, there is a research gap identified in analysing the effects of urban form on two environmental indicators that have differing morphological requirements for improvement. Figure 1 summarises the gap thus observed between environmental modelling, urban planning practice, and comparing indicator performance using a simplified workflow.

This project addresses the research gap by allowing users to analyse their built environment as well as future scenarios using open-source methodologies and software. Allowing for ease of use and replicability using Graphic Modelers in QGIS environments as well as open-source physics-based plugins and programming where necessary, the set of workflows explains and navigates the user through the data transformations and conversions necessary to conduct the analysis, while also giving the freedom to manipulate future scenarios as per the user.

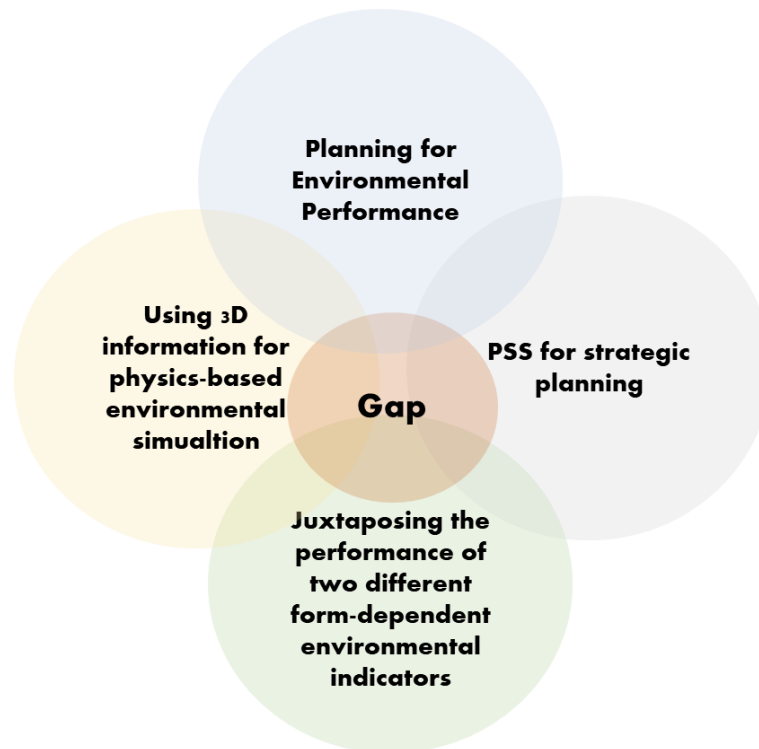


Figure 1 - Research Gap of the project

1.5. Conceptual Framework

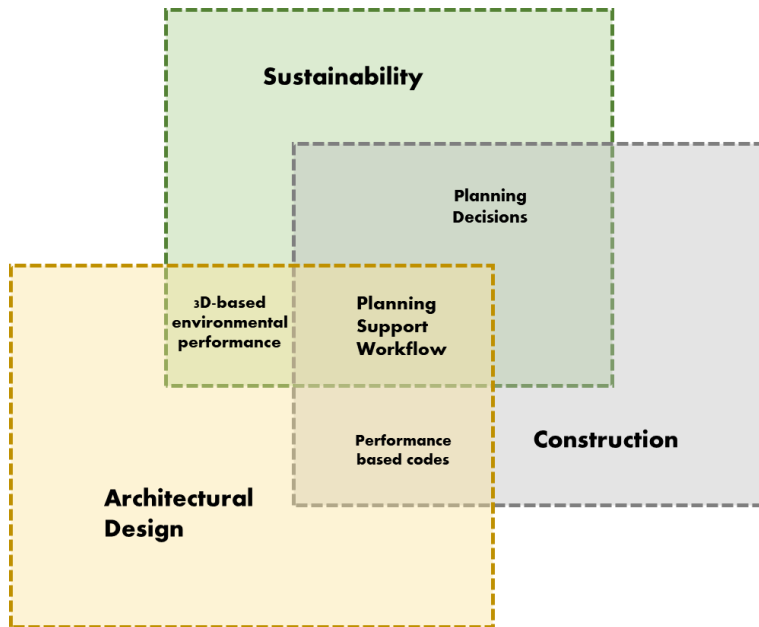


Figure 2 - Conceptual Framework of the project.

The conceptual framework outlines the vision of the project to serve as a technical aid to the urban planning process of neighbourhood-scale development. Taking cues from policies at multiple scales, the PSS Workflow is aimed to aid in 3D urban planning for performance-based planning, which in turn will improve local sustainability by analysing and visualizing climate comfort and feasibility of energy transition for existing and simulated 3D scenarios.

1.6. Thesis Structure

This thesis is divided into multiple chapters. Chapter 1 introduces the topic of the thesis, along with the aims and objectives. Chapter 2 is literature review, which revolves around Sub-Objective 1. Chapter 3 introduces the study area of Twekkelerveld. Chapter 4 details the research methodology. Chapter 5 consists of the results of the analysis, and Chapter 6 discusses the results. Chapter 7 comprises of conclusions and recommendations, as well as scope for further study.

2. LITERATURE REVIEW

Urban morphology has a direct effect on multiple environmental indicators, and this has been corroborated by research. This section of literature review discusses on defining the concepts of environmental indicators used within this research, summarizes the current state of research on exploring the effect of morphological changes on the selected environmental indicators, and throws more light on the broader context of national and local policies at play in the study area of Enschede in the Netherlands. In addition, it also underlines the importance of using 3D as an input as well as an output of the research in order to make the results easily comprehensible. The Literature Review section also answers Sub-Objective 1.

2.1. Effect of Urban Form on Environmental Indicators

2.1.1. Defining Environmental Indicators

As the research dives into the components and contributors to environmental performance and its measurement, it is crucial to clarify the terminology. Variables are any modifiable factors within a system, such as building orientation, or roof area. They may be dependent or independent in nature and can be measurable or qualitative. Parameters are measurable variables, such air temperature, or percentage of shadowing of roof surfaces. Indicators describe the state of the environment and are used to assess performance (European Environment Agency, n.d.). They may be defined as a parameter, a combination of parameters or value derived from such that provides information of significance about a system beyond the numeric value, such as the PET (indicator for thermal comfort) (Höppe, 1999) or Solar Potential estimate in kilowatt-hour per unit area (kWh/m²) (Polo & García, 2023).

2.1.2. Morphological parameters influencing environmental performance

The effect of morphology on environmental performance has been widely studied, with many studies focusing on the effect of urban form and geometry on daylighting, ventilation, building energy demand and so on (Clifton et al., 2008; Ratti et al., 2005; Rode et al., 2014; Silva et al., 2017; Steadman et al., 2014). The effects of different neighbourhood and building morphological characteristics on the indicators selected for this research are discussed further in this section.

2.1.2.1. Effect of building and neighbourhood morphology on Solar Potential

The national Renewable Energy laboratory (NREL) defines Solar irradiance as the “*average energy flux received from the sun*” in form of electromagnetic radiation (NREL - U.S. Department of Energy, 2012). Usually measured in W/m² or kW/m², solar irradiance can be expressed as Global Horizontal irradiance, Direct normal irradiance, or Diffuse Horizontal irradiance.

Global Horizontal irradiance is “*the amount of irradiance falling on a surface horizontal to the surface of the earth*” (Sandia National Laboratories, 2024). Diffuse Horizontal irradiance is the “*terrestrial irradiance received by a horizontal surface after being scattered by the atmosphere*” (Sandia National Laboratories, 2024), whereas Direct Normal irradiance is the “*amount of solar radiation received per unit area by a surface area normal to the rays of the sun*” (Kosmopoulos, 2024).

Thus, the relationship of GHI, DNI and DHI is as follows:

$$GHI = DHI + DNI \cdot \cos(\theta_z) \dots\dots\dots (1)$$

Where (θ_z) is the angle between the sun and the zenith direction. The three variables can also be estimated from each other due to availability of advanced estimation models.

The US Department of Energy defines solar potential of a singular rooftop as the amount of solar capacity that can be installed on that rooftop based on its size, shading, tilt, and other locational factors and roof characteristics, whereas the solar rooftop potential for a country (or in this case, of a neighbourhood), is the number of rooftops that are suitable for solar panel installation (US DOE, n.d.).

Solar potential highly depends on geographic, neighbourhood as well as roof characteristics. The key data used for the estimations is the solar irradiation data. Recent models can also estimate Global Horizontal irradiation (GHI) and Direct normal Irradiation (DNI) using cloud cover information from satellite-based datasets (Solargis et al., n.d.). These datasets are now also available as free datasets within the Global Solar Atlas, funded by the World Bank. Major factors affecting solar potential of rooftops are individual building characteristics, i.e., the morphological factors, as well as geographic and choice-dependent factors, which are summarised in Table 1.

Table 1 - Morphological and non-morphological factors affecting solar potential and harvest

Morphological Factor	Effect
Urban density and shadowing	Sky View factor and shadowing can help in determining direct and indirect irradiation on a surface (Calcabrini et al., 2019). Variations in building heights in a neighbourhood can affect shadowing on neighbouring rooftops, reducing the amount of received irradiation (Bardhan et al., 2020; Li-Lian, 2022)
Building and installation Orientation	Visibility of placement of PV module affects the rooftop potential, with modules at the west edge having the highest visibility (Zhou et al., 2023). Building orientation should have the long side facing south (Bardhan et al., 2020)
Roof design and geometry	Slope needs to be 10-45 degrees for optimal utilisation (Yorulmaz, 2023). This is to capture maximum DNI. PV modules should be placed on flat roofs or larger roof plates so that they are not visible to the public – especially in the case of monumental buildings(Zhou et al., 2023) Roof aspect should not be facing North as that receives the least amount of usable irradiation (Yorulmaz, 2023). Minimum roof area 20sqm is needed to have a viable installation (Yorulmaz, 2023). Available roof area without obstructions is essential for a rooftop to have solar potential (Li-Lian, 2022)
Aspect ratio and street orientation	Parameters like average and range of building heights, orientation of buildings, plot ratio and site coverage, height to width ratio (Street width: building height), compactness can impact annual solar irradiance. Sky View factor can be used as an indicator for evaluating solar irradiation on surfaces (Poon et al., 2020).
Geographic/locational factor	Effect on Solar potential
Annual solar irradiation	At least 800 kWh or more is beneficial to realise the investment cost of setting up the solar panels (Yorulmaz, 2023). This is dependent on latitude, day length and altitude of the location.
Cloud Cover and Weather Patterns	Frequent cloud cover can reduce solar potential due to diffused sunlight (Nevins & Apell, 2021).
Atmospheric pollution	High level of pollutants can scatter and absorb sunlight, effectively blocking the amount of sunlight reaching the PV panels (Ramanathan et al., 2001)
Non-Morphological factor	Effect of solar harvest
Choice of PV cells	Different PV cells and systems have different efficiencies and costs. Thus, their suitability also differs as per location, slope, and other factors. (Zhou et al., 2023)

Maintenance of cells	Not keep surfaces clean from dust deposition can reduce the conversion rate from solar energy to electricity (Nezamisavojbolaghi et al., 2023).
----------------------	---

2.1.3. Effect of building and neighbourhood morphology on Thermal comfort.

Centre for Disease Control and Prevention (CDC) (NIOSH/CDC, 2020) defines heat stress as a “health hazard stemming from exposure to extreme heat or hot working conditions, potentially leading to conditions such as dehydration, heat strokes, exhaustion, morbidity, and, in severe cases, even death, as the body struggles to regulate its internal temperatures”. Within the European context, there is escalating concern on heat waves, with the Lancet reporting that the surface air temperature increase in the continent has surpassed the global average by almost 1°C (van Daalen et al., 2022). The year 2022 marked the hottest European summer on record, and the trend marks a grim future.

The sharper increase in recorded temperatures in urban areas as compared rural or vegetated areas lead to creating Urban Heat Islands, and its effect on humans can be measured by indicators of thermal comfort such as Physiological Equivalent temperature (PET), which takes into account the effect of the air temperature, relative humidity, and wind speed, along with surface albedo on the human body (Matzarakis et al., 1999). PET is based on the Munich Energy-balance Model for Individuals (MEMI) and is a holistic indicator of thermal comfort. The ranges of temperatures and the physiological stress they correspond to are explained below (Table 2).

Table 2 - Estimated ranges of PET, its thermal perception, and the Grade of Physiological Stress

PET/°C	Thermal perception	Grade of physiological stress
≤4.0	Very cold	Extreme cold stress
4.1–8.0	Cold	Strong cold stress
8.1–13.0	Cool	Moderate cold stress
13.1–18.0	Slightly cool	Slight cold stress
18.1–23.0	Comfortable/Neutral	No thermal stress
23.1–29.0	Slightly warm	Slight heat stress
29.1–35.0	Warm	Moderate heat stress
35.1–41.0	Hot	Strong heat stress
41.1≤	Very hot	Extreme heat stress

Source: Matzarakis and Mayer (1997)

Multiple factors that have been studied to decrease thermal comfort have been summarised in Table 3.

Table 3 - Summary of literature review of the effect of morphology on UHI/Thermal comfort

Morphological Factor	Effect on Thermal Comfort
Natural light and ventilation	Hindrance to natural ventilation can decrease thermal comfort and increase the dependence on mechanical cooling (Lau et al., 2018)
Building Orientation	Airflow blocking by building orientation can reduce thermal comfort (Stewart & Oke, 2012). Building orientation towards south will have a negative effect on thermal comfort (Nakata-Osaki et al., 2018)
Aspect ratio and street orientation	Lack of air paths along with closely packed buildings can hinder ventilation (Deng & Wong, 2020; Lau et al., 2018; Nasrollahi et al., 2021; Siu et al., 2021)
Taller, voluminous buildings and dense neighbourhoods	Taller buildings increase surface areas for absorption of solar radiation. Thus, high rise, dense neighbourhoods report higher temperatures compared to less dense areas

(Hong et al., 2023). However, shadowing between buildings may reduce local heat stress (Nasrollahi et al., 2021).

Non-Morphological factors	Effect on Thermal Comfort
Built material and albedo	Surface materials influences UHI by material properties of absorption and reflectivity (Cascone & Leuzzo, 2023)
Plantations and water bodies in proximity	Presence of greenery reduces UHI (Cascone & Leuzzo, 2023)

Literature suggests that using solar panels can have a positive effect in reduction of UHI as radiation is either absorbed or reflected away from the panels (Masson et al., 2014). Thus, one strategy in planning can be to combat increasing UHI by introducing tall buildings is to offset it by increasing the number of solar panels, but this is yet to be comprehensively tested. Instead, the reduction in UHI by introducing non-building elements such as plantations and water bodies in the neighbourhoods have been proven as summarised in Table 3.

2.2. National and local policies in effect in the study area

This research attempts to understand the local context and how the results from this workflow can be used to aid these policies in effect. This section summarises some of the local policies and vision plans in the city of Enschede to contextualise the research problem.

The Spatial Planning Act (WRO) (Ministry of Infrastructure and the Environment the Netherlands, 2013) guides broad urbanisation trends in the Netherlands. The new Omgevingswet released in 2024 allows the Gemeente (municipality) to decide on building details at plot level, and the Gemeente Enschede decides on permission to build by consultation. Thus, there is no strict ban against introducing taller buildings in residential areas and can potentially done in consultation with the municipality.

2.2.1. Housing in the Netherlands

Netherlands has been going through a housing shortage over the past few years, with the gap between demand and supply standing at almost 400,000 houses in 2023 and slated to rise to over 980,000 homes by 2030 (ABF Research, 2023). In line with many other European cities, Dutch cities have shown trends of densification within residential zones of cities rather than creating urban sprawl at the city peripheries (Broitman & Koomen, 2015). The strict zoning regulations effectively maintain open spaces and thus contain urban development by concentrating them (Koomen et al., 2008). The Housing Vision Plan for Enschede - Woonvisie2024 Enschede outlines the plan by the Gemeente to build 9400 new homes in Enschede, trying to unite Almelo-Hengelo -Enschede as an urban corridor in the region of Twente.

2.2.2. Solar Energy in the Netherlands

Transition to using solar energy is encouraged by the Dutch government with the use of energy tax rebates, grant schemes, supplying electricity back to grid and other help via subsidies (Government of the Netherlands, n.d.). The potential annual yield of electricity generated through solar installations in the country is 200TWh, which is 73% higher than the national consumption (Netherlands Enterprise Agency (RVO) et al., 2020). Due to this, the national Dutch government is aiming for at least 7TWh to be generated from small scale solar installations in the built environment (Netherlands Enterprise Agency (RVO) et al., 2020).

Regarding this, the municipality of Enschede envisions their Energy goals for the city in their *Energie Visie* document, which states “*With the spatial policy for solar energy, the municipality wants to achieve that at least 530 Terajoules, or 147,000 MWb, will be produced in Enschede by 2030. This is the electricity that can be generated annually with 442,300 solar panels. This is electricity for approximately 53,000 households.*” (Gemeente Enschede, 2021b, 2021a)



Figure 3 - Municipal Goal for transition of energy demand to renewable energy.

Thus, not only is feasible energy transition a goal for the city, but the vision document lists three major pillars to achieve this as seen in Figure 4. In the creation of green energy, the aim is to identify rooftops and public open space that may be conducive for exploiting solar potential to reach municipal goals by 2030 (Gemeente Enschede, 2021b, 2021a).

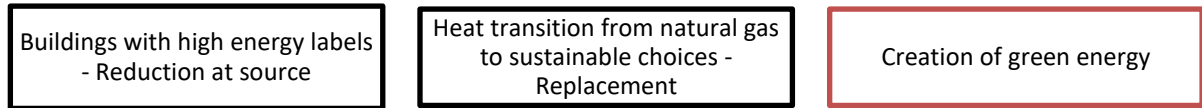


Figure 4 - Municipal Vision for Energy in Enschede

2.2.3. UHI in the Netherlands

The Netherlands has a mild Oceanic (Cfb) climate (Koppen-Geiger Climate Classification (Steenveld et al., 2011) and thus, UHI was not considered as a critical issue historically, but now it is also seen as a growing concern in city centres (Van Hove et al., 2011). There exist multiple studies spanning hundreds of cities worldwide, out of which the study of the city of Den Haag found strong correlation between measured UHI and the properties of urban space such as the degree of hardness of surfaces, absence of greenery, shadowing and built volume (van der Hoeven et al., 2019). An increased UHI leads to poor thermal comfort for the residents.

PET is one of the many indicators that is used to study the impact of this urban heat stress on humans. In the Netherlands, a standardised way to calculate PET in direct sunlight is described by (Koopmans et al., 2020) as:

$$\begin{aligned}
 PET_{sun} = & -13.26 + 1.25T_a + 0.011Q_s - 3.37\ln(u_{1.2}) + 0.078T_w + 0.0055Q_s \ln(u_{1.2}) + 5.56\sin(\phi) - \\
 & 0.0103Q_s \ln(u_{1.2}) \sin(\phi) + 0.0546B_b + 1.94S_{vf} \\
 & \dots\dots\dots (2)
 \end{aligned}$$

- where a = 2-m air temperature (°C),
- Qs = solar irradiation (W m⁻²)
- u_{1.2} = wind speed at 1.2-m height (m s⁻¹),
- T_w = wet-bulb temperature,
- σ the Stefan Boltzmann constant (5.67.10⁻⁸ W m⁻² K⁻¹),
- φ = solar elevation angle (degrees),
- B_b = Bowen ratio (ratio between sensible and latent heat flux),
- S_{vf} = sky-view factor
- Q_d = diffuse irradiation (W m⁻²)
- For impervious surfaces, Bowen's ratio is taken as the constant 3.

The municipality at Enschede recognizes UHI as a risk to urban liveability in the city and has included it in their risk matrix for heat stress (Gemeente Enschede & Royal HaskoningDHV, 2022). Other national datasets have also conducted nationwide studies of heat measurement in the country, such as *Klimaat-effectatlas* (Stichting Climate Adaptation Services, 2023), and the results show a concentration of UHI in the core of the city.

2.2.4. Easement rights

Environmental performance can be measured at different scales. While the most common is that of building scale, i.e., to check whether an individual building is performing in an acceptable manner, the effect of introducing new built forms on the performance of its neighbours is not commonly measured. Easement rights protect individual homeowners from poor design decisions of neighbours. One such easement is of solar easement, which allows property users access to their share of sunshine onto their plots (Thoubboron,

2021). These are necessary as increased shade due to taller neighbouring buildings or tall trees can hinder solar energy generation through rooftop panels. Similarly, change in urban form and building material can affect the perception of thermal comfort in its immediate neighbourhood (Elkhazindar et al., 2022) as it can result in changed sky view factor, albedo, and shadowing.

2.3. Energy Modelling for cities and City Modelling in 3D

In the recent years, there has been many attempts to create 3D models of cities, and also to monitor several environmental and non-environmental parameters using these 3D models. The increased interest in using physics-based models in urban energy modelling has also seen a steady increase over the past decade (Kamel, 2022). However, the accuracy of using these models for an entire city remains a challenge as most papers that test Urban Building Energy Modelling (UBEM), do so on a micro-scale of less than 1000 buildings. There are simplifications made UBEM models in order to make them more accessible for analyses, such as development of the UBEM.io interface by MIT labs (Ang et al., 2022). Examples of aggregated 3D simulations of individual buildings scaled to city-scale include the SimStadt model which was developed on CityGML and uses the extension Energy ADE to simulate the energy metrics (Scartezzini et al., 2015). Salter et al (2020) have devised a methodology to model the effects of environmental policy interventions using variations in the built environment, which involves a method of comparing the performance of the future built form and policy scenarios to the existing condition.

The concept of Digital Twins and the desire to view the model results in 3D has led to many academic and commercial projects to map cities in 3D, examples of which include 3D Amsterdam and other projects by Geodan (Kuster, 2023). The use of 3D visualisations while presenting analyses and results to stakeholders is widely recognised for increasing the amount of understanding and engagement over the given results. Compared to traditional 2D visualisations, such as a map, 3D visualisations in forms of building models improve spatial awareness and quality of insights in spatial analyses (Bleisch & Dykes, 2015).

The use of 3D visualizations can lead to more effective decision-making. A meta-analysis of the effectiveness of 3D visualizations in discrete-event simulations (DES) concludes that 3D displays outperform 2D displays in model verification, validation, and analysis of results, thus leading to more efficient decision-making (Akpan & Shanker, 2019).

3D geo-visualizations enable the display of quantitative data in context, which can be crucial for fields like urban planning and environmental management. Although some studies report minimal differences in performance between 2D and 3D visualizations, specific contexts show clear benefits of using 3D for conveying spatial data (Seipel, 2013). Herbert & Chen (2015) argue that the use of 3D is beneficial depending upon the type of analysis in urban planning and cannot be said to always be the better option of visualization.

2.4. Summary and Conclusion

There are multiple studies on the effects of morphology on UHI and on Solar Potential, where parameters such as size, orientation, roof angle, spacing, shadowing, and material selection is commonly studied (Liu et al., 2023; Xu et al., 2019). Some of the common morphological parameters are summarized in Table 4. In that, the factors marked in red affect the desired environmental performance negatively, while the factors marked in green affect the performance positively.

The Urban Heat Island effect is exacerbated by building arrangement configurations such as street canyons, i.e., the ratio of building height: width of streets, which plays a role in affecting wind flow and effectively affects air temperature (Karimimoshaver et al., 2021). In addition, surface materials (Cascone & Leuzzo, 2023) and presence of greenery (Cascone & Leuzzo, 2023) also influence UHI and thus reduce thermal comfort.

Solar potential is highly dependent on geography, as the intensity and number of sun hours have a direct effect on the electricity generation (UNDP, 2000). While these cannot be changed by design, morphological parameters such as roof size and building orientation, optimal roof tilt of installation, avoiding shadows from self or other structures can positively influence solar electricity generation using PV rooftop installations (Li-Lian, 2022; Poon et al., 2020).

Table 4 - Morphological parameters affecting solar potential and UHI, derived from literature review.

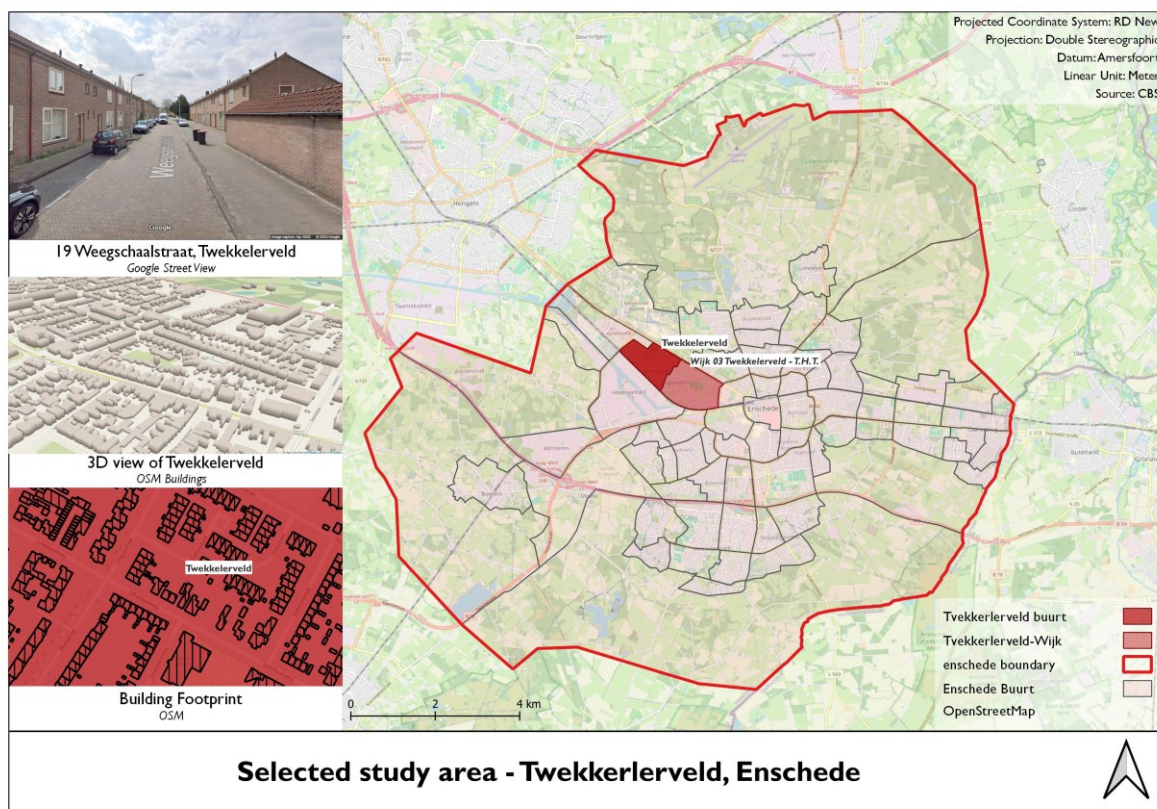
UHI	Source	Solar Potential	Source
Average building height: street width ratio - urban canyon	(Deng & Wong, 2020; Nasrollahi et al., 2021; Siu et al., 2021)	Available roof area (not too small, without major obstructions)	(Li-Lian, 2022)
Shadowing from neighbouring buildings – height ratio between adjacent buildings	(Nasrollahi et al., 2021; Siu et al., 2021)	Shadowing from neighbouring buildings – height ratio between adjacent buildings	(Bardhan et al., 2020; Li-Lian, 2022)
Building orientation – long side towards south	(Nakata-Osaki et al., 2018)	Roof angle/orientation – long side towards south	(Bardhan et al., 2020; Li-Lian, 2022)
Airflow blocking due to building arrangement	(Stewart & Oke, 2012)	Obstruction to roof e.g., trees	(Li-Lian, 2022)

The literature review highlights the importance using 3D data and visualisation contextually for ease of comprehension of results by the stakeholders. In addition, the national laws and policies governing the chosen study area focus not only on increasing housing stock, but also focus on increasing liveability by decreasing the threat of Urban Heat Island while increasing Solar electricity generation via PV modules on suitable rooftops and open spaces. As one of the methods of increasing housing stock while not horizontally expanding the city is in-situ densification by building taller, this thesis intends to utilise taller built-form options to see its subsequent effect on the chosen environmental indicators.

3. STUDY AREA

3.1. Rationale

In discussion with the Enschede municipality, three prospective neighbourhoods were discussed as potential study areas which are planned to undergo urban redevelopment in terms of building and utilities in the near future. Using this planned proposal of urban redevelopment as the main motivation, the administrative neighbourhood of Twekkelerveld is selected for simulating probable 3D built configurations to analyse the predicted environmental performance. The selected site also falls on the route towards Hengelo municipality, in the Almelo-Hengelo-Enschede axis that the Gemeente plans to urbanise in.



Map 1 - location of selected neighbourhood as study area. Source: author, using data from CBS, OSM, Google Maps

3.2. Characteristics

The neighbourhood is fairly homogeneous in its built pattern, with 2-3 storey buildings and having sloped roofs with only one taller building in proximity to the neighborhood (Figure 6). It is also characterized by absence of trees and plants in many residential streets. The BAG (Basisregistratie Adressen en Gebouwen) extract – which records data of land registrations in the Netherlands - shows that most of the houses in this zone are privately owned. This is acceptable as the Dutch municipalities work in partnerships with private owners and also with land purchasing in order to realise their urbanisation plans (Götze & Jehling, 2023; Meijer & Jonkman, 2020). Figure 5 visualises a modelled study site created using available open-source data (AHN-4, BAG extracts).



Figure 5 - 3D textured model made in CityEngine using LIDAR and rule packages. Source: author.



Figure 6 - There is only one tall building in the extended neighbourhood beyond the study area. Source: Google Street View

4. RESEARCH METHODOLOGY

4.1. Selection of open-source data sources and processing software

Keeping in mind that the main user of this workflow will be a municipality with constrained resources and funding, the project specifically uses open-source datasets and software in the workflow. Open-source GIS software QGIS is used for mapping and analysis, while CloudCompare is used to visualize and edit Point Cloud information, and Blender is used to visualize and edit 3D city models. From an array of modules, plug-ins, and models available to process 3D LIDAR information, conversion to DEM and use of UMEP and GRASS GIS as the primary plug-ins are selected as it is robust and well-supported. Code-based scripting is used as required to reduce manual work and errors. The major datasets used in this research as are listed in Table 5.

Table 5 - Datasets used in developing the workflow.

<i>S.N^o</i>	<i>Topic</i>	<i>Dataset</i>	<i>Source/ Owner</i>	<i>Data form</i>	<i>Link to Access/Citation</i>
1	LIDAR/point cloud data	AHN4 dataset	Geotiles.nl	.laz	(Dataset: Actueel Hoogtebestand Nederland 4 (AHN) & PDOK, 2023)
2	Building footprint	BAG dataset	PDOK/Kadaster	.gpkg	https://app.pdok.nl/lv/bag/download-viewer/
3	EPW Weather data – Typical Meteorological Year	PVGIS, Ladybug tools	EU-JRC	.epw, .csv	(EU-JRC, n.d.)
4	3D building models in Netherlands	3D BAG building models	3D geoinformation research group (TU Delft) and 3DGI	.obj, CityJSON	(Peters et al., 2022)

4.2. Phasing

The methodology is divided 4 phases that mirror the 4 sub-objectives and their respective research questions, as seen in Figure 7. The detailed research methodology is explained in the flowchart in Figure 8.

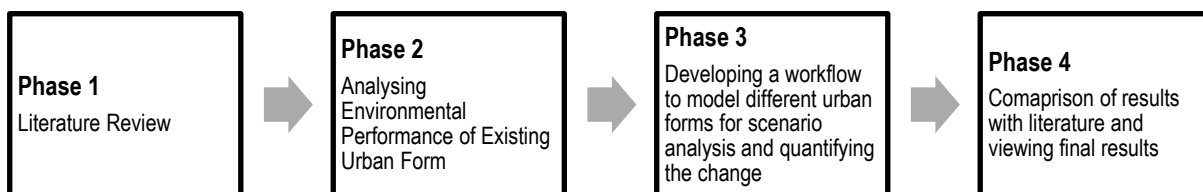


Figure 7 - Phasing of the project.

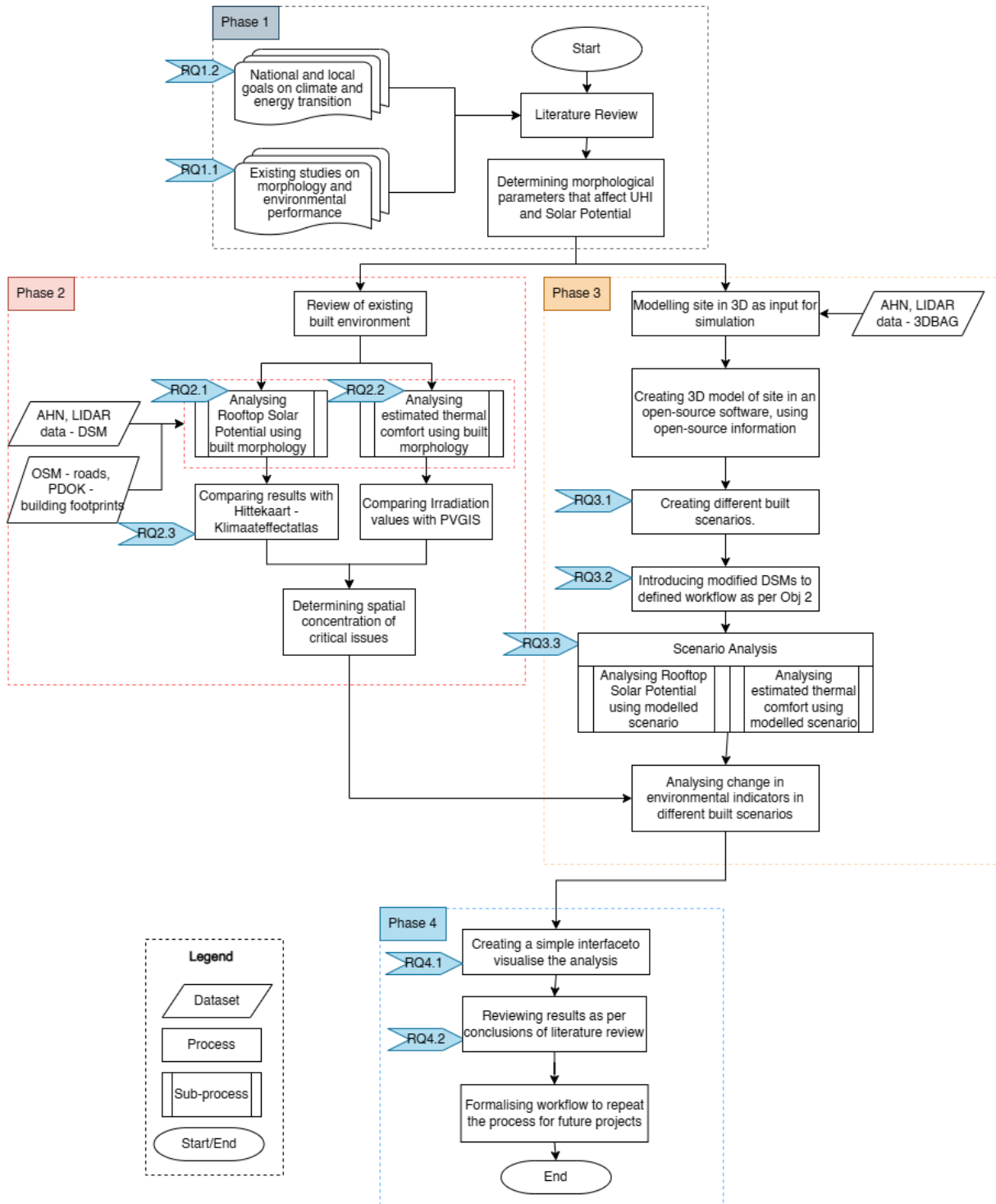


Figure 8 - Research Methodology

4.2.1. Phase 1 – Literature Review

Phase 1 focuses on conducting a literature review (Chapter 2) on existing knowledge of the effect of morphology on UHIP and SEP, and on existing Sustainable Development Goals, national and local vision plans on making built environment more sustainable and liveable. The aim is to have a comprehensive understanding of the role of urban form in affecting its immediate environment, and also understand the direction in which the local government wants to guide future developments and policies.

4.2.2. Phase 2 - Analysing Environmental Performance of Existing Urban Form

Phase 2 focuses on analysing the existing state of environmental performance of the two selected indicators in a selected neighbourhood in Enschede. Using freely available 2D and 3D geoinformation and weather datasets, the current state of solar potential of rooftops, as well as the estimated thermal comfort using PET is studied. The methodological processes to quantify an approximation are intentionally kept simple and easy to replicate, so that they may be adopted by local government departments with ease. The method is tested and then formalised into a simple interface input using QGIS Graphic Modeler, to allow for ease of repetition in Phase 3.

4.2.2.1. Pre-processing

For creating the main input files of DSM and DTM, AHN-4 LIDAR data is processed in CloudCompare. The point clouds are filtered by the desired scalar value and then processed to a DEM within CloudCompare. The tutorial for this can be found in the Annexure.

For calculation of annualised solar irradiance, the data from the entire EPW (Energy Weather Plus) file is used, which contains multiple weather variables. However, for estimation of Mean Radiant Temperature (TMRT) and PET, an extract of the file is used as the calculation is computationally heavy. It contains weather information of the hottest day in 2017, on June 22, which is just one day after the summer solstice. Thus, the weather file is from June20 (00:00)-June23 (23:00), capturing both the longest as well as the hottest day in 2017. 2017 is used as it was the latest year in the EPW with information of the summer months. The records of 2019 do not have information over June-August.

The inputs used to create the meteorological file for input in UMEP uses the following inputs, and the input into the UMEP interface is as per Figure 9:

- **T2m**: This typically stands for air temperature at 2 meters above ground level.
- **RH**: Relative Humidity, which is the amount of moisture in the air compared to what the air can hold at that temperature.
- **G (h)**: Global horizontal irradiance, which is the total amount of shortwave radiation received from above by a horizontal surface. This includes both direct solar radiation and diffuse sky radiation. (Sandia National Laboratories, 2024)
- **G_b (n)**: Direct beam normal irradiance, which is the amount of solar radiation on a surface perpendicular to the sun's rays.
- **G_d (h)**: Diffuse horizontal irradiance, which is the amount of solar radiation diffused by the atmosphere and then received on a horizontal surface.
- **IR (h)**: Infrared radiation (or longwave radiation) received by a horizontal surface, typically emitted from clouds and the atmosphere.
- **WS10m**: Wind Speed at 10 meters above ground level.
- **WD10m**: Wind Direction at 10 meters above ground level, usually given in degrees from true north.

Figure 9 - Input variables to make the meteorological text file for UMEP calculations.

4.2.2.2. Analysing solar potential using open-source methods

To analyse solar potential, data regarding building information such as roof size, building orientation and roof slope are required. These are collected from the Dutch information portal top10NL (via PDOK, Kadaster), and the DTM and DSM is derived from AHN-4 (LIDAR data) at 0.5m of spatial resolution. Weather information is collected from an EPW file of the location (meteorological information in an Energy Plus Weather file format). This includes information on Global irradiation as well as direct and diffuse shortwave radiation (EU-JRC, n.d.).

Using these open-source datasets, slope and aspect of roof is calculated in GIS tools, and clipped to building footprints, which are then filtered by suitability. Suitability of pixels are decided using 3 factors – that the pixel is shadow-free at least 60% of the time, receives solar irradiation over 900 kWh/m² per annum and has a contiguous area of at least 2sqm.

Shadows are estimated using the UMEP plug-in in QGIS, which uses the DSM to create shadows (Li-Lian, 2022). Solar panel output can be estimated by the Solar Energy on Building Envelopes (SEBE) function in UMEP, which uses solar irradiance data from the EPW file (Lindberg et al., 2015).

Total irradiance is calculated as the sum of direct, diffuse and reflected radiation as given in Equation 3 ((Lindberg et al., 2015; Polo & García, 2023), and stored as an attribute of the pixel.

$$R = \sum_{i=0}^p [(I\omega S + DS + G(1 - S)\alpha)]$$

Equation 3 - Calculating total irradiance on a pixel.

Where: p is the number of patches on the hemisphere.

I is the incidence direct radiation,

D is diffuse radiation

G is the global radiation originating from the i th patch.

α is the surface albedo

S is the shadow calculated to each pixel.

ω is the Sun incidence angle as explained in (Lindberg et al., 2015)

This method estimates an approximation of total solar irradiation per pixel, accounting for shadow as well as the angles and orientation of the roof surfaces derived from the DSM. A suitability analysis is done to extract only the usable pixels using raster process of `r.clump` in GRASS GIS and GDAL, and the usable areas and estimated production values are joined back to the building roof vector file via Zonal Statistics.

Energy estimates are calculated as per a global approximation formula: $\mathbf{E} = \mathbf{A} * \mathbf{r} * \mathbf{H} * \mathbf{PR}$,

Where \mathbf{E} =Energy (kWh)

\mathbf{A} =Total solar panel Area (m²)

\mathbf{r} =solar panel yield or efficiency (%)

\mathbf{H} =Annual average solar radiation on tilted panels (shadings not included)

\mathbf{PR} = Performance ratio, coefficient for losses (ranges between 0.5 and 0.9, default value 0.75)

- Here, A is calculated in Field calculator as $\text{Area} = \text{count of pixel} * 0.5 * 0.5$ (as the cell size is 0.5m)
- H is the average annual solar irradiation obtained from SEBE - taken here as the median kWh/m² received by the roof.
- PR is assumed at default value 0.75 r is assumed at 14%

PR is the solar module efficiency. This is assumed at 14% because PVGIS uses 14% for Crystalline Silicone modules. The process is simplified and explained in Figure 10.

The output map of pixel-wise average solar irradiation can be validated against the PVGIS dataset which uses insolation maps (EU-JRC, n.d.).

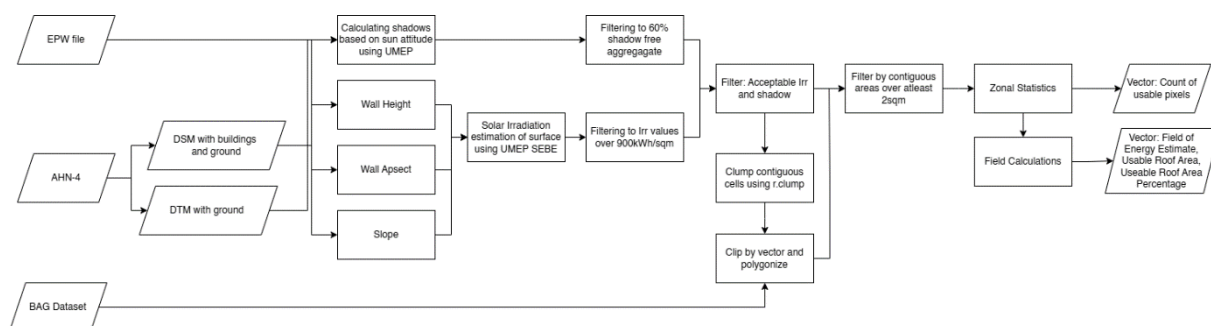


Figure 10 - Simplified open-source methodology for determining approximate solar potential per rooftop.

4.2.2.3. Analysing thermal comfort using morphological parameters – SOLWEIG, UROCK and PET

In addition to the analysis of solar potential, the research estimates outdoor human thermal comfort using the Physiological Equivalent Temperature (PET) indicator, but only retaining the built morphology as the input. This is done, as in this research, the contribution of vegetation, water bodies and major surface material variations are not accounted for, which is proven in literature to strongly affect the thermal comfort.

Thus, the analysis estimates an approximation of PET using only information of building form derived from DEM and DSM, and weather information of the location, and should not be treated as an estimation of the real temperatures that are expected to be experienced in a real, complex environment with different building materials, plantations and water bodies that effectively lower the experienced thermal comfort. The variables thus used in the calculation is as per Figure 11.

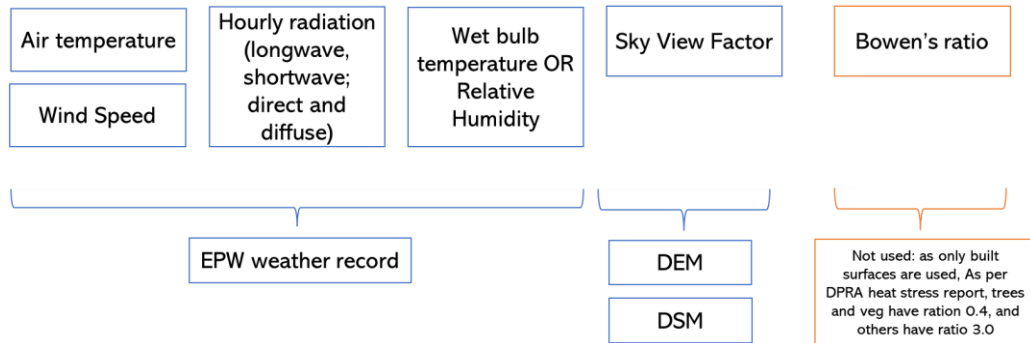


Figure 11 - Variables used to estimate PET. Bowen’s ratio is not included.

Outdoor human thermal comfort is dependent on radiation (Gál & Kántor, 2020). To analyse thermal comfort, two major sub-indicators are calculated using UMEP Processors (Lindberg et al., 2018)– Thermal Mean Radiant temperature (Tmrt) using SOLWEIG (The solar and longwave environmental irradiance geometry model) (Kong et al., 2022; Lindberg et al., 2008), and wind modelling using URock2023a (Johansson et al., 2016). Tmrt or Mean Radiant Temperature is a variable in the SOLWEIG model in UMEP to estimate “*spatial variations of 3D radiation fluxes*” in urban scenarios. It can give an understanding of thermal comfort by simulating the absorption and emissions of radiation of different materials and surfaces in given urban scenarios.

Tmrt using the SOLWEIG model considers radiation fluxes from six directions using Höppe’s (1992) method. While the full model of SOLWEIG has the capability to incorporate vegetation as well as ground cover data along with built form, it is used in this research to only estimate spatial variations of 3D fluxes using the urban built form. Figure 12 lists the variables used to estimate Tmrt.

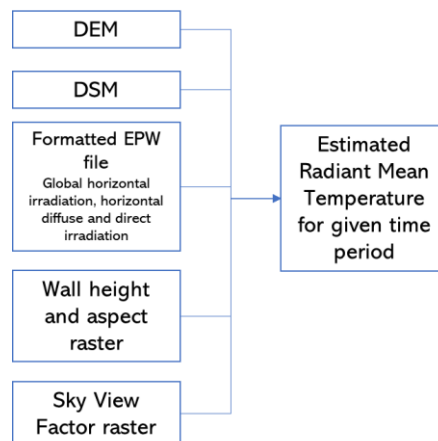


Figure 12 - Variables used to estimate Tmrt.

URock estimates wind fields using a ‘semi-empirical wind model’ adapted from Röckle (1990) (Bernard et al., 2023). Using the value of wind velocity recorded at 10m height in the EPW file for June 22, 2017, the wind flow rasters are calculated. The URock model estimates the wind flow velocity at human height based on the WSD10m parameter (Bernard et al., 2023). The outputs of these sub-indicators are fed into a Spatial Thermal Calculator Model which estimates the Physiological Equivalent Temperature based on the TMRT and the wind flow raster.

Thus, as discussed, modifying the input into the accepted formula for PET (Koopmans et al., 2020), air temperature, solar irradiation, solar elevation (through latitude/longitude information), relative humidity

and sky view factor are used within the SOLWEIG model while wind speed is modelled using URock2023a. Only the effect of surface perviousness and vegetation calculated through Bowen’s ratio is omitted from the study, modifying the formula. Thus, the result is the effect of simply the contribution of the built form and weather to estimating human thermal comfort. The methods are explained in Figure 13.

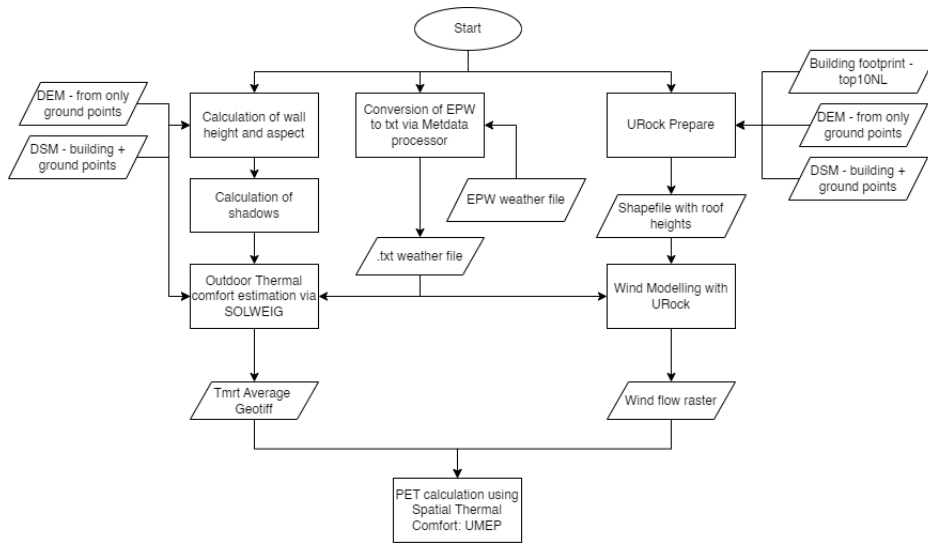


Figure 13 - Simplified open-source methodology for approximating thermal comfort.

These two sub-processes set the base conditions of environmental performance of the existing urban form, which will then be compared with the results obtained from the modified urban forms created in Phase 3.

4.2.3. Phase 3 – Modifying the Urban Form

Phase 3 is centred around designing a workflow that allows users to modify the built form in 3D and feed it back into the analysis phase for re-evaluation of environmental performance. As input to the model, the existing 3D environment will be created using the 3DBAG in Blender. The 3DBAG model can be imported into Blender as both an .obj file as well as a CityJSON file using the ‘Up3date’ Blender plugin (Mastorakis, 2020). Using edits in Blender, the 3D model can be modified as required – introducing or eliminating built forms, changing heights, widths etc. This can then be exported via Cloud Compare, converting from .obj to .pcd to DEM. This process uses open-source software and allows the user to customize built form as needed. For testing the workflow, different configurations are tested such as introducing one tall building and a cluster of tall buildings.

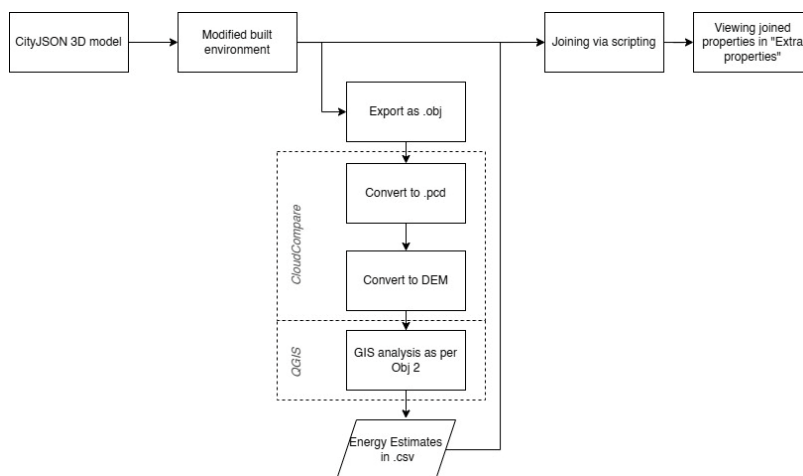


Figure 14 - Methodology used for modifying built form in 3D and related data processing.

The second part of this phase focuses on running the same analysis as Phase 2 on the new DSMs, and analysing the difference in results, if any, attributed to introducing modified morphology, as all other variables are kept constant. The data of the usable roof area and the suitable pixels thus found via GIS analysis are joined to the 3D model using python Blender scripting, and then model is saved in the glTF 2.0 format, which can be read by Cesium (Figure 14).

4.2.4. Phase 4 – Quantification of Improvement and Interface Design

Phase 4 focuses on visualizing the results of the analyses in a 3D environment. For visualizing the analysis using a 3D environment, Cesium JS library, along with Cesium Ion and Cesium Stories are used. Cesium is popularly used in game interface development and supports geographical information. Web-based models created via Cesium Ion/Stores can be easily shared and are easy to interact with.

Phase 4 will conclude by comparing the results with the conclusions of the literature review and giving form-based recommendations for the selected neighbourhood.

4.3. Operationalisation of sub-objectives – Research Matrix

Table 6 summarise the sub-objectives, research questions, the data used in answering each sub-question and the expected output of each step.

Table 6 - Proposed Research Matrix of the project

Obj1 - To review existing body of literature on the effect of built form on neighborhood environmental performance, and relevant policies guiding urban development in the context of the study area, with a focus on transition to solar energy and improving thermal comfort.			
<i>Research Questions</i>	<i>Methodology</i>	<i>Data</i>	<i>Expected output</i>
RQ1.1 – What is the current state-of-the-art in analyzing environmental performance at neighbourhood-scale using morphological indicators?	Literature Review	Scientific papers and publications	Understanding of the morphological parameters and indicators, specially building height and volume, and the effect of changing building typology on solar potential and thermal comfort of neighbours.
RQ1.2 – What are the goals of the local municipality regarding increasing energy transition and improving thermal comfort, and how can that be utilized for designing the PSS?	Literature Review	Government documents and Vision Plans	Clarity on goals and visions of the government regarding increasing energy transition and decreasing UHI effect.
Obj2 – To investigate and apply appropriate GIS-based methodologies for evaluating Solar Energy Potential of rooftops and Thermal Comfort (via Physiological Equivalent Temperature estimate) of the existing built form in a selected neighbourhood in Enschede.			
<i>Research Questions</i>	<i>Methodology</i>	<i>Data</i>	<i>Expected output</i>
RQ2.1 - What is the Solar Energy Potential of the rooftops in the existing state of the selected neighbourhood?	GIS-based methods using open-source plugins	PDOK, BAG shapefile), AHN/DSM, EPW 15-year weather data	Map output showing potential solar energy harvest per rooftop in the selected neighbourhood on selected dates.
RQ2.2 - What is the state of Thermal Comfort in the existing state of the selected neighbourhood?	GIS-based methods using open-source plugins	As RQ 2.1	Map output showing estimated Physiological Equivalent Temperature in the selected neighbourhood on a particular date.

RQ2.3 - What openly available data on solar potential and thermal comfort can be compared with the results from the workflows used in RQ2.1?	Comparison of raster of predicted maps and validation data	Hittekaart – Klimateffect atlas, PVGIS portal for solar illumination	Comparison of analysis done in RQ2.1 and RQ2.2 with global and national datasets.
Obj3 - To develop a workflow using 3D geoinformation to model new urban landscapes for scenario analysis, which can work seamlessly with the analysis in Objective2, and simulate the environmental performance of the scenario models.			
<i>Research Questions</i>	<i>Methodology</i>	<i>Data</i>	<i>Expected output</i>
RQ3.1 - How can 3D geoinformation be visualized and modified by user in an open-source software?	Visualized and edited in Blender	3DBAG (made using AHN) .obj and CityJSON	Using this workflow, different built scenarios will be created such as introducing one single tall building and a cluster of tall buildings.
RQ3.2 - What is the observed change in the balance of environmental performance when the pattern of urban form is modified?	As per RQ 2.1 and RQ 2.2	As per RQ 2.1 and RQ 2.2, DSMs from RQ 3.2	Comparing the results obtained in Obj2 and Obj3.
Obj4 - To visualise the results of the simulations in a 3D environment and compare results with literature review.			
<i>Research Questions</i>	<i>Methodology</i>	<i>Data</i>	<i>Expected output</i>
RQ4.1 - How can the results of the scenarios be visualized 3D model-based environment?	Viz on Cesium (Ion/JS library)	From Obj2 and Obj3	Shareable web models of scenarios which can be turned, zoomed etc.
RQ4.2 – How do the results compare to the conclusions of the literature review? What further recommendations can be made for form-based planning in the selected neighbourhood?	Literature review	From Obj 1,2,3	Conclusions from the research and further recommendations.

4.4. Ethical considerations, risks and contingencies

The project proposes to use freely available data sourced from national and international datasets to develop this decision support workflow. It does not make use of any personal data or involves citizen data collection. The datasets used will be referenced to their data owner.

The results of the project are meant to be used by the municipalities to guide their decisions regarding built form and are not designed to inform individual homeowners about the potentials of their property.

4.5. Summary

To create a workflow that can analyse environmental performance, the acquired 3D data is processed and converted to 2D. The majority of the analysis are done in 2D using height values obtained from the 3D. Finally, the results are joined back to the 3D so that the final results can be viewed using a 3D model. The components of the workflow are summarised in Figure 15.

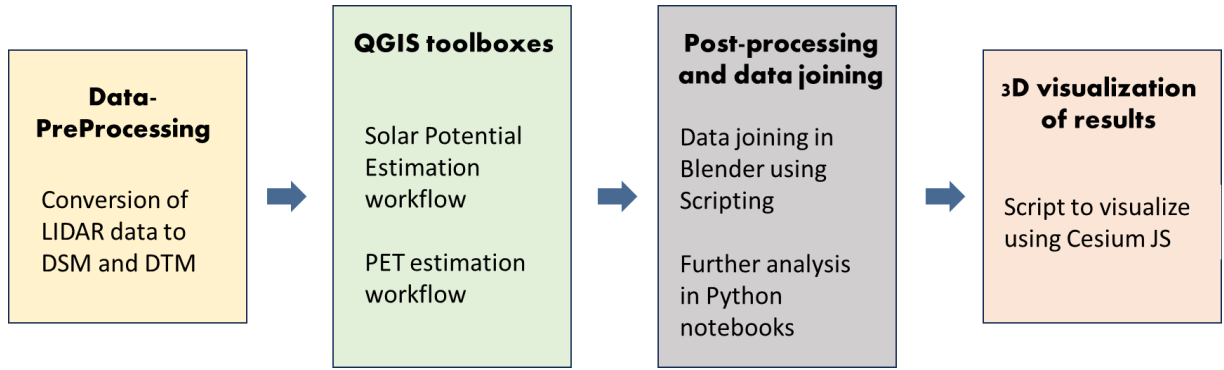


Figure 15 - Summary of the sub-workflows in the proposed PSS

Using code scripting in Python/JS as required and employing robust and well-supported plug-ins as needed, the workflow simplifies using 3D data to visualise results in 3D.

5. RESULTS

5.1. Visualising the site in 3D

As discussed in the previous chapter, for the Netherlands, the AHN-4 data is freely available, and is used to make the 3DBAG dataset, which models the buildings at LOD 2.5 with detailed roof forms (Dataset: Actueel Hoogtebestand Nederland 4 (AHN) & PDOK, 2023). Using the CityJSON file of the 3DBAG model available online, the site is visualised in Blender. Using Up3Date plugin (Mastorakis, 2020) in Blender, this workflow processes the CityJSON file of the 3DBAG in Blender and converts it to a .obj format.

Three built form scenarios are analysed using the designed workflow (Figure 16):

- Case A: Original built form
- Case B: Addition of one tall building. In this, a 30m tall building (10 storeys) is introduced which is aligned N-S. This is done to see the difference of taller buildings and the effect of its subsequent shading on environmental performance.
- Case C: Addition of 3 tall buildings. This case, two more tall buildings (12 storeys) are introduced in close proximity to the building introduced in Case B. One of these is also aligned N-S, while the other is aligned E-W. The different in alignment is also made to see the effect of building orientation on environmental performance.

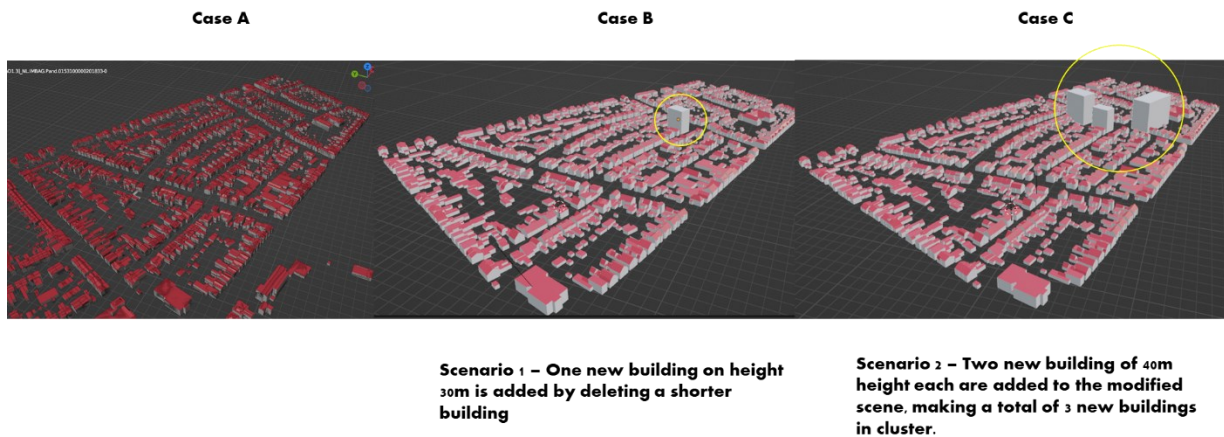


Figure 16 - 3D built-form scenarios.

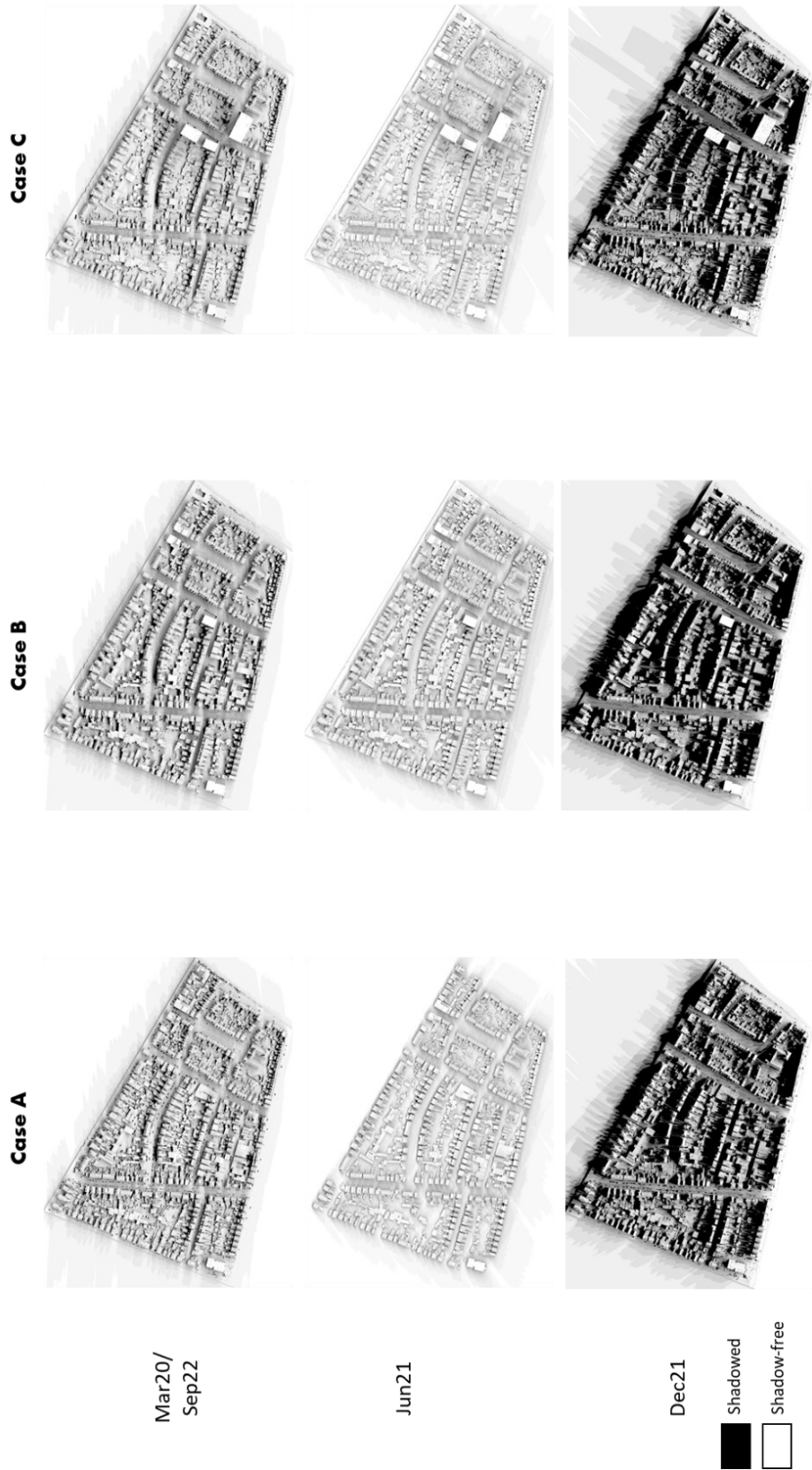
5.2. Analysing environmental performance of original and modified scenarios

5.2.1. Estimating Solar Potential per rooftop

Following the given methodology, solar energy potential per rooftop was estimated. To get meaningful results from the workflow for further analysis, the entire workflow was calculated on 3 days in the year – on the two equinoxes (Mar 20, Sep 22) – which should show almost equal shadow patterns, on the summer solstice (Jun21) and on the winter solstice (Dec 21).

5.2.1.1. Shadow Patterns

Shadow plays an important role in modifying the expected conversion of solar power to electricity. The shadow patterns estimated on the selected three days are shown in Map 2. Here, shadow-free pixels are seen in white, while pixels under partial or complete shadow are seen in black.

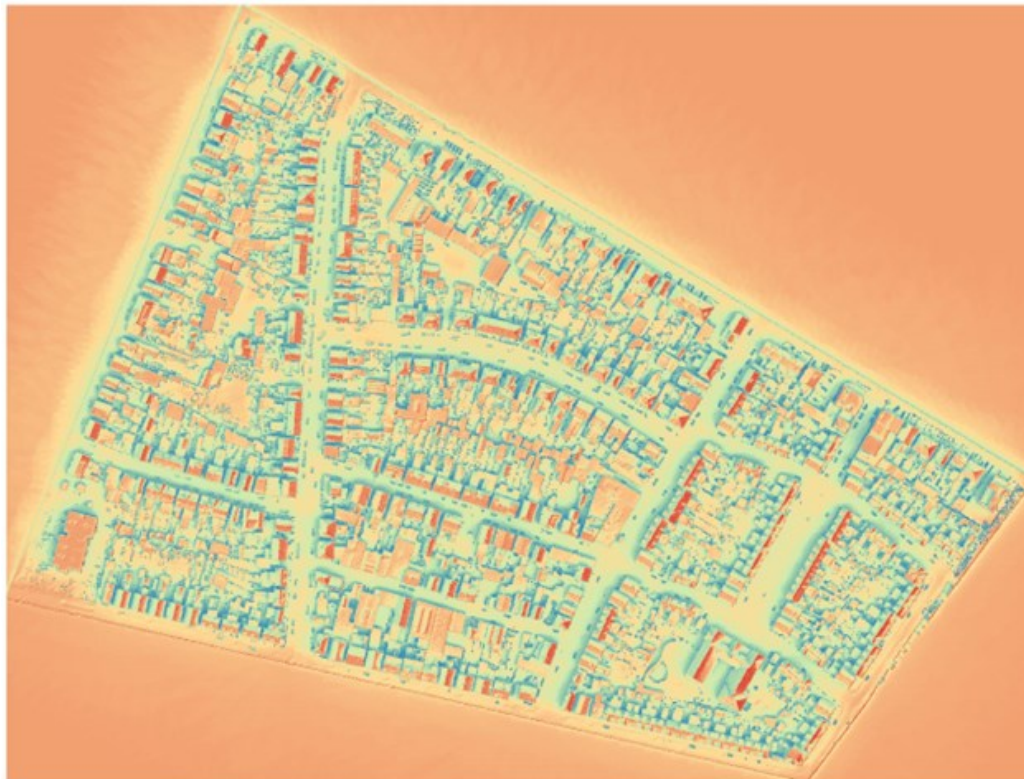


Map 2 - Shadow Pattern of the built-form scenarios, on 3 selected dates of the Equinox and Summer and Winter Solstice

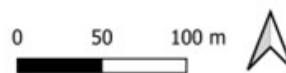
5.2.1.2. Estimation of solar irradiance

Using the input of the aggregated shadow raster files calculated per hour for Mar 20th, June 21st, Sep20nd and Dec 21st, as well as the annual solar irradiance data estimated from the TMY5.2 weather file, average annual solar irradiation in kWh/m² was estimated per pixel for each of the built-form scenarios, as seen in Map 3, Map 4 and Map 5, using SEBE in UMEP.

Case A

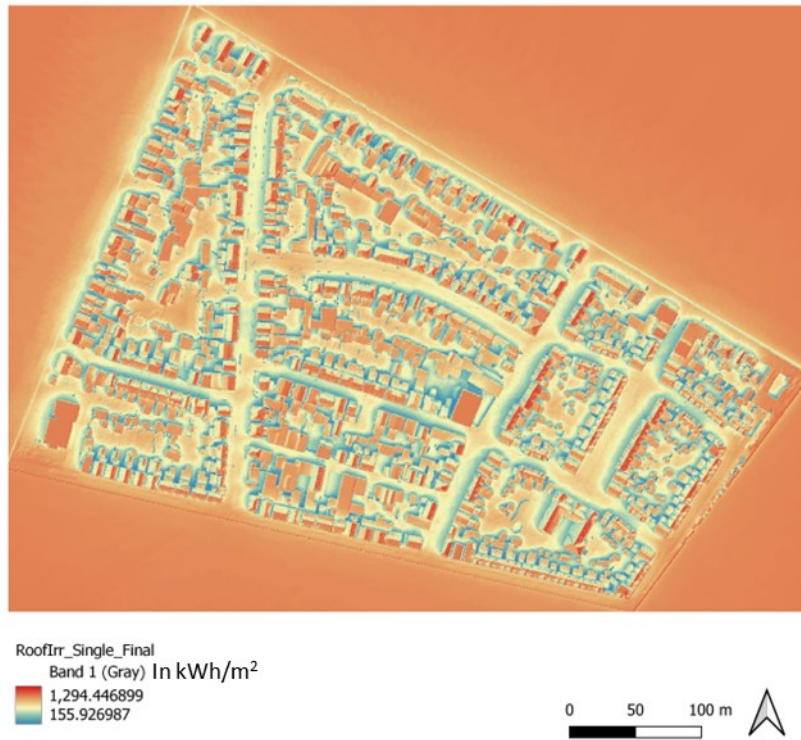


ROOFIRR_Original
Band 1 (Gray) In kWh/m²
1,285.51062
155.926987



Map 3 - Estimation of Annualised Solar Irradiation values of the original scenario – in kWh/m²

When comparing the Irradiation maps of Case B (Map 4) and Case C (Map 5) to the original Case A, it is immediately visible that there is a loss of irradiation recorded in the pixels North-West of the introduced tall buildings. This can be attributed to the new shadowing pattern introduced due to the modified built forms.



Map 4 - Estimation of Annualised Solar Irradiation values of the Modified scenario with a Single tall building – in kWh/m²



Map 5 - Estimation of Annualised Solar Irradiation values of the modified scenario with a cluster of Multiple Tall buildings – in kWh/m²

5.2.1.3. Comparing solar Irradiation values with PVGIS

Comparing the ranges of solar irradiation estimated by the SEBE model (approximate maximum of 1290 kWh/m²) and the PVGIS yearly in-plane radiation of the best-case scenario (1308 kWh/m²) (Figure 17) shows that the SEBE model is quite reasonable in its estimation. Thus, the values are acceptable and taken ahead in the workflow.

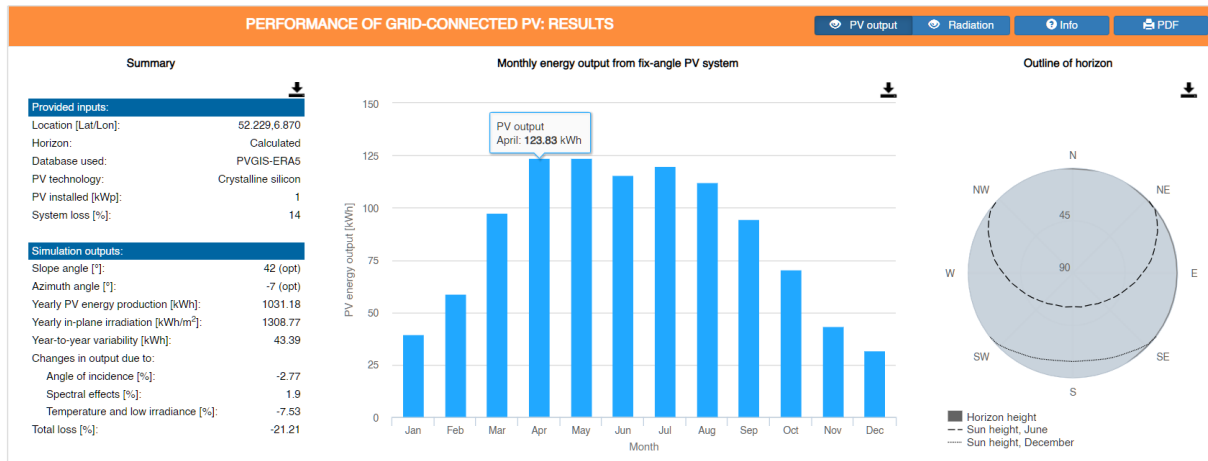
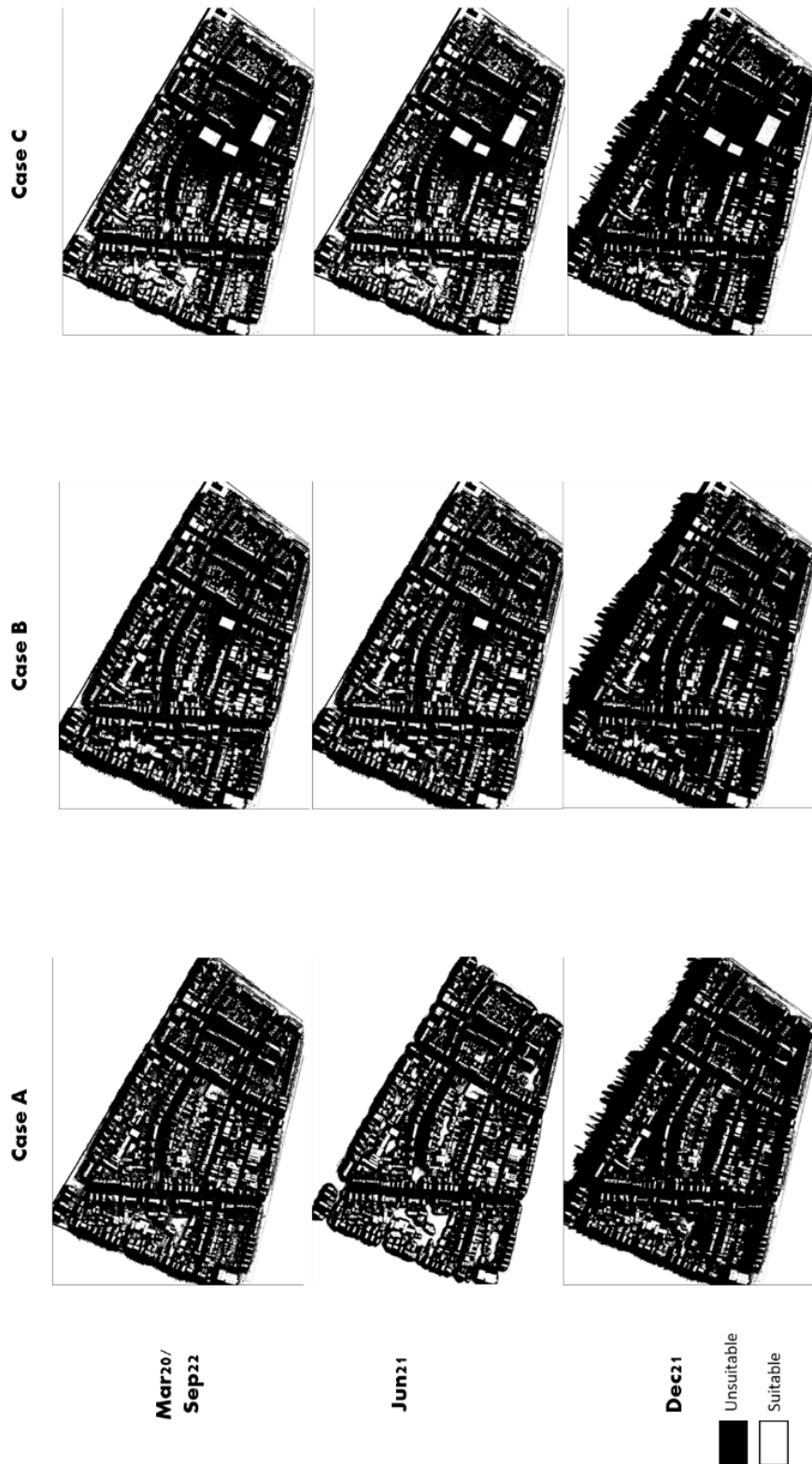


Figure 17 - An extract from PVGIS showing the best-case solar irradiance estimate for the given study area. Source:(EU-JRC, n.d.)

5.2.1.4. Suitable pixel identification

Using a combination of raster processes as discussed in the methodology, suitable pixels are identified. They are selected on the basis of being free of shadows for at least 60% of the day, receiving over 900kWh/m² and in contiguous clusters over 2sqm (as one single solar panel is 1.6 sqm) are identified per rooftop. The restrictions used here to decide on suitability are strict and are used in a way to compensate for the expected variations in irradiation estimation made by UMEP-solar modelling. The results of this suitability analysis seen in Map 6. As the cells marked black are unsuitable, it is seen that the number of black cells in the

immediate vicinity of the introduced buildings in Case B and C record an increase as they are now deemed unsuitable.



Map 6 - Shadow x Irradiance X contiguous cells - Suitable cell identification.

5.2.1.5. Estimation of Solar Energy

Using the output of the suitability analysis in raster format, the values are transferred to the rooftop vector shapefiles using Zonal Statistics, as seen in Map 7. This suitability analysis is repeated for all 3 built scenarios, in all 3 selected dates to get a more holistic idea of the annual production potential. This suitability analysis is modifiable by users to determine their own cutoff irradiance levels, acceptable shadowing, and contiguous usable areas. Thus, the accepted levels can be much lower than what is used in these particular analyses, allowing the workflow to be modified to be used in different geographic and economic conditions.

The entire workflow is made concise and replicable using Graphic Modeller and allows for variation in input data and assumptions. The graphical representation of the process is explained in Figure 18, which reduces the long, tedious 15-step process to one-step. The suitability analysis is modifiable by users so as to determine their own cutoff irradiance levels, acceptable shadowing, and contiguous usable areas.

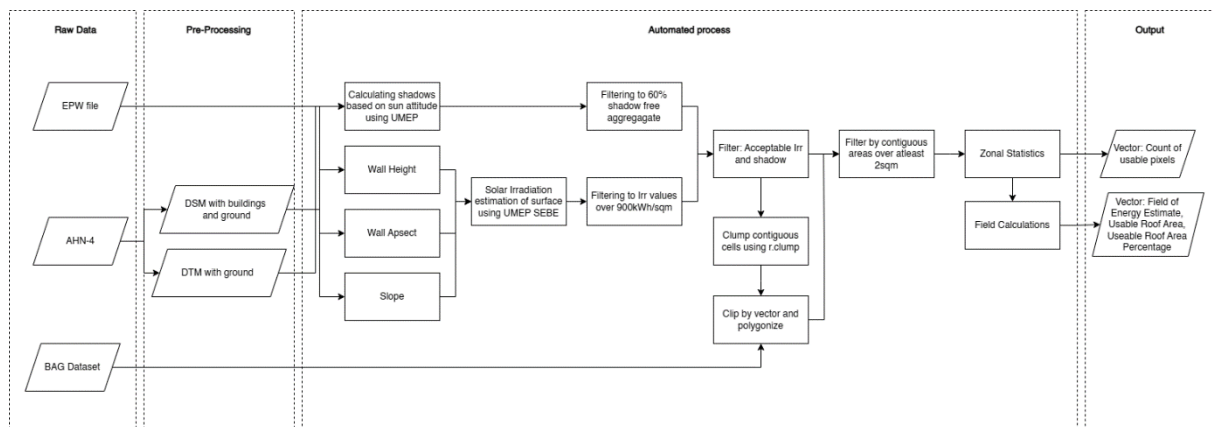


Figure 18 - Simplified workflow of the automation as a part of the whole process.

Using the derived suitability and irradiation per pixel, calculations of the predicted Energy Estimate and Usable roof area are done using field calculators. Maps in Map 7 and Map 8 show the variations due to different built forms and also the variations in different seasons.

It is also understood that the Energy estimate derived using the shadow patterns of March/September provide a more realistic annual number as compared to the extremes of summer and winter months.

Figure 19 displays the final interface made using Graphic Modeller. Thus, the proposed workflow can be used to quickly estimate an approximate energy yield and rooftop utilization percentage in assisting to visualize the differences caused due to different built form scenarios.

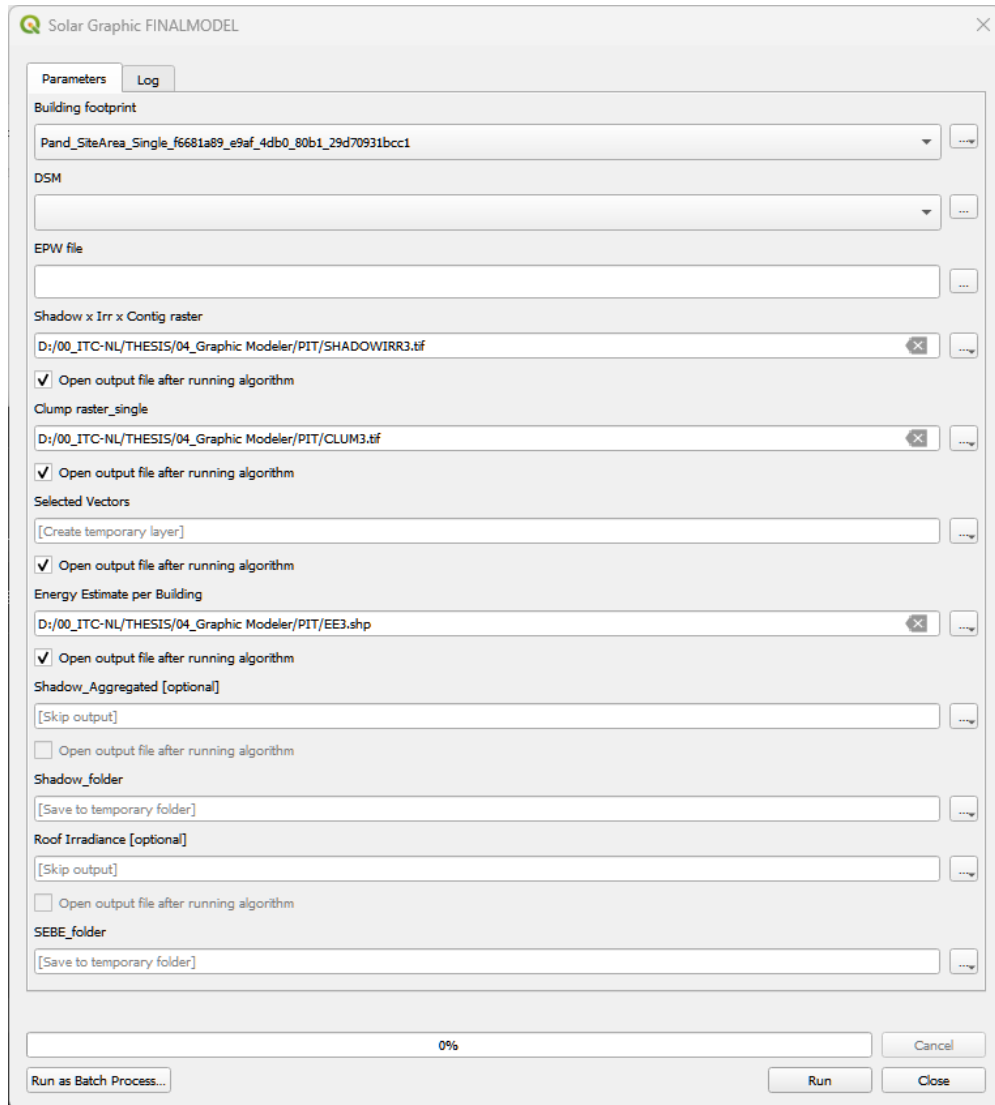
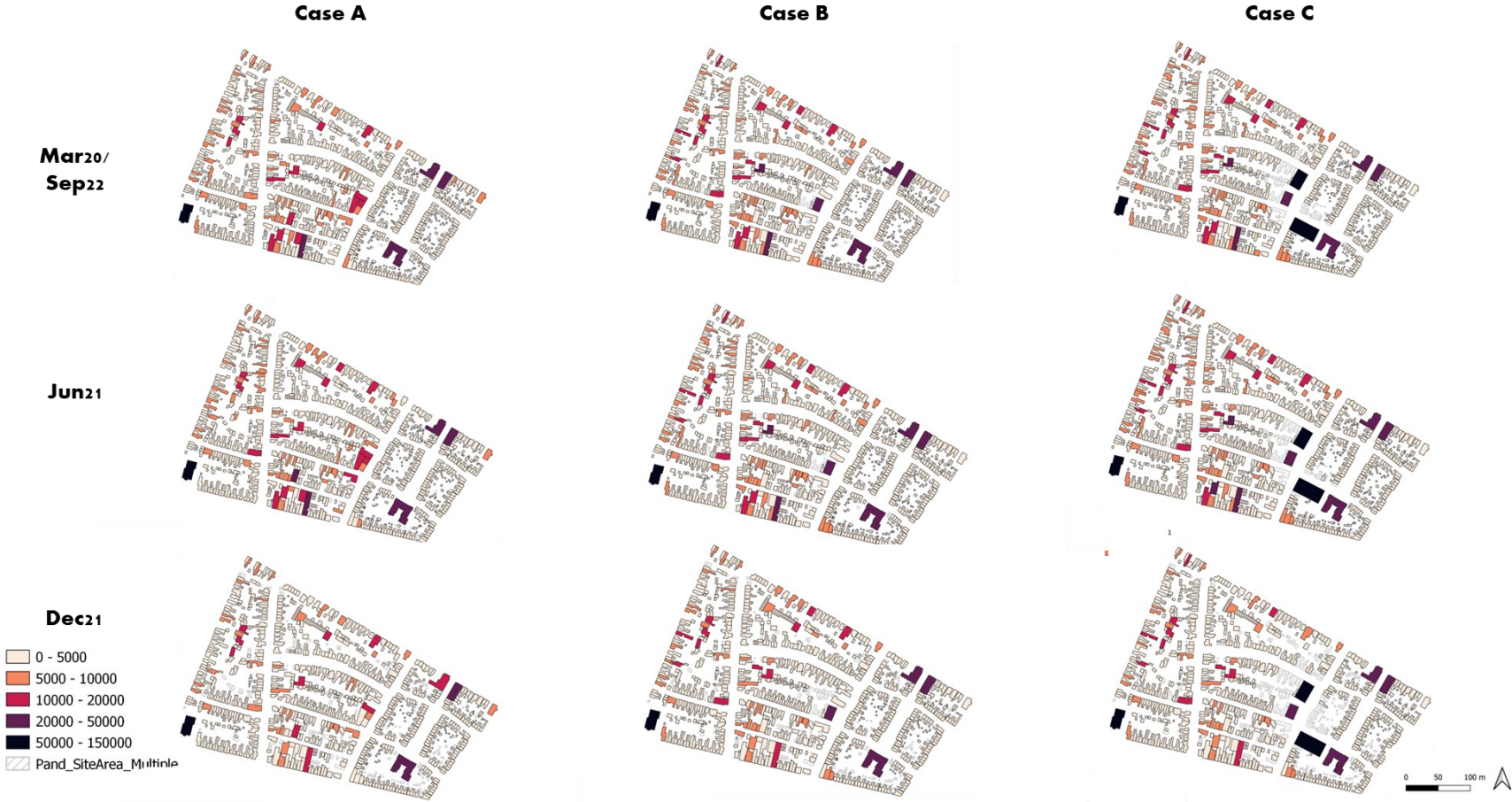
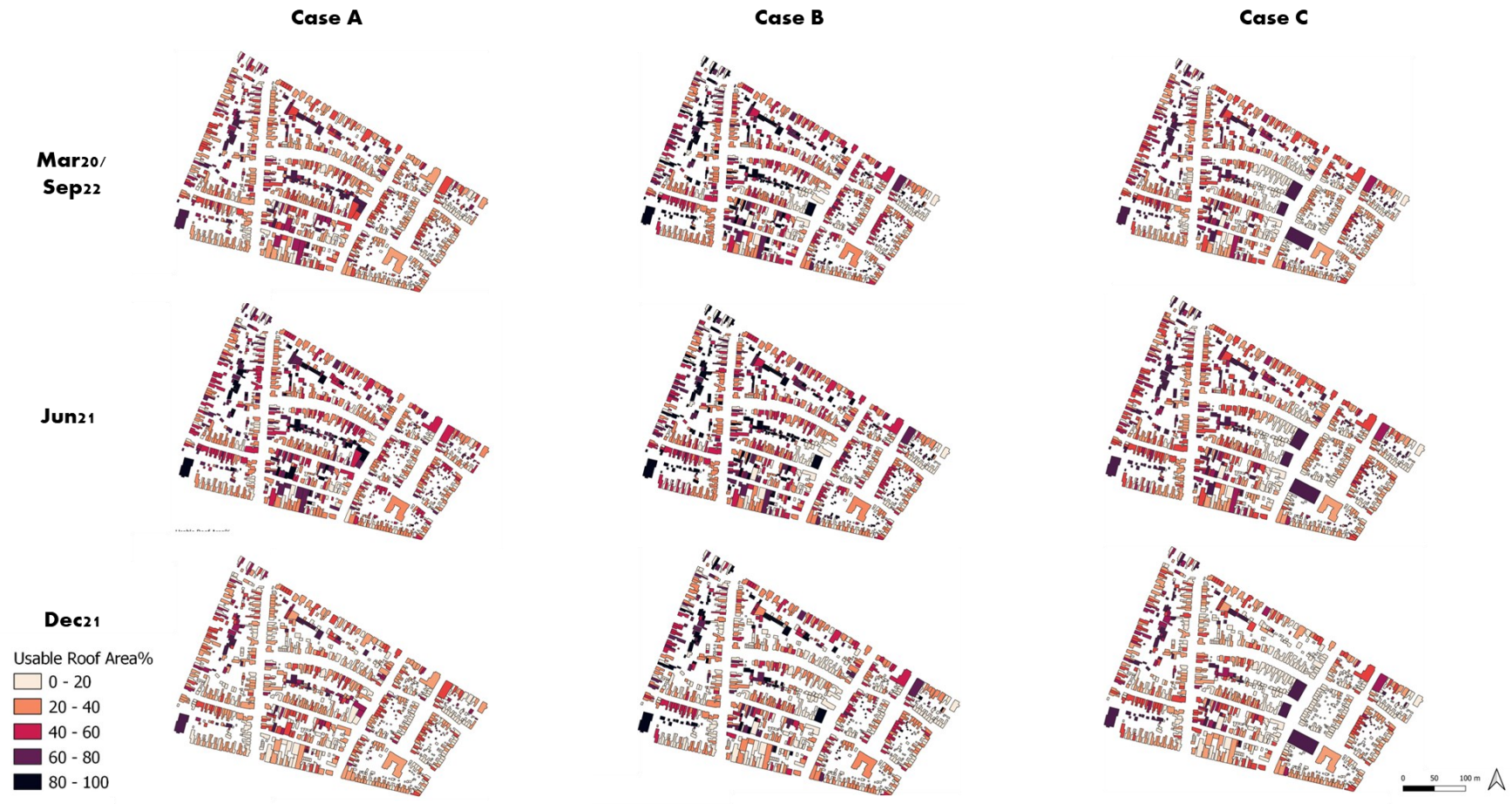


Figure 19 - Interface of the Solar Potential analysis Model



Map 7 - Energy production potential estimates made from suitable cells – in kWh per annum per rooftop



Map 8 - Usable roof area in percentage in each built case and season

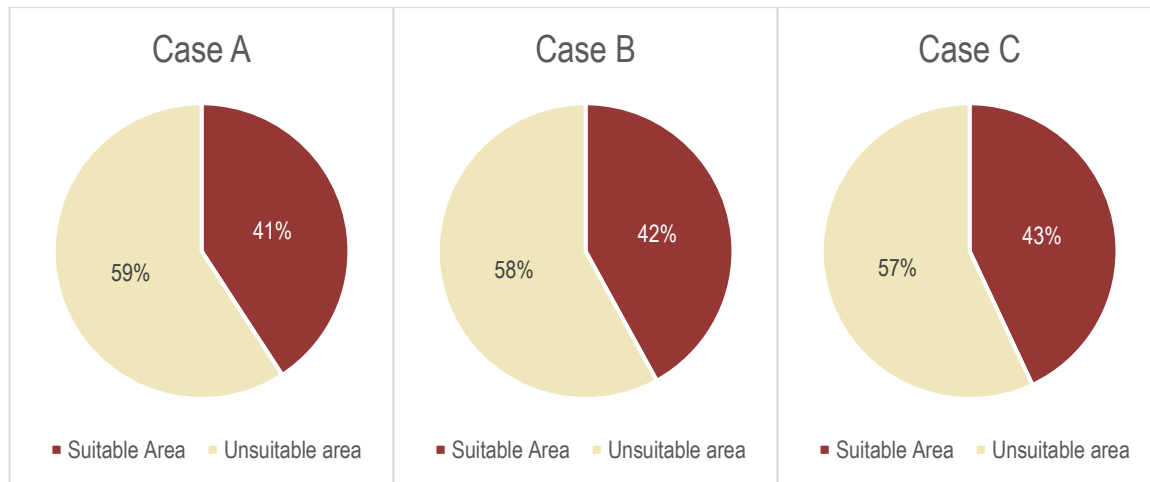


Figure 20 - Suitable v/s unsuitable roof area for harvesting solar energy in each of the built form cases.

As seen in Figure 20, there is a small increase in suitable rooftop percentage from Case A to case C. However, it is also be noted that the amount of rooftop area also increases as the newly introduced buildings have a much bigger roof surface than the previous buildings. Thus Table 7 summarises the change observed in numbers from Case A to Case C.

Table 7 - Summary of suitable pixels, average irradiation per suitable pixel and energy estimates in the three built form scenarios

	Case A	Case B	Case C
Total Area (sqm)	50,070.258	50,170.231	50,640.033
Suitable Area (sqm)	20,432.509	21,073.839	21,782.021
Unsuitable area (sqm)	29,637.749	29,096.392	28,858.012
Irradiance average value (kWh/m ²)	994.940	989.301	984.787
Count of suitable cells	81,730	84,295	87,128
Energy Estimate in kWh per annum	2,134,557.241	2,189,079.427	2,252,319.029
Predicted value in Euro (at 35 cents per kWh)	747,095.03	766,177.79	788,311.66

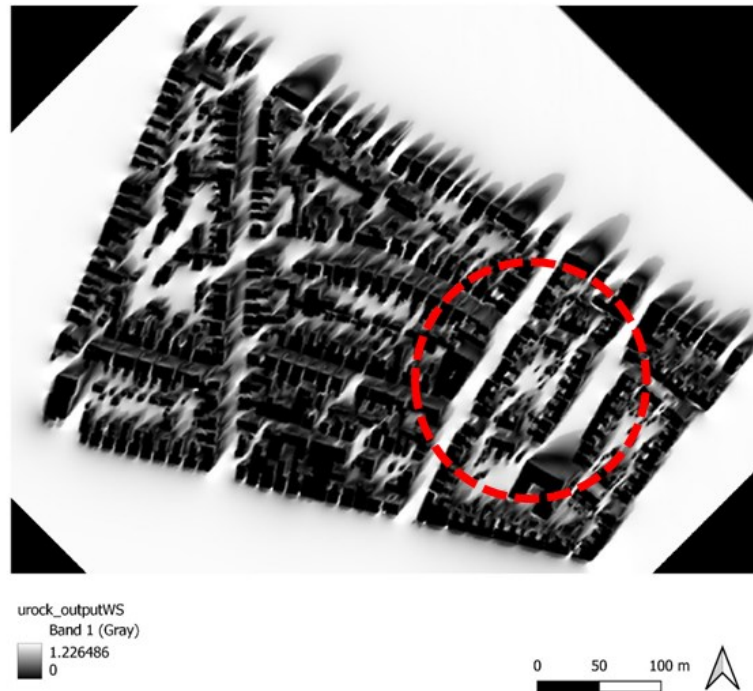
5.2.2. Thermal Comfort Estimation using PET.

For calculating PET, the date of June 22, 2017, at 1pm was selected as it was the hottest record in the summer months in the TMY5.2 dataset. Keeping in mind that it is a Typical Meteorological Year, the temperature of 33°C is not the most extreme, but is a temperature regularly seen in the study area in the summer months.

5.2.2.1. Estimating Wind flow

Using the methodology described above, PET was calculated in two steps. In the first stage, wind flow estimation is done using URock2023a. A wind direction of SW at 225 degrees was selected as it is the predominant wind direction for the study area.

As seen in Map 9, the wind flow speed is derived from the WD10 value in the TMY5.2 dataset, which records wind speed and direction at 10m height. URock2023a shows a derived output at 1.5m height, which can be considered for human thermal comfort.



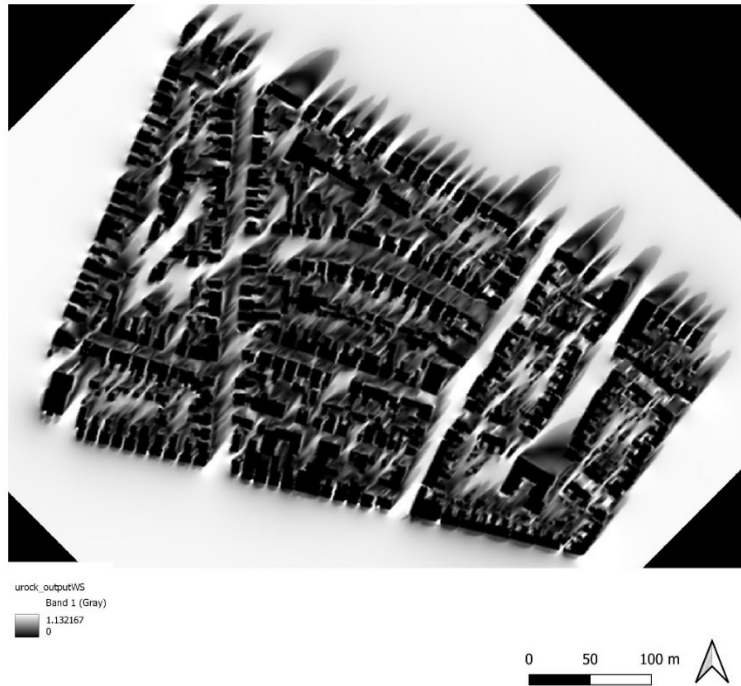
Map 9 - Wind flow speed in m/s calculated for Case A using the on-ground wind conditions in the EPW file for WS10m

Map 10 shows the direction of wind flow and the behaviour of the wind as it is restricted by the buildings. Seen here, the N-S alignment of the streets allows wind flow while the houses pose as barriers. Due to this the backyards record reduced wind velocity at human height.



Map 10 - Wind Flow intensities on ground for Case A.

Similarly, for Case B and C, wind flow velocities in meters per second are calculated (Map 11, Map 13)

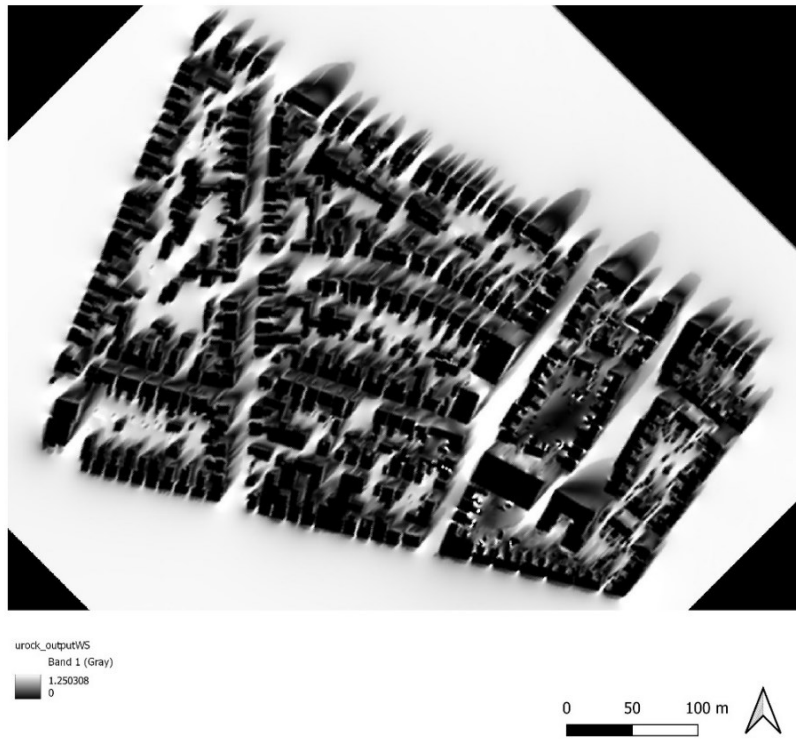


Map 11 - Wind flow speed in m/s calculated for Case B using the on-ground wind conditions in the EPW file for WS10m

The wind flow intensity for Case B (Map 12) shows a reduction in estimated speed of wind to the North-East of the newly introduced tall building, possibly indicating that the tall building is hindering wind flow.



Map 12 - Wind Flow intensities on ground for Case B. Wind pattern is seen to be changing around the introduced tall building.



Map 13 - Wind flow speeds in m/s calculated for Case C using the on-ground wind conditions in the EPW file for WS10m.

In case C, as three tall buildings are introduced in a cluster, the wind speed in the neighbourhood to the North-East of the cluster records a sharp drop in wind flow (Map 14).



Map 14 - Wind Flow intensities on ground for Case C. There is considerable change in wind pattern observed due to introducing the tall building aligned E-W, which blocks wind effectively.

5.2.2.2. Sky view Factor Estimation

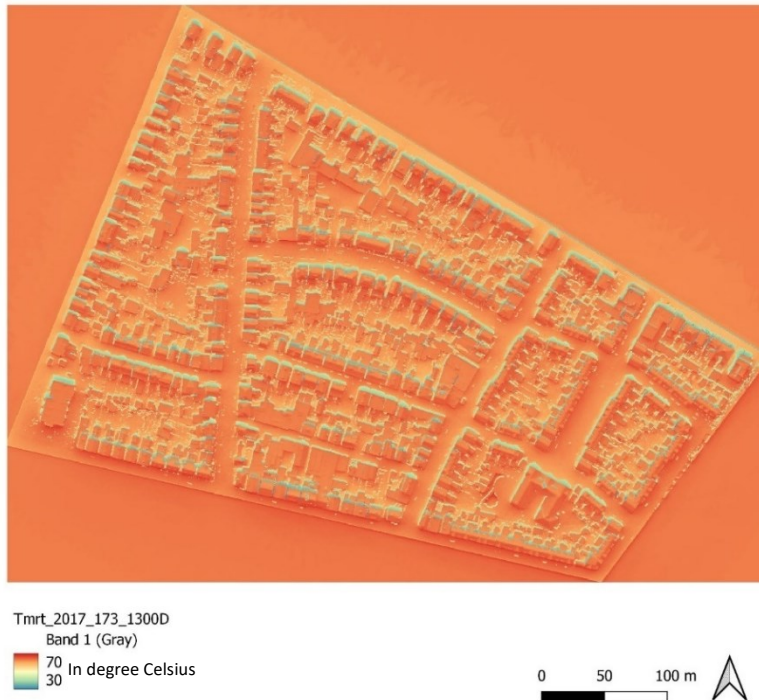
Sky View factor estimation using DEM is used as an input to estimate the TMRT. Sky view factor ranges between 0 to 1, where 0 is completely unobstructed, while 1 is totally obstructed from all sides. It can be seen that the areas in immediate vicinity of the introduced tall buildings show a lower Sky View factor estimation due to the presence of the tall facades (Map 15). (Here, black is 0 (obstructed) while white is 1 (unobstructed)).



Map 15 - Sky View factor estimations for all 3 built form scenarios.

5.2.2.3. Estimating Mean Radiant Temperature

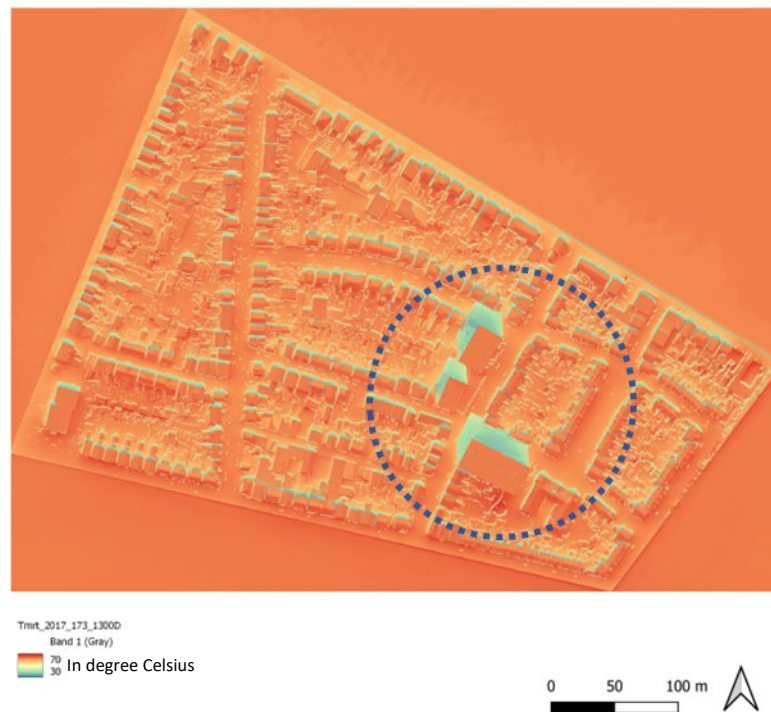
Following the methodology described in section 4.2.2.3, sky view factor per pixel is calculated in UMEP, as well as wall height and aspect rasters. All these inputs are then utilised to produce the Mean Radiant Temperature estimation for 1pm on June 22nd, 2017, which shows extremely high flux estimations. However, interestingly, in Case b (Map 17) and Case C (Map 18), there is a drop recorded in the Tmrt to the North-West of the buildings, possibly where urban shadowing is expected.



Map 16 - Tmrt - Mean radiant temperature estimate using SOLWEIG for Case A



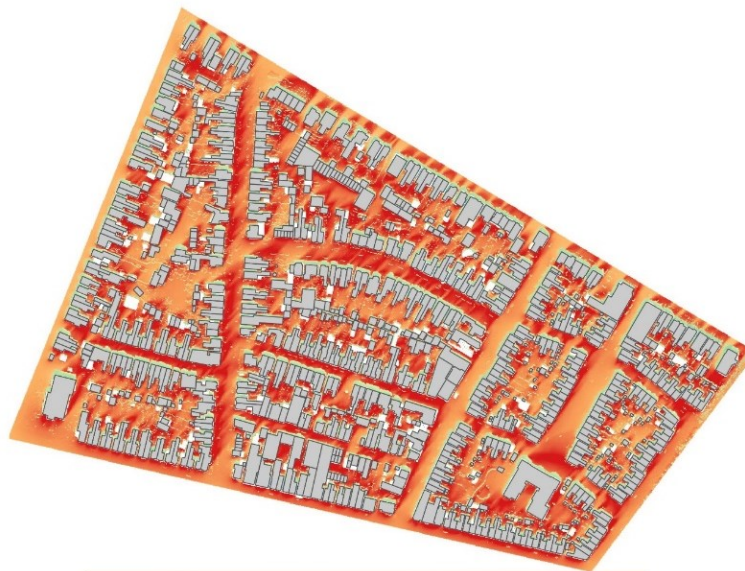
Map 17 - Tmrt - Mean radiant temperature estimate using SOLWEIG for Case B



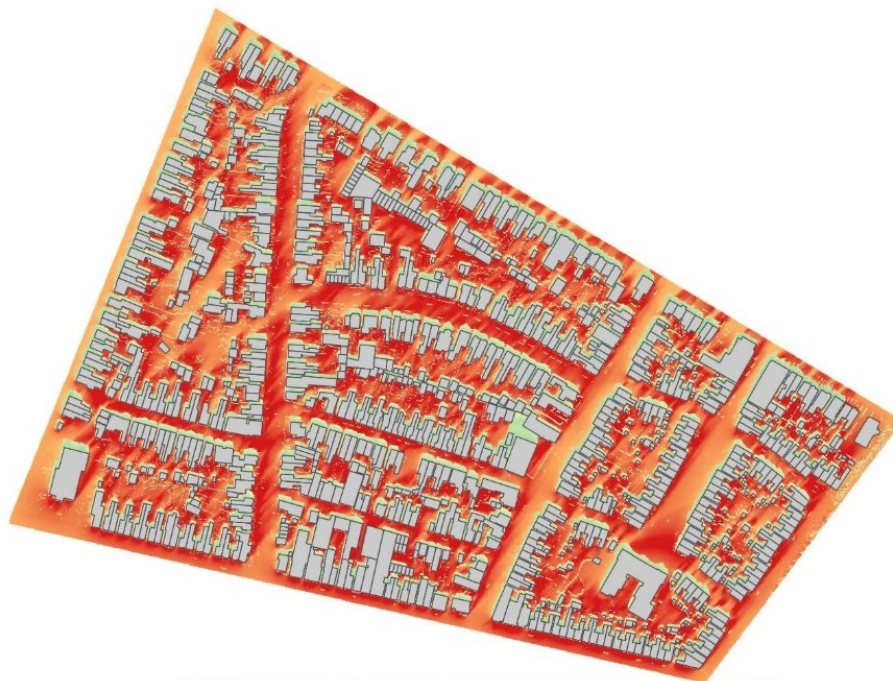
Map 18 - Tmrt - Mean radiant temperature estimate using SOLWEIG for Case C

5.2.3. Calculating PET

Using Tmrt in 5.2.2.3 and Wind Flow intensity estimation in 5.2.2.1, and also using standard assumptions as per the SOLWEIG model of thermal comfort, PET is estimated as seen in Map 19, Map 20 and Map 21.



Map 19 - PET estimate at 1pm, 22nd June 2017 – case A



Map 20 - PET estimate at 1pm, 22nd June 2017 – Case B



Map 21 - PET estimate at 1pm, 22nd June 2017 - Case C

The entire workflow and results can be summarised as in Figure 21.

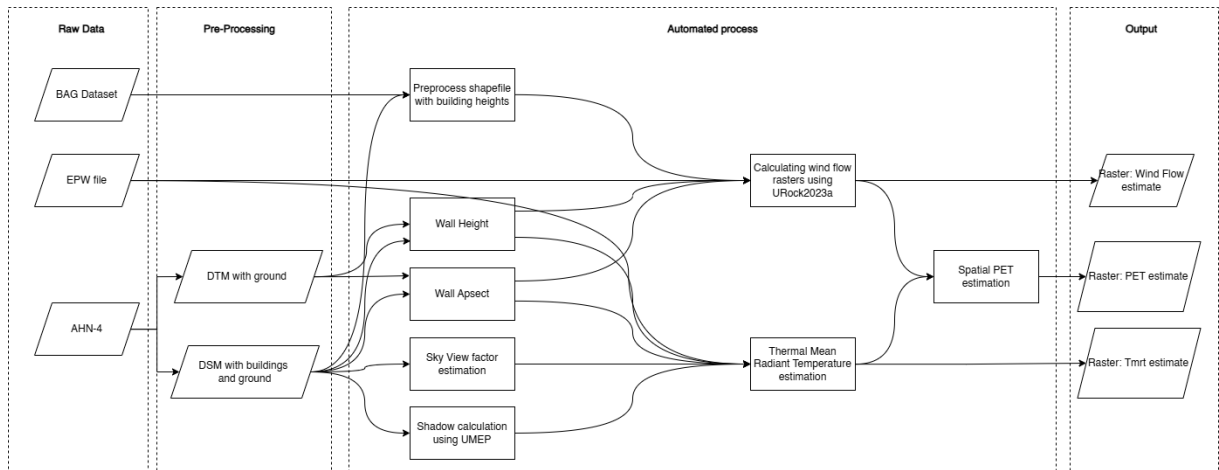


Figure 21 - Summarising the automated workflow for estimating PET using only built form variables.

The created interface using Graphic Modeller is as seen in Figure 22.

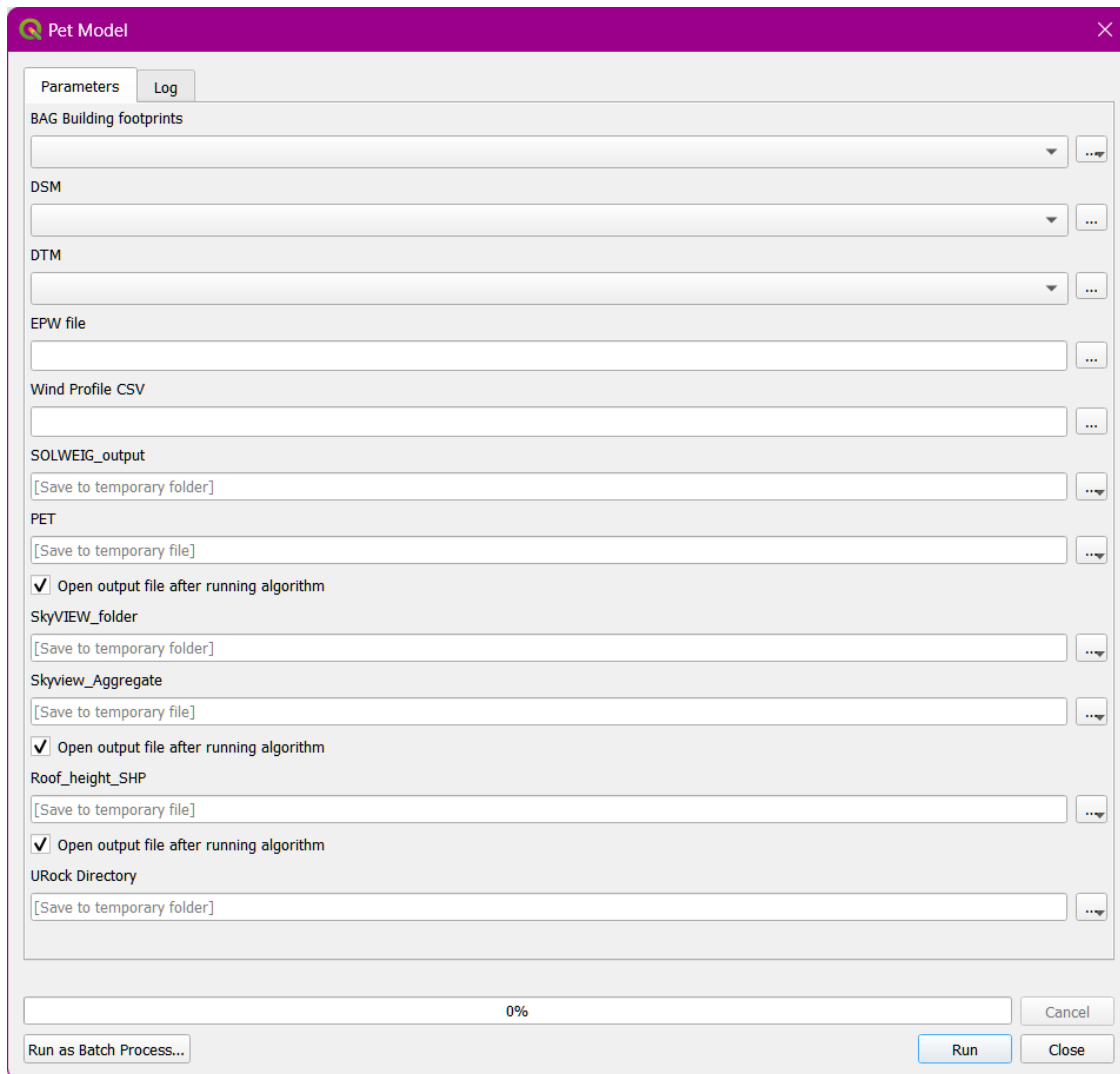


Figure 22 - Interface for data input for the calculation for PET

5.2.4. Comparing with the Klimateffectatlas

On comparing the results from the modified PET analysis in the previous section and comparing with the Risk map of UHI in the Klimateffectatlas (Figure 23) (Stichting Climate Adaptation Services, 2023), there is a difference seen as the risk of UHI computed by Klimateffectatlas takes into account the influence of the greenery and water bodies near the site. This stresses on the fact that the result maps obtained through the workflow only show the effect of the morphology and should not be considered as an estimate of the on-ground scenario with the influence of plants and water bodies.

klimateffect_UHI



Figure 23 - A map extract of the site area from Klimateffectatlas, showing the potential UHI effect.
Source:(Stichting Climate Adaptation Services, 2023)

5.3. Visualising results in 3D

The data from the solar analysis is joined to the 3D model in Blender by a custom script, as seen in Figure 24.

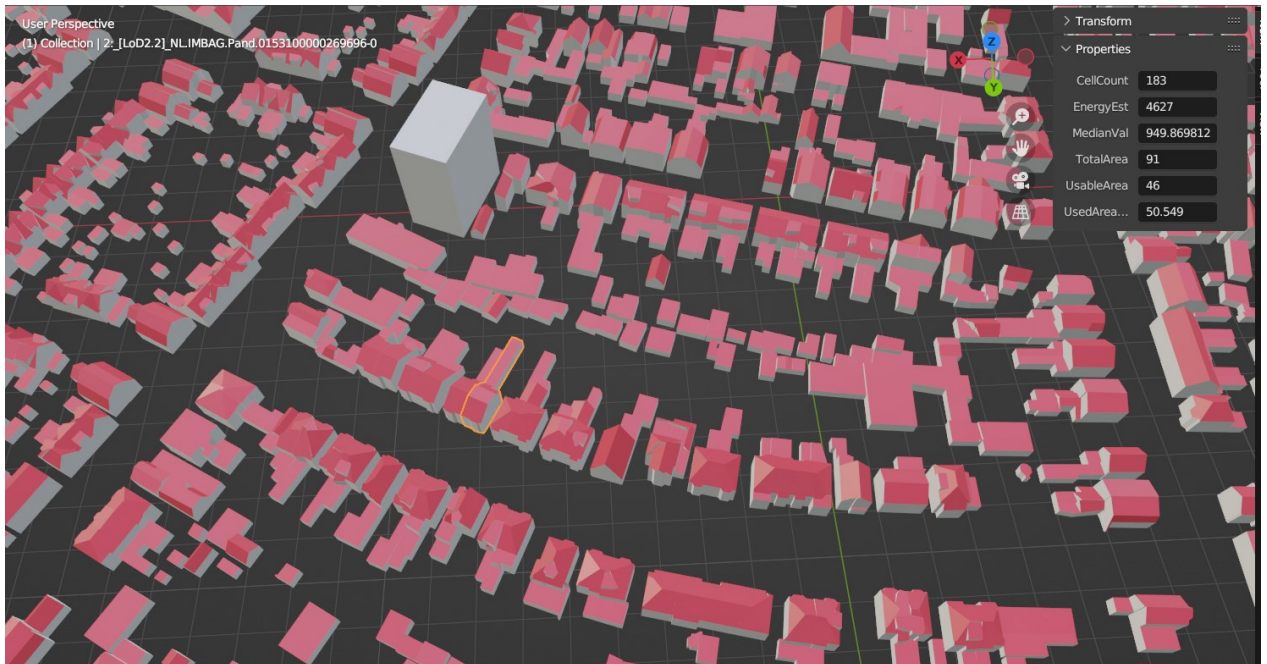


Figure 24 - data from the analysis is joined to the 3D model in Blender.

The 2D raster of PET is overlaid in Blender (Figure 25). This allows for querying the value of individual rooftops while also seeing the trend of the estimated outdoor temperatures at the same time.

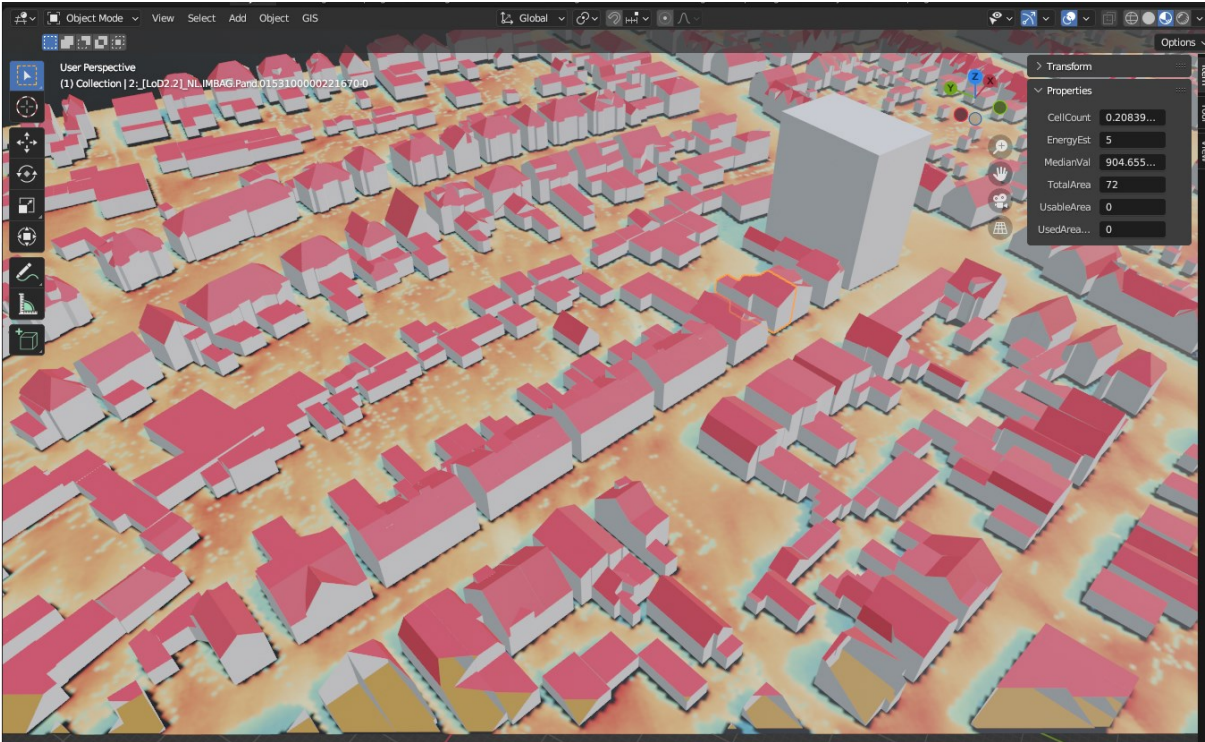


Figure 25 - Visualising on local system using Blender.

The attempt is made to view both the 2D and 3D in Cesium Viewer using Javascript code. This can be seen as under:

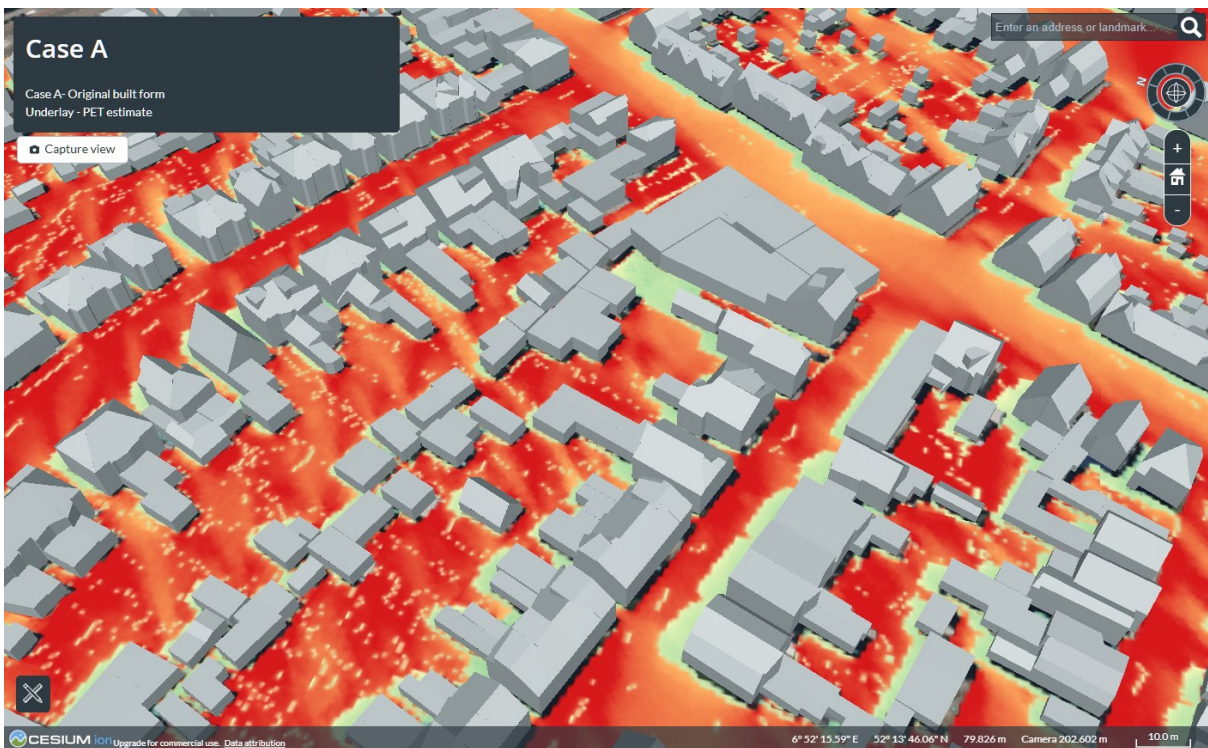


Figure 26 - Visualising the results on the analysis using Cesium – Case A

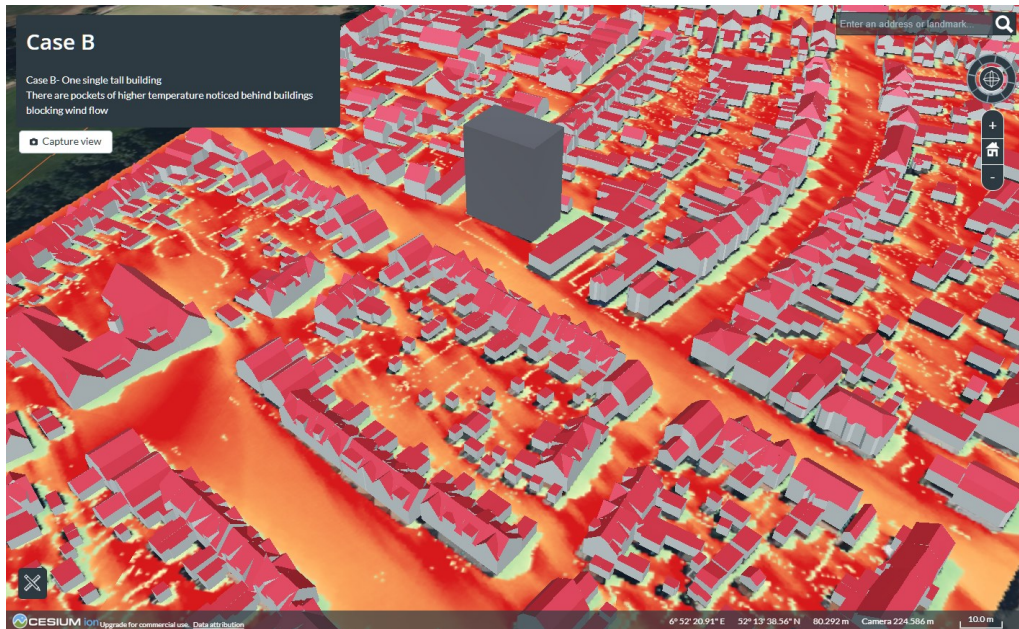


Figure 27 - Visualising the results on the analysis using Cesium – Case B

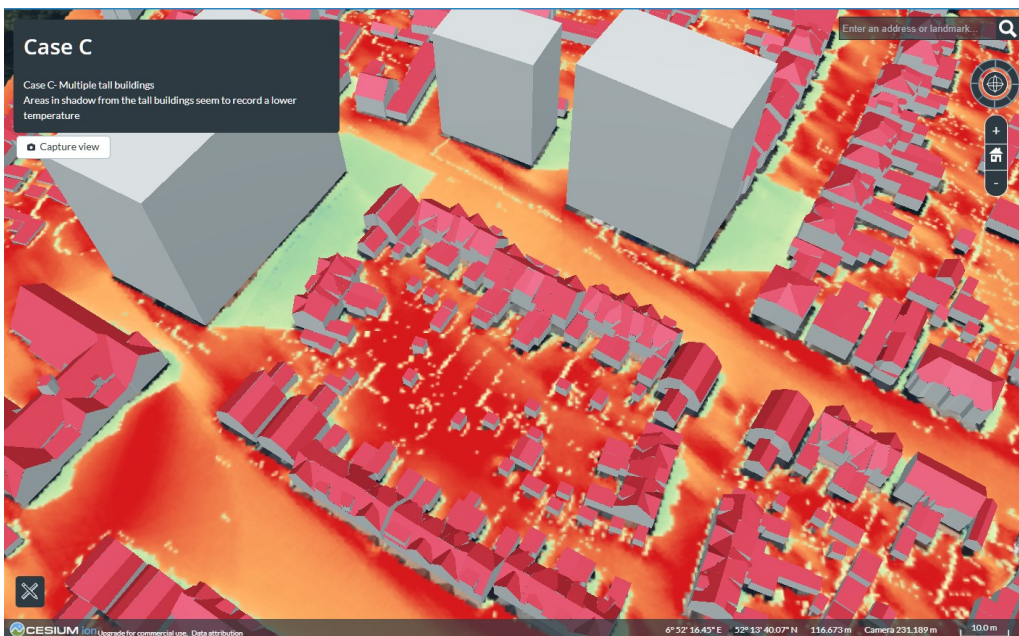


Figure 28 - Visualising the results on the analysis using Cesium – Case C

The model can be viewed in Cesium Stories on: <https://ion.cesium.com/stories/viewer/?id=d2667679-81e9-4069-9e97-db9c98711f68>. In addition, the code for doing the same using a local host and Cesium JS is given in the Annex.

5.4. Summary

This section has listed all the map outputs derived from using the workflow as designed. Thus, it discusses the 3D model scenarios that are created, the results obtained from using the created QGIS toolboxes, and the final data joining, and model visualisation as planned. An analysis of these results are done in the next chapter to aid decision-making further. Testing the workflow on different dates and different built forms also demonstrates the expected changes in environmental indicators in a visual manner and demonstrates the key takeaways from the literature review in a spatial context.

6. DISCUSSION

This research reinforces the key takeaway from literature review that modifications in the urban form have a direct effect on the environmental indicators at the scale of the neighbourhood. The results in the previous chapter revealed the direct impact of increasing building height on limiting the solar potentials of their neighbours and also on influencing the pattern of predicted thermal comfort in the neighbourhood. The direction and distance of impact varies over the seasons as it depends on the movement of the sun and the consequent shadow pattern formed. This Discussion section discusses some of the many analyses that can be carried out of the derived results and model outputs, and how they can help support informed decision-making.

6.1. Analysis of results from Solar Workflow

On conducting the analysis initially for summer conditions on June 21, the results of neighbourhood-level performance gave an expected result. While the number of individual rooftops with a viable energy estimate declined as new buildings are inserted (Figure 29), the mean value of the Energy Estimate per rooftop increases as the value of energy that can be produced by the newly introduced rooftops is far higher than the rooftops that have lost their suitability (Figure 30).

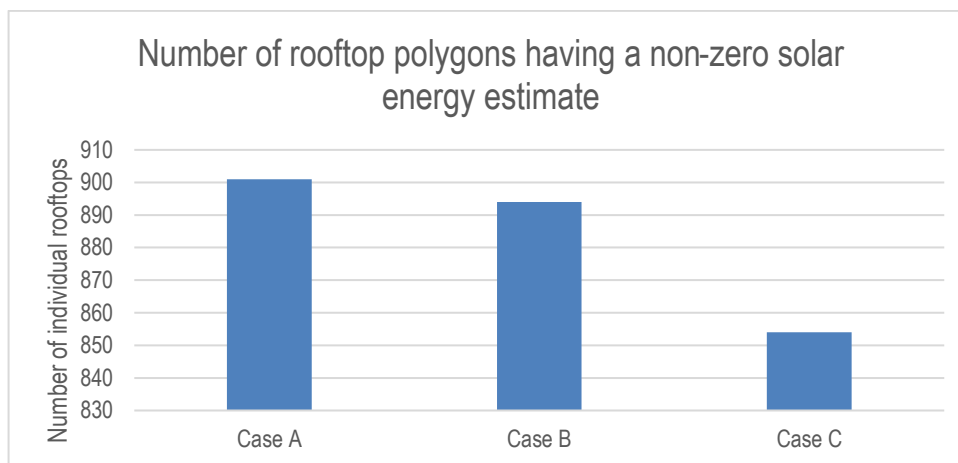


Figure 29 - number of housing rooftop polygons that record an energy estimate.

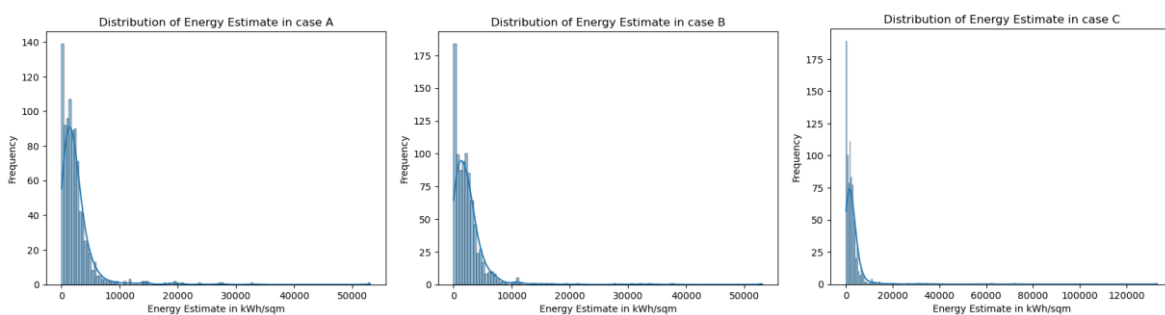


Figure 30 - Distribution of Energy Estimate values per rooftop in each of the built form cases.

Figure 30 also demonstrates that the number of rooftops with value 0 rise from 140 in Case A to over 175 in Case C, but the x-Axis of maximum value per rooftop increases as the newer, bigger rooftops have significantly higher potential than the smaller rooftops they have replaced.

Similarly, the usable rooftop area of the whole neighbourhood increases (Figure 20) (as discussed in the previous section) on the introduction of the new buildings – demonstrating that while there may be unfair losses at the scale of individual households, there is a net gain in the scale of the neighbourhood. Overlaying the distributions between Case A and Case B (Figure 31), shows the increase in rooftops having zero potential, possibly due to the shadowing caused by the introduction of the tall building.

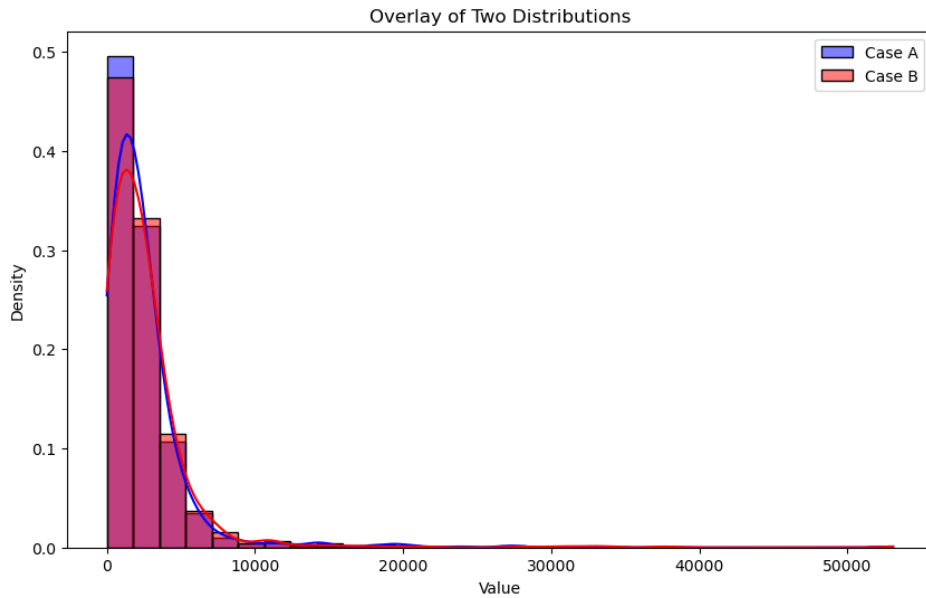


Figure 31 - Probability of Energy Estimate of a given rooftop in the neighbourhood. Maximum probability is of generating Energy below 5000kWh.

On further analysing the roof surfaces that lose their suitability in all 3 temporal scenarios, it is observed that the houses to the North-West of the new construction are affected the most. While the suitability changes in the 3 temporal scenarios, the rooftops identified in Map 23 seem to have permanently lost their suitability due to the two new built scenarios. It should be noted that the number of households thus affected are small, being in the ranges of 5-10 for Case B (Map 22) and 20-25 for Case C (Map 23).



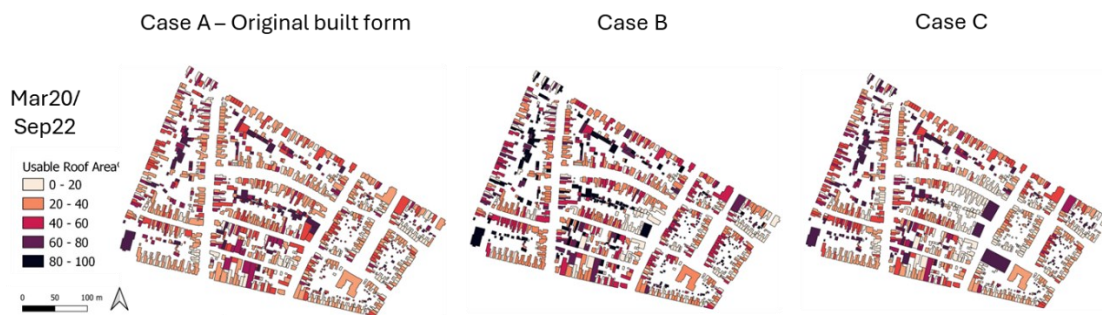
Map 22 - Rooftops showing loss of suitability in the built-form scenario of Case B- One Single Tall Building



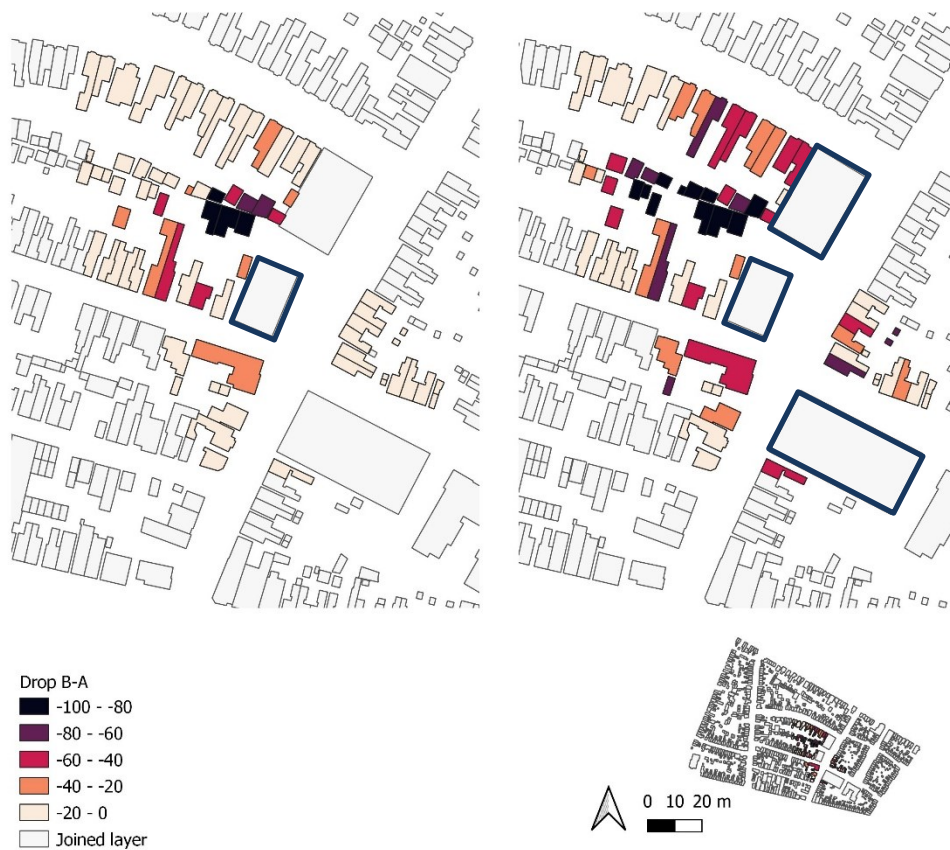
Map 23 - Rooftops showing loss of suitability in the built-form scenario of Case C - Multiple Tall Buildings

To understand this further, the immediate neighbourhood of the modified cases are analysed again. Map 24 reiterates the percentage of roof area that is suitable in each case. However, on subtracting the percentage of roof area in each of the modified cases from the original, the loss of suitable roof area can be visualised in Map 25. For example, if a roof lies in the range of loss from 40-60%, it means that 40-60% of actual roof area is now unusable in addition to the unsuitable roof area already derived for Case A.

Thus, if roof area utilisation was 60% in Case A and 30% in Case B, the further unsuitability is $60 - 30 = 30\%$. This ensures that the roofs that were already showing low utilisations, say 10%, do not show a large drop such as 50% when the actual area drops from 10% to 5%.



Map 24 - Roof Area utilization (in percentage) in March/Sep



Map 25 - reduction in usable roof area (in percentage) on introducing new buildings.

However, it is to be noted that the loss of suitability is dependent on the conditions that have been applied for estimating said suitability. Thus, if the condition for 60% shadow-free surface is relaxed, the loss of suitability then estimated will be lower, and the number of rooftops affected will be lower. In this manner, this workflow can give a snapshot of expected change, but the ‘damage’ thus shown is not definite and is very dependent of the conditions of suitability that are used.

To understand the variation of the pattern of energy estimates as a neighbourhood cluster, the Kullback-Leibler divergence was calculated over the predicted energy estimates per rooftop. KL divergence is used here to understand the difference of one probability distribution of one dataset from another.

KL divergence is calculated between the Rooftop Energy Estimate dataset of Case A and case B to see the divergence of results due to the introduction of one tall building: **KL Divergence: 0.1787**

KL divergence between Rooftop Energy Estimate dataset of Case C and case A: **KL Divergence: 0.2467**

These values show that there is not a great difference in the probability distributions on the introduction of different tall buildings, leading to the conclusion that their effect on the distributions is hyper-local. Thus, the sample size is reduced to an even smaller neighbourhood, we can expect a higher divergence score.

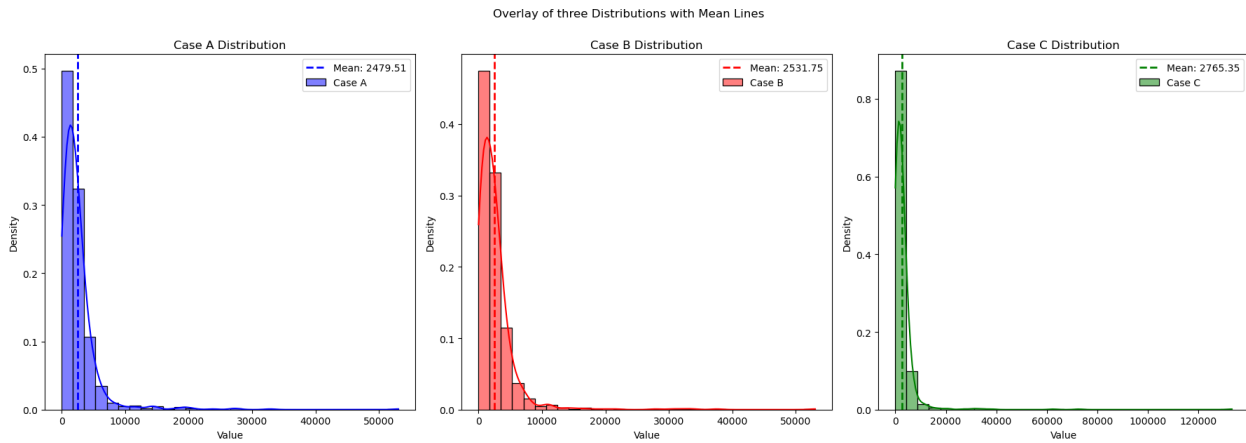


Figure 32 - The average EE probability also rises. Thus, a singular average household can get approx. 300kWh more per year

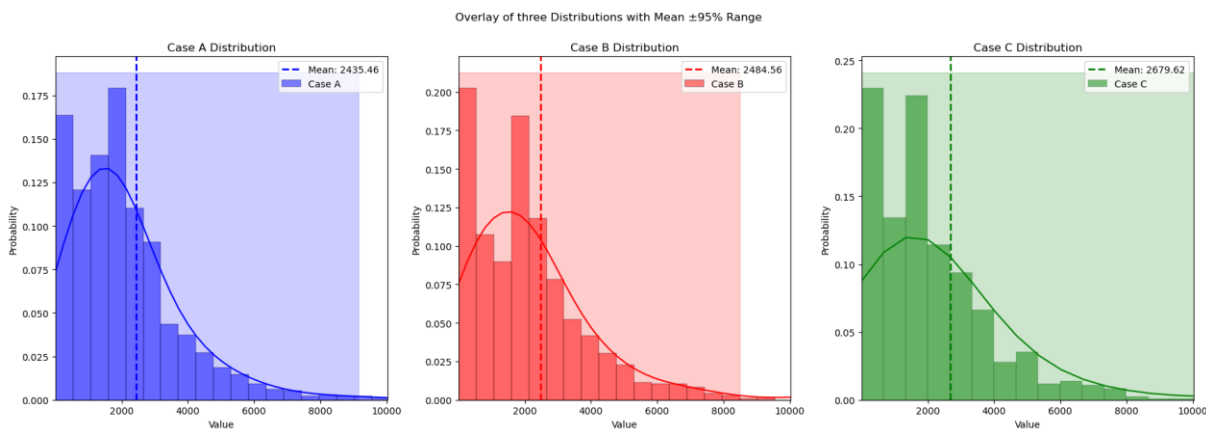


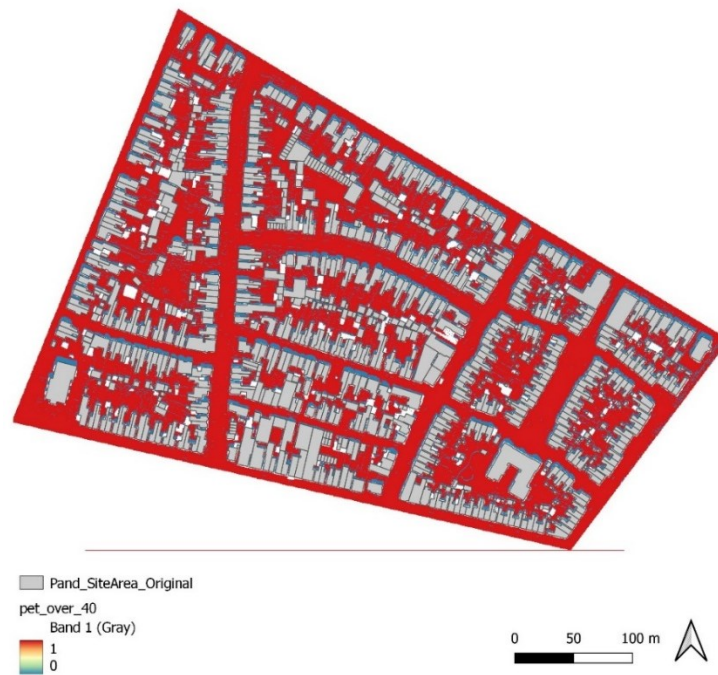
Figure 33 - Distributions with the mean range from 2.5-97.5 percentile range to remove extreme outliers.

Figure 32 shows that the mean value of the Solar potential per rooftop rises as the bigger roof plates are introduced in Case B and C. In an ideal scenario where 100% of the suitable area is utilised for solar energy harvesting, and the energy is shared locally, each building will gain an extra 300kWh of production in Case C as compared to Case A. On using on the middle 95% of values by removing extreme outliers, it is seen that the probability of rooftops with 0KWh is increasing (Figure 33). In addition, the smooth tapering of the distribution as seen in case A seems to have reduced as well, leading to the conclusion that while the overall energy estimates have increased, individual rooftops seem to have decreased in their potentials.

This makes a strong case advocating for neighbourhood-scale energy sharing policies by localised grid networks and can help counter the seemingly negative effects of tall buildings on their neighbour's rooftop solar potential.

6.2. Analysis of results from PET estimation

Critical areas recording Strong heat stress, here noted as zones estimated having temperatures above 40 °C are calculated (via Raster Calculator) in each built form case to identify zones predicted to experience very high thermal discomfort. In Case A, the zones below 40 °C are seen to be in the shadows of other buildings, towards the North. Here, zones recording PET values below 40 c are marked in blue, while areas recording PET estimate over 40 °C is marked in red.



Map 26 - PET values over 40 °C in Case A

Similarly, in Case B, temperatures are seen to be lower to the Northwest of the new built form, possibly as per the shadow pattern. This trend continues for Case C, however, as the orientation of the third building is E-W, there is a larger area that is seen to be recording below 40 degrees due to shadowing.



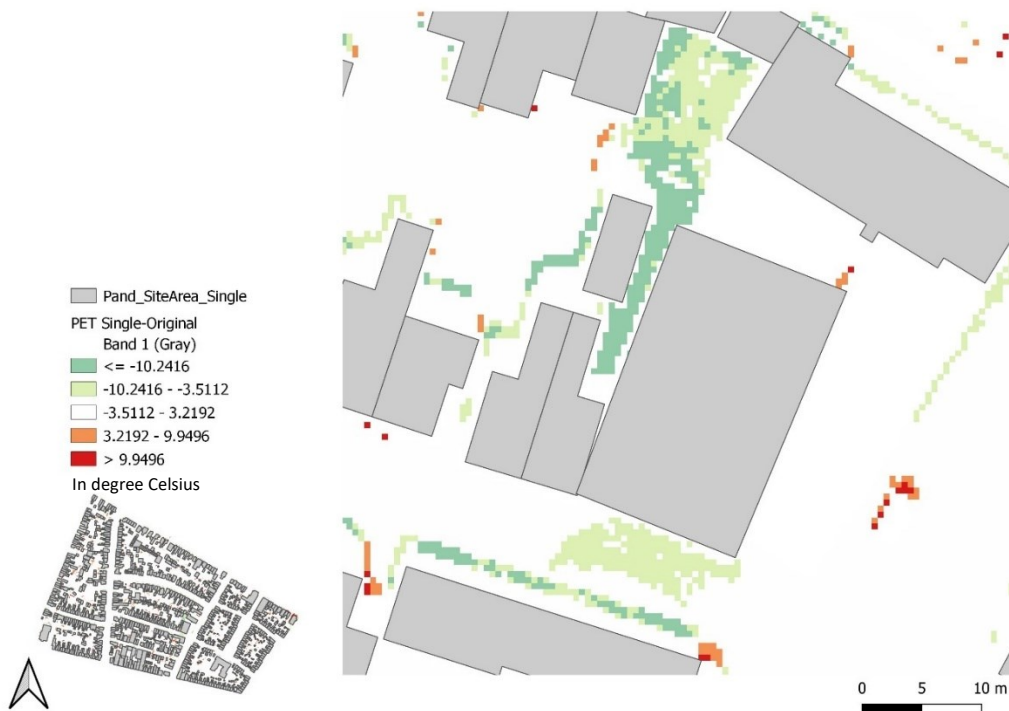
Map 27 - PET values over 40 °C in Case B.



Map 28 - PET values over 40 °C in Case C.

Thus, while literature suggests that taller, voluminous buildings can increase local temperatures by retaining more heat (Allen et al., 2011; Dirksen et al., 2019; Hong et al., 2023; Zhou et al., 2017), the results here show a local decrease in the estimated PET values.

To test whether temperature is only reducing, which seems to be contrary to literature review, additional raster calculations were carried out. Subtracting the predicted map of the built cases from the predicted PET map of the original built case showed interesting results.



Map 29 - PET values (Case B-CaseA)



Map 30 - PET values (Case C- Case A)

As seen in Map 29, the area to the North-west of the singular tall building does indeed record a lowering of experienced temperatures. However, on zooming out further for Case C in Map 30, it is clear to see the effect of building orientation of the effect on local neighbourhood. While the buildings aligned to the expected wind flow seem to only lower the predicted temperature, buildings hindering the wind flow have two-part effect – they lower predicted temperatures by shadowing, but hindering the wind flow causes two pockets of increased temperatures.

This seems to indicate the limitations of the estimation model being used in the analysis, which is highly dependent on the wind flow to dissipate the radiated flux. In addition, another limitation of the estimation that the accurate building materials and their albedo is not known, which could alter the estimation of PET. The effect of planation and water bodies is also not accounted for.

Figure 34 shows an overlay of the raster value distributions of the PET estimates, which shows that Case A shows a lower temperature estimate than both of the other built cases. Case B shows a spike in temperatures below 40 degrees, possibly due to the shadowing effect, while Case C shows a spike in temperatures around 45 degrees, possibly due to blocking of the wind flow.

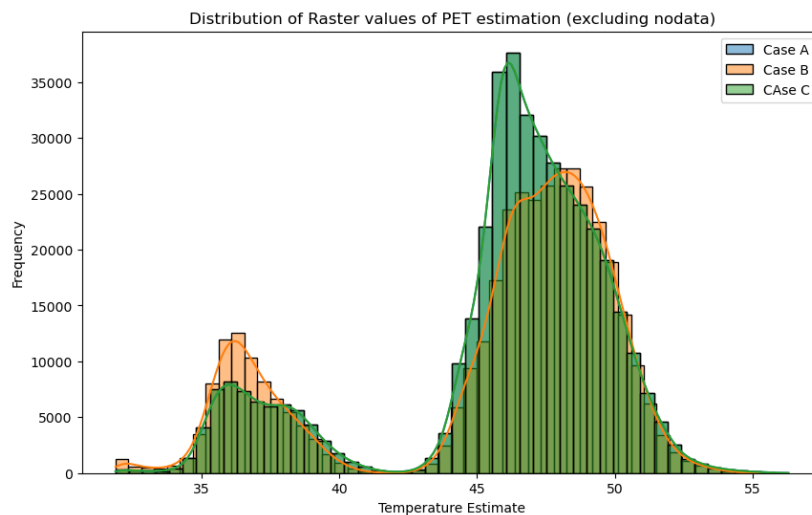


Figure 34 - Overlaid frequencies of temperature estimates of the three built cases.

Thus, it can be seen that it is not correct to make strong assumptions on the nature of environmental performance of a neighbourhood by modifying the built form, such as tall buildings *always* worsen solar potential. While there may be losses at a disaggregated level, there may be a net positive at an aggregated level, as seen in the results of the solar analysis. Similarly, the prediction of thermal comfort is complex and dependent of multiple variables that can cause local gains and losses, which may even out by additions of another kind, such as including more greenery, or painting surfaces in highly reflective paint, or using building finishes of lower albedo.

The workflow thus used makes multiple analyses possible, only a few of which have been discussed here to highlight the versatility of using free and open-source data along with GIS tools.

6.3. Comparison of results and analysis with literature study

In Chapter 2, multiple morphological parameters and characteristics were discussed that influence the two selected environmental indicators of thermal comfort and solar potential. A majority of the results behave in accordance with the conclusions of the literature review and are summarised in Table 8.

Table 8 - Comparison of literature with the results and analysis – Solar Potential estimation and analysis

Morphological Factor	Effect on Solar Potential of rooftops as per literature review	Notes from the Results and Analysis of Results
Urban density and shadowing	Sky View factor and shadowing can help in determining direct and indirect irradiation on a surface (Calabrini et al., 2019). Variations in building heights in a neighbourhood can affect shadowing on neighbouring rooftops (Bardhan et al., 2020; Li-Lian, 2022)	Urban shadowing has a major effect on reducing the suitability of a rooftop to solar potential and is demonstrated in Map 22 and Map 23.
Building and installation Orientation	Visibility of placement of PV module affects the rooftop potential, with modules at the west edge having the highest visibility (Zhou et al., 2023). Building orientation should have the long side facing south (Bardhan et al., 2020)	Suitability of rooftops is visible in Map 3, Map 4 and Map 5, where due to the irradiation estimation model used in UMEP, there is a discrepancy seen in the suitability of Eastern and Western facing roof slopes.
Roof design and geometry	Slope needs to be 10-45 degrees for optimal utilisation (Yorulmaz, 2023). This is to capture maximum DNI. PV modules should be placed on flat roofs or larger roof plates so that they are not visible to the public – especially in the case of monumental buildings (Zhou et al., 2023) Roof aspect should not be facing North as that receives, the least amount of usable irradiation (Yorulmaz, 2023). Minimum roof area 20sqm is needed to have a viable installation (Yorulmaz, 2023). Available roof area without obstructions is essential for a rooftop to have solar potential (Li-Lian, 2022)	When the suitable pixels of the rooftops are overlaid on the slope, it can be seen that most of them lie within the 0–45-degree slope range. In addition, North facing roof slopes are not deemed suitable in the results.
Aspect ratio and street orientation	Parameters like average building height, orientation of buildings, plot ratio and site coverage, height to width ratio (Street	The decrease in sky view factor in the immediate neighbourhood of the taller buildings in case B and c corroborate to a

width: building height), compactness, and the range of building heights can impact annual solar irradiance. Sky View factor can be used as an indicator for evaluating solar irradiation on surfaces (Poon et al., 2020).

lowered solar potential of the neighbouring rooftops.

As geographic and weather parameters are held constant over all three built form scenarios, the effect of modifying control parameters is not discussed.

Table 9 - Comparison of literature with the results and analysis - PET estimation and analysis

Morphological Factor	Effect on Thermal Comfort	Notes from Analysis and Results
Natural light and ventilation	Hindrance to natural ventilation can decrease thermal comfort and increase the dependence on mechanical cooling (Lau et al., 2018)	Map 12 and Map 14 show the effect of reduction in wind flow due to introducing the tall buildings, which is demonstrated more clearly in Map 29 and Map 30.
Building Orientation	Airflow blocking by building orientation can reduce thermal comfort (Stewart & Oke, 2012). Building orientation towards south will have a negative effect on thermal comfort (Nakata-Osaki et al., 2018)	Same as above.
Aspect ratio and street orientation	Lack of air paths along with closely packed buildings can hinder ventilation (Deng & Wong, 2020; Lau et al., 2018; Nasrollahi et al., 2021; Siu et al., 2021)	Same as above. In addition, wind flow directions can also be clearly seen in the streets (Map 12, Map 14)
Taller, voluminous buildings and dense neighbourhoods	Taller buildings increase surface areas for absorption of solar radiation. Thus, high rise, dense neighbourhoods report higher temperatures compared to less dense areas (Hong et al., 2023). However, shadowing between buildings may reduce local heat stress (Nasrollahi et al., 2021).	Higher ranges of Thermal Mean radiant temperatures as observed due to the larger volumes of the newly introduced buildings, as seen in Map 17 and Map 18.

6.4. Selection of plugins

Urban Heat and Thermal Comfort are widely studied topics, and there exist a multitude of methods to calculate it. This workflow is intended to be used, and thus the plug-in UMEP was selected as it was free, tested and is still regularly supported with troubleshooting on GitHub. It was important that anyone using the method could also raise questions on how to implement the code or plug-ins.

In addition, GRASS GIS plugin is also utilised in the workflow, along with well supported GDAL functions. The availability of these plug-ins ensures that there is no great need to develop models from scratch unless it is to improve upon it.

7. CONCLUSIONS AND RECOMMENDATIONS

This research attempted to define a workflow to analyse and visualise the environmental performance of not simply the existing neighbourhood but allowed testing new built forms and its possible effects. The workflow was then tested on a small neighbourhood of Tweckelerveld in Enschede, on many significant dates. In doing so, it answered many research questions.

The literature review carried out in Chapter 2 discussed the general literature on the effect of urban form on environmental performance and described the Dutch context in terms of governance and current conditions. The goals of the municipality in wanting to increase their housing stock, to combat thermal stress and to also encourage rooftop solar panels was recognised and incorporated into the research. Due to the literature insisting that changing built form did influence solar potential and thermal comfort, tall buildings of 30m+ in height were modelled.

Workflows were defined in pre-processing AHN-4 LIDAR data and the QGIS operations were made simple using QGIS Graphic Modeller. The current pattern of solar energy potential and thermal comfort was recorded, and the workflow was re-run on different dates and built form scenarios to capture any changes in estimation. The results were also compared with the freely available national and global datasets.

The results were analysed further to record the nature of predicted changes, and the same was compared with the literature review to ensure that the workflow was not giving results anomalous to expectations. In addition, the results were also visualised on the local system using Blender and also on the web using Cesium JS and Cesium Stories.

Implementation of global plans to reduce the effect of climate change require localisation and implementation at the municipal scale. However, conscientious, and effective adaptation often requires data-driven analysis to aid planning decisions. Resource, capacity, and time constraints are common constraints in this process, and often small municipalities are lagging behind (Fila et al., 2024). This highlights the importance of high quality open-source data and solutions that is reliable, consistent, and verified as there are many smaller municipalities that may not be able to afford creating or buying expensive data or costly software.

The proposed PSS workflow has relevance in the domain of form-based urban design, especially in the pursuit of analysing environmental parameters using modified urban forms. The proposed PSS workflow allows for users to modify the 3D environment and then test to visualise the effect of their decisions on the immediate environment, allowing for visual aid to see the repercussions of built-form decisions.

In essence, this research directly addresses the practical needs of professionals in urban planning and design, offering them a workflow to visualize the consequences of modifying urban cityscapes in the chosen environmental parameters. It is designed to serve as an approximation to aid feasibility studies, rather than to provide absolute final numerical results. The planning system is influenced by the goals of different government levels, and the output directly affects current and future residents. It also involves technical experts such as developers, architects and engineers who may or may not be directly employed by the municipality but have a stake in developing and using the output of the workflow.

One of the main contributions of this research is to not simply derive a workflow, but also make it easily replicable using Graphic Modeller. The toolbox thus created requires the pre-installation of UMEP, and then produces the final output of Solar Energy Potential estimation per rooftop, and PET from single input windows. By reducing manual steps, the processes now rely solely on the processing system's capabilities to produce results, while still allowing customization in key aspects. The development of these open-source workflows also highlighted the laborious and repetitive steps in raster processing, which can require more familiarity with GIS software and handling the output of spatial data analysis. These can be simplified using a Graphic Modeller or done entirely in a Python environment. While QGIS allows for a familiarity of environment, in many steps such as DEM conversion or repetitive processing, it is indeed to use a python environment, or a toolbox made by Graphic Modeller to save on processing time.

As the chosen pixel size is kept relatively small at 0.5m, visualising the effect of singular buildings becomes clearer. This extends to modelling future built scenarios, where the modification of environmental indicators can be visualised due to the modification of the built form, for example, decreased solar potential due to a

tall neighbouring building, or decreased thermal comfort due to new developments blocking wind flow. The effect of roof angles and aspect is clear in the solar potential estimation, underlining the importance of location and roof orientation as found in the literature review. Similarly, it is interesting to see the direct effect of building morphology in hindering wind flow, which then directly affects the estimated thermal comfort on the streets, as also stated by Rijal (Rijal, 2012). Thus, as the global meteorological values are kept constant, different morphological parameters of building height, angle, orientation, and grouping affect the environmental indicators.

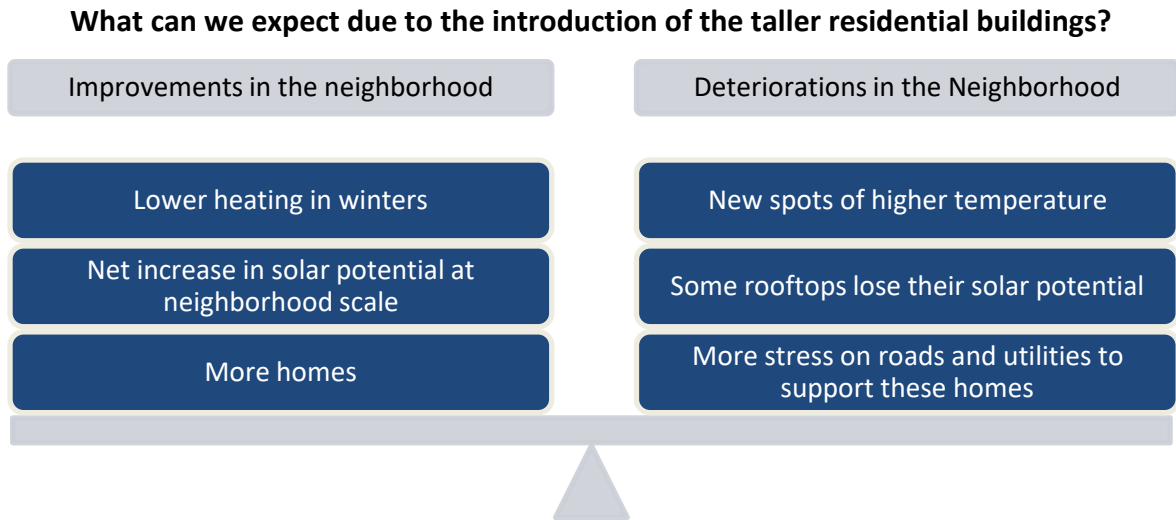


Figure 35 - Some key trade-offs noticed in this simulation and analysis.

It was also interesting to note the trade-off observed in the analysis of both indicators. While the two new built-form cases reduced the solar potential of the immediate neighbouring rooftops, they contributed to increasing the overall solar potential of the neighbourhood. Similarly, while the tall buildings seem to increase thermal comfort in the immediate neighbourhood due to shadowing, the overall neighbourhood experiences a slight increase in the upper range of predicted temperatures as well as new pockets of higher temperature due to blocking of wind flow. In addition to this, being 10 storeys tall each, the new built form can potentially house residents, partly fulfilling the housing requirements outlined in the WoonVisie (Housing Vision plan). While this research has tried to understand the difference in metrics by suitable roof area and roof utilisation percentages, another method of analysis can be to treat households as the functional units and see the net positive or negative effect when divided by a growing number of households that will be affected by this. Thus, keeping multiple goals and vision plans in mind, this highlights the complexity of predicting the effects of modifying building morphology and that strong statements cannot be made for or against introducing new building typologies. The summarization in Figure 35 reinforces the requirement of an Integrated Impact Assessment to understand the nature of change that can be expected by introducing new built forms for accommodating more housing units via densification.

7.1. Limitations of study

This study is limited to exploring the effect of morphology on the two selected environmental indicators. The research and development of the PSS is limited by the accuracy of the UMEP plug-in (Lindberg et al., 2018) which has been used extensively in the analysis. However, according to studies, UMEP is found as a good compromise between accuracy and processing time (Mutani & Beltramino, 2022). As processing time, or strength of processor is also a part of resource constraint, using this simplified workflow using UMEP can be a cost and time-effective solution for initial analysis for urban planners in small municipalities. In addition, the variables used for PET estimation are severely restricted as albedo (material) is kept constant and water and trees are omitted from the estimation. Thus, the modified results cannot be considered as real thermal comfort temperature estimations as they model T_{mrt} on constrained variables.

The importance of scenario and variable selection can be deduced from the results. The projected results as well as the existing condition varies greatly as the underlying climatic variables are modified. This drives

home the importance of selecting scenarios – extremes, medians or means – as this greatly influences the projected outcomes of different built scenarios. It is also noteworthy that the thermal comfort estimation is done for a standard of a 35-year-old male in comfortable clothing and is thus only an approximation of human comfort. The results will also vary as the target population of children, or the elderly is considered.

7.2. Avenues for future research and development

In future research, the current set of workflows can be expanded to include more indicators to get a holistic view of the changes triggered by a change in urban form. In addition, there can be development on running the entire experiment on python code, independent of a GIS environment. In addition, PET estimation calculations can be re-run for different surface albedo if such data is available, and also for different target population conditions – such as comfort conditions for the elderly, for children and for women.

Further development in visualisation and usability can be conducted in making a single interface for modelling new buildings and visualising their results. Visualising on the web gives users the ability to quickly share models by link, instead of needing local devices. This can be used in cases of stakeholder meetings, where models can be shared before the meeting so that the stakeholders have time to interact and understand the models and come with more contextual questions. This may also help in driving up attendance in stakeholder meetings as now the stakeholders have a reference of new projects and their effects. There are already many 3D city models in use in the Dutch context such as the 3D Amsterdam, and the novelty and use of these interfaces may help in driving citizen engagement. Some of the conclusions of testing the viewing interface using different software is listed in Table 10.

Table 10 - Characteristics of different platforms for viewing results.

	Blender	Cesium local host	Unity
Shareability	Not shareable	Cesium stories can be shared by link	Not shareable
Ability to query	Individual houses can be selected for viewing extra properties	No querying in Cesium stories. Querying needs good grasp of JavaScript for Cesium Ion	Querying needs good grasp of C#
Cost	Free	Free	Free only for individual use
Computing capacity	Not a very heavy software, works on local device.	No demand for high computing capacity, uses code and local host/Cesium cloud.	Requires more graphic capacity as it is a game engine but works on local device in gaming laptops.

7.3. Policy recommendations

PlanSchade is a great example of paying back the damages caused due to building approvals that can cause in loss of value to houses (Rijksoverheid, n.d.). The method outlined in this research can aid in serving as a guide to the *PlanSchade* as well as it can reveal the extent of area that can lose their solar potentials, or experience heightened temperatures in the summer due to disruptive built forms.

In a country facing a severe housing crisis and planning to build almost a million more homes without expanding into agricultural land, it is obvious that there will be some form of urban densification – by raising heights of buildings or reducing the distance between them. It can thus become important to see whether the prospective increase in temperature caused by the built form can be reduced by alternate measures such as increasing greenery rates, or by including that in the *PlanSchade* as a form of damage. In addition to policy instruments, it is necessary to also adopt local initiatives of painting reflective coatings on roads and

pavements to combat expected increases in PET (Sankar Cheela et al., 2021) and also stress on greenifying residential neighbourhoods (Cascone & Leuzzo, 2023).

Furthermore, the analysis also shows that modification of the built environment in this manner can potentially generate more solar electricity as the new building with a large footprint also has a large, suitable rooftop. Thus, it becomes important to include an energy sharing clause into the approvals, and creating hyper-local grids that can overcome the potential energy losses (SolarPower Europe, 2023) and improve the quality of living while also achieving the plan to house more people within the city boundaries.

LIST OF REFERENCES

- ABF Research. (2023, July). *Rapportage Primos Prognose 2023*. Primos Prognose. <https://abfresearch.nl/2023/07/12/rapportage-primos-prognose-2023/>
- Akpan, I. J., & Shanker, M. (2019). A comparative evaluation of the effectiveness of virtual reality, 3D visualization and 2D visual interactive simulation: an exploratory meta-analysis. *Simulation*, *95*(2), 145–170. https://doi.org/10.1177/0037549718757039/ASSET/IMAGES/LARGE/10.1177_0037549718757039-FIG1.JPEG
- Allen, L., Lindberg, F., & Grimmond, C. S. B. (2011). Global to city scale urban anthropogenic heat flux: Model and variability. *International Journal of Climatology*, *31*(13), 1990–2005. <https://doi.org/10.1002/JOC.2210/ABSTRACT>
- Ang, Y. Q., Berzolla, Z. M., Letellier-Duchesne, S., Jusiega, V., & Reinhart, C. (2022). UBEM.io: A web-based framework to rapidly generate urban building energy models for carbon reduction technology pathways. *Sustainable Cities and Society*, *77*, 103534. <https://doi.org/10.1016/J.SCS.2021.103534>
- Bardhan, R., Debnath, R., Gama, J., & Vijay, U. (2020). REST framework: A modelling approach towards cooling energy stress mitigation plans for future cities in warming Global South. *Sustainable Cities and Society*, *61*. <https://doi.org/10.1016/J.SCS.2020.102315>
- Bernard, J., Lindberg, F., & Oswald, S. (2023). URock 2023a: an open-source GIS-based wind model for complex urban settings. *Geoscientific Model Development*, *16*(20), 5703–5727. <https://doi.org/10.5194/GMD-16-5703-2023>
- Bleisch, S., & Dykes, J. (2015). Quantitative data graphics in 3D desktop-based virtual environments – an evaluation. *International Journal of Digital Earth*, *8*(8), 623–639. <https://doi.org/10.1080/17538947.2014.927536>
- Boccalatte, A., Fossa, M., Gaillard, L., & Menezo, C. (2020). Microclimate and urban morphology effects on building energy demand in different European cities. *Energy and Buildings*, *224*. <https://doi.org/10.1016/j.enbuild.2020.110129>
- Broitman, D., & Koomen, E. (2015). Residential density change: Densification and urban expansion. *Computers, Environment and Urban Systems*, *54*, 32–46. <https://doi.org/10.1016/J.COMPENVURBSYS.2015.05.006>
- Calcabrini, A., Ziar, H., Isabella, O., & Zeman, M. (2019). A simplified skyline-based method for estimating the annual solar energy potential in urban environments. *Nature Energy*, *4*(3), 206–215. <https://doi.org/10.1038/s41560-018-0318-6>
- Cascone, S., & Leuzzo, A. (2023). Thermal Comfort in the Built Environment: A Digital Workflow for the Comparison of Different Green Infrastructure Strategies. *Atmosphere 2023, Vol. 14, Page 685*, *14*(4), 685. <https://doi.org/10.3390/ATMOS14040685>
- Clifton, K., Ewing, R., Knaap, G. J., & Song, Y. (2008). Quantitative analysis of urban form: A multidisciplinary review. *Journal of Urbanism*, *1*(1), 17–45. <https://doi.org/10.1080/17549170801903496>
- Dataset: Actueel Hoogtebestand Nederland 4 (AHN), & PDOK. (2023). Actueel Hoogtebestand Nederland 4 (AHN). In <https://www.pdok.nl/introductie/-/article/actueel-hoogtebestand-nederland-abn>.
- Deng, J. Y., & Wong, N. H. (2020). Impact of urban canyon geometries on outdoor thermal comfort in central business districts. *Sustainable Cities and Society*, *53*, 101966. <https://doi.org/10.1016/J.SCS.2019.101966>
- Dirksen, M., Ronda, R. J., Theeuwes, N. E., & Pagani, G. A. (2019). Sky view factor calculations and its application in urban heat island studies. *Urban Climate*, *30*, 100498. <https://doi.org/10.1016/J.UCLIM.2019.100498>

- Elkhazindar, A., Kharrufa, S. N., & Arar, M. S. (2022). The Effect of Urban Form on the Heat Island Phenomenon and Human Thermal Comfort: A Comparative Study of UAE Residential Sites. *Energies*, *15*(15), 5471. <https://doi.org/10.3390/en15155471>
- EU-JRC. (n.d.). *JRC Photovoltaic Geographical Information System (PVGIS) - European Commission*. Retrieved November 28, 2023, from https://re.jrc.ec.europa.eu/pvg_tools/en/tools.html
- European Environment Agency. (n.d.). *environmental indicator - definition*. Retrieved April 22, 2024, from <https://www.eea.europa.eu/help/glossary/eea-glossary/environmental-indicator>
- Fila, D., Fünfgeld, H., & Dahlmann, H. (2024). Climate change adaptation with limited resources: adaptive capacity and action in small- and medium-sized municipalities. *Environment, Development and Sustainability*, *26*(3), 5607–5627. <https://doi.org/10.1007/S10668-023-02999-3/TABLES/2>
- Gál, C. V., & Kántor, N. (2020). Modeling mean radiant temperature in outdoor spaces, A comparative numerical simulation and validation study. *Urban Climate*, *32*, 100571. <https://doi.org/10.1016/J.UCLIM.2019.100571>
- Geis, A. (2023). Housing Supply in the Netherlands: The Road to More Affordable Living. *Selected Issues Papers*, *2023*(023), 1. <https://doi.org/10.5089/9798400236389.018>
- Gemeente Enschede. (2021a). *Beleidsregels Zonne Energie (Solar Energy Policies)*.
- Gemeente Enschede. (2021b). *Energie Visie*.
- Gemeente Enschede, & Royal HaskoningDHV. (2022). *Water- en Klimaatadaptatieplan Gemeente Enschede 2022-2026*.
- Götze, V., & Jehling, M. (2023). Comparing types and patterns: A context-oriented approach to densification in Switzerland and the Netherlands. *Environment and Planning B: Urban Analytics and City Science*, *50*(6), 1645–1659. https://doi.org/10.1177/23998083221142198/ASSET/IMAGES/LARGE/10.1177_23998083221142198-FIG4.JPEG
- Government of the Netherlands. (n.d.). *Stimulating the growth of solar energy | Renewable energy | Government.nl*. Retrieved December 1, 2023, from <https://www.government.nl/topics/renewable-energy/stimulating-the-growth-of-solar-energy>
- Herbert, G., & Chen, X. (2015). A comparison of usefulness of 2D and 3D representations of urban planning. *Cartography and Geographic Information Science*, *42*(1), 22–32. <https://doi.org/10.1080/15230406.2014.987694>
- Hong, C., Wang, Y., & Gu, Z. (2023). How to understand the heat island effects in high-rise compact urban canopy? *City and Built Environment* *2023* *1:1*, *1*(1), 1–13. <https://doi.org/10.1007/S44213-022-00002-9>
- Höppe, P. (1999). The physiological equivalent temperature - A universal index for the biometeorological assessment of the thermal environment. *International Journal of Biometeorology*, *43*(2), 71–75. <https://doi.org/10.1007/S004840050118/METRICS>
- Johansson, L., Onomura, S., Lindberg, F., & Seaquist, J. (2016). Towards the modelling of pedestrian wind speed using high-resolution digital surface models and statistical methods. *Theoretical and Applied Climatology*, *124*(1–2), 189–203. <https://doi.org/10.1007/S00704-015-1405-2>
- Kamel, E. (2022). A Systematic Literature Review of Physics-Based Urban Building Energy Modeling (UBEM) Tools, Data Sources, and Challenges for Energy Conservation. *Energies* *2022*, *Vol. 15*, Page *8649*, *15*(22), 8649. <https://doi.org/10.3390/EN15228649>
- Karimimoshaver, M., Khalvandi, R., & Khalvandi, M. (2021). The effect of urban morphology on heat accumulation in urban street canyons and mitigation approach. *Sustainable Cities and Society*, *73*, 103127. <https://doi.org/10.1016/J.SCS.2021.103127>
- Kong, F., Chen, J., Middel, A., Yin, H., Li, M., Sun, T., Zhang, N., Huang, J., Liu, H., Zhou, K., & Ma, J. (2022). Impact of 3-D urban landscape patterns on the outdoor thermal environment: A modelling

- study with SOLWEIG. *Computers, Environment and Urban Systems*, 94. <https://doi.org/10.1016/J.COMPENVURBSYS.2022.101773>
- Koomen, E., Dekkers, J., & van Dijk, T. (2008). Open-space preservation in the Netherlands: Planning, practice and prospects. *Land Use Policy*, 25(3), 361–377. <https://doi.org/10.1016/J.LANDUSEPOL.2007.09.004>
- Koopmans, S., Heusinkveld, B. G., & Steeneveld, G. J. (2020). A standardized Physical Equivalent Temperature urban heat map at 1-m spatial resolution to facilitate climate stress tests in the Netherlands. *Building and Environment*, 181, 106984. <https://doi.org/10.1016/J.BUILDENV.2020.106984>
- Kosmopoulos, P. (2024). Solar irradiance and exploitation of the Sun's power. *Planning and Management of Solar Power from Space*, 1–20. <https://doi.org/10.1016/B978-0-12-823390-0.00006-5>
- Kuster, C. (2023, January 27). *Digital Twin: The Netherland in game engines*. Geodan Research. <https://research.geodan.nl/digital-twin-the-netherland-in-game-engines/>
- Lau, K. K. L., Ng, E., Ren, C., Ho, J. C. K., Wan, L., Shi, Y., Zheng, Y., Gong, F., Cheng, V., Yuan, C., Tan, Z., & Wong, K. S. (2018). Defining the environmental performance of neighbourhoods in high-density cities. *Building Research and Information*, 46(5), 540–551. <https://doi.org/10.1080/09613218.2018.1399583>
- Li, Y., Schubert, S., Kropp, J. P., & Rybski, D. (2020). On the influence of density and morphology on the Urban Heat Island intensity. *Nature Communications* 2020 11:1, 11(1), 1–9. <https://doi.org/10.1038/s41467-020-16461-9>
- Li-Lian, A. (2022, August 31). *Estimating Solar Panel Output with Open-Source Data*. Towards Data Science | Medium. <https://towardsdatascience.com/estimating-solar-panel-output-with-open-source-data-bbca6ea1f523>
- Lindberg, F., Grimmond, C. S. B., Gabey, A., Huang, B., Kent, C. W., Sun, T., Theeuwes, N. E., Järvi, L., Ward, H. C., Capel-Timms, I., Chang, Y., Jonsson, P., Krave, N., Liu, D., Meyer, D., Olofson, K. F. G., Tan, J., Wästberg, D., Xue, L., & Zhang, Z. (2018). Urban Multi-scale Environmental Predictor (UMEP): An integrated tool for city-based climate services. *Environmental Modelling and Software*, 99, 70–87. <https://doi.org/10.1016/J.ENVSOFT.2017.09.020>
- Lindberg, F., Holmer, B., & Thorsson, S. (2008). SOLWEIG 1.0 - Modelling spatial variations of 3D radiant fluxes and mean radiant temperature in complex urban settings. *International Journal of Biometeorology*, 52(7), 697–713. <https://doi.org/10.1007/S00484-008-0162-7>
- Lindberg, F., Jonsson, P., Honjo, T., & Wästberg, D. (2015). Solar energy on building envelopes – 3D modelling in a 2D environment. *Solar Energy*, 115, 369–378. <https://doi.org/10.1016/j.solener.2015.03.001>
- Liu, K., Xu, X., Huang, W., Zhang, R., Kong, L., & Wang, X. (2023). A multi-objective optimization framework for designing urban block forms considering daylight, energy consumption, and photovoltaic energy potential. *Building and Environment*, 242. <https://doi.org/10.1016/j.buildenv.2023.110585>
- Masson, V., Bonhomme, M., Salagnac, J. L., Briottet, X., & Lemonsu, A. (2014). Solar panels reduce both global warming and urban heat island. *Frontiers in Environmental Science*, 2(JUN), 81306. <https://doi.org/10.3389/FENVS.2014.00014/BIBTEX>
- Mastorakis, K. (2020). *An integrative workflow for 3D city model versioning*. <https://repository.tudelft.nl/islandora/object/uuid%3Aa7f7f0c8-7a34-454e-973a-d55f5b8b0dfe>
- Matzarakis, A., Mayer, H., & Iziomon, M. G. (1999). Applications of a universal thermal index: Physiological equivalent temperature. *International Journal of Biometeorology*, 43(2), 76–84. <https://doi.org/10.1007/S004840050119/METRICS>
- Meijer, R., & Jonkman, A. (2020). Land-policy instruments for densification: the Dutch quest for control. *Town Planning Review*, 91(3), 239–258. <https://doi.org/10.3828/TPR.2020.14>

- Méndez Echenagucia, T., Capozzoli, A., Cascone, Y., & Sassone, M. (2015). The early design stage of a building envelope: Multi-objective search through heating, cooling and lighting energy performance analysis. *Applied Energy*, *154*, 577–591. <https://doi.org/10.1016/j.apenergy.2015.04.090>
- Ministry of Infrastructure and the Environment the Netherlands. (2013, June 24). *Spatial Planning in The Netherlands | Spatial planning | Government.nl*. <https://www.government.nl/topics/spatial-planning-and-infrastructure/spatial-planning-in-the-netherlands>
- Mussawar, O., Mayyas, A., & Azar, E. (2023). Built form and function as determinants of urban energy performance: An integrated agent-based modeling approach and case study. *Sustainable Cities and Society*, *96*, 104660. <https://doi.org/10.1016/j.scs.2023.104660>
- Mutani, G., & Beltramino, S. (2022). Geospatial Assessment and Modeling of Outdoor Thermal Comfort at Urban Scale. *International Journal of Heat and Technology*, *40*(4), 871–878. <https://doi.org/10.18280/IJHT.400402>
- Nakata-Osaki, C. M., Souza, L. C. L., & Rodrigues, D. S. (2018). THIS – Tool for Heat Island Simulation: A GIS extension model to calculate urban heat island intensity based on urban geometry. *Computers, Environment and Urban Systems*, *67*, 157–168. <https://doi.org/10.1016/j.compenvurbysys.2017.09.007>
- Nasrollahi, N., Namazi, Y., & Taleghani, M. (2021). The effect of urban shading and canyon geometry on outdoor thermal comfort in hot climates: A case study of Ahvaz, Iran. *Sustainable Cities and Society*, *65*, 102638. <https://doi.org/10.1016/j.scs.2020.102638>
- Netherlands Enterprise Agency(RVO), FME, TKI Urban Energy, & Top Sector Energy. (2020). *Next-generation solar power Dutch technology for the solar energy revolution*.
- Nevens, M. G., & Apell, J. N. (2021). Emerging investigator series: quantifying the impact of cloud cover on solar irradiance and environmental photodegradation. *Environmental Science: Processes & Impacts*, *23*(12), 1884–1892. <https://doi.org/10.1039/D1EM00314C>
- Nezamisavojbolaghi, M., Davodian, E., Bouich, A., Tlemçani, M., Mesbahi, O., & Janeiro, F. M. (2023). The Impact of Dust Deposition on PV Panels' Efficiency and Mitigation Solutions: Review Article. *Energies*, *16*(24), 8022. <https://doi.org/10.3390/en16248022>
- NIOSH/CDC. (2020, August 31). *Heat Stress | NIOSH | CDC*. <https://www.cdc.gov/niosh/topics/heatstress/default.html>
- NREL - U.S. Department of Energy. (2012). *Life Cycle Greenhouse Gas Emissions from Solar Photovoltaics*.
- Peters, R., Dukai, B., Vitalis, S., van Liempt, J., & Stoter, J. (2022). Automated 3D Reconstruction of LoD2 and LoD1 Models for All 10 Million Buildings of the Netherlands. *Photogrammetric Engineering & Remote Sensing*, *88*(3), 165–170. <https://doi.org/10.14358/PERS.21-00032R2>
- Polo, J., & García, R. J. (2023). Solar Potential Uncertainty in Building Rooftops as a Function of Digital Surface Model Accuracy. *Remote Sensing*, *15*(3), 567. <https://doi.org/10.3390/rs15030567>
- Poon, K. H., Kämpf, J. H., Tay, S. E. R., Wong, N. H., & Reindl, T. G. (2020). Parametric study of URBAN morphology on building solar energy potential in Singapore context. *Urban Climate*, *33*. <https://doi.org/10.1016/j.uclim.2020.100624>
- Ramanathan, V., Crutzen, P. J., Kiehl, J. T., & Rosenfeld, D. (2001). Atmosphere: Aerosols, climate, and the hydrological cycle. *Science*, *294*(5549), 2119–2124. https://doi.org/10.1126/SCIENCE.1064034/SUPPL_FILE/1064034S2_THUMB.GIF
- Ratti, C., Baker, N., & Steemers, K. (2005). Energy consumption and urban texture. *Energy and Buildings*, *37*(7), 762–776. <https://doi.org/10.1016/j.enbuild.2004.10.010>
- Rijal, H. B. (2012). Thermal adaptation outdoors and the effect of wind on thermal comfort. *Ventilating Cities: Air-Flow Criteria for Healthy and Comfortable Urban Living*, 33–58. https://doi.org/10.1007/978-94-007-2771-7_3/FIGURES/18

- Rijksoverheid. (n.d.). *Waar kan ik schadevergoeding aanvragen na planschade?* | *Rijksoverheid.nl*. Retrieved June 20, 2024, from <https://www.rijksoverheid.nl/onderwerpen/ruimtelijke-ordening-en-gebiedsontwikkeling/vraag-en-antwoord/waar-kan-ik-schadevergoeding-aanvragen-na-planschade>
- Rode, P., Keim, C., Robazza, G., Viejo, P., & Schofield, J. (2014). Cities and energy: Urban morphology and residential heat-energy demand. *Environment and Planning B: Planning and Design*, 41(1), 138–162. <https://doi.org/10.1068/B39065>
- Salter, J., Lu, Y., Kim, J. C., Kellett, R., Girling, C., Inomata, F., & Krahn, A. (2020). Iterative ‘what-if’ neighborhood simulation: energy and emissions impacts. *Buildings and Cities*, 1(1), 293–307. <https://doi.org/10.5334/BC.51>
- Sandia National Laboratories. (2024). *Global Horizontal Irradiance*. PV Performance Modeling Collaborative (PVPMC). <https://pvpmc.sandia.gov/modeling-guide/1-weather-design-inputs/irradiance-insolation/global-horizontal-irradiance/>
- Sankar Cheela, V. R., John, M., Biswas, W., & Sarker, P. (2021). Combating Urban Heat Island Effect—A Review of Reflective Pavements and Tree Shading Strategies. *Buildings 2021*, Vol. 11, Page 93, 11(3), 93. <https://doi.org/10.3390/BUILDINGS11030093>
- Scartezzini, J.-L., Nouvel, R., BRASSEL, K.-H., BRUSE, M., Duminil, E., Coors, V., Eicker, U., & Robinson, D. (2015). *SimStadt, a new workflow-driven urban energy simulation platform for CityGML city models*. https://www.researchgate.net/publication/312997307_SimStadt_a_new_workflow-driven_urban_energy_simulation_platform_for_CityGML_city_models
- Seipel, S. (2013). Evaluating 2D and 3D geovisualisations for basic spatial assessment. *Behaviour & Information Technology*, 32(8), 845–858. <https://doi.org/10.1080/0144929X.2012.661555>
- Shach-Pinsly, D., & Capeluto, I. G. (2020). From Form-Based to Performance-Based Codes. *Sustainability*, 12(14), 5657. <https://doi.org/10.3390/su12145657>
- Sheng, W., Kan, X., Wen, B., & Zhang, L. (2021). Design matters: New insights on optimizing energy consumption for residential buildings. *Energy and Buildings*, 242, 110976. <https://doi.org/10.1016/j.enbuild.2021.110976>
- Silva, M., Oliveira, V., & Leal, V. (2017). Urban Form and Energy Demand: A Review of Energy-relevant Urban Attributes. *Journal of Planning Literature*, 32(4), 346–365. <https://doi.org/10.1177/0885412217706900>
- Siu, S., Lau, Y., & Qin, H. (2021). *Investigation of The Impacts of Urban Morphology On Summer-Time Urban Heat Island Using GIS And Field Measurement*. <https://doi.org/10.21203/RS.3.RS-902622/V1>
- Solargis, World Bank Group, & ESMAP. (n.d.). *Global Solar Atlas 2.0*. Retrieved June 12, 2024, from <https://globalsolaratlas.info/map?c=52.283072,6.745605,11&s=52.273238,6.857941&cm=site>
- SolarPower Europe. (2023). *Regulatory framework for Energy Sharing*. https://api.solarpowereurope.org/uploads/Final_collective_self_consumption_report_133b88bb28.pdf?updated_at=2023-03-03T13:42:12.001Z
- Steadman, P., Hamilton, I., & Evans, S. (2014). Energy and urban built form: An empirical and statistical approach. *Building Research and Information*, 42(1), 17–31. <https://doi.org/10.1080/09613218.2013.808140>
- Steenefeld, G. J., Koopmans, S., Heusinkveld, B. G., Van Hove, L. W. A., & Holtslag, A. A. M. (2011). Quantifying urban heat island effects and human comfort for cities of variable size and urban morphology in the Netherlands. *Journal of Geophysical Research Atmospheres*, 116(20). <https://doi.org/10.1029/2011JD015988>
- Stewart, I. D., & Oke, T. R. (2012). Local Climate Zones for Urban Temperature Studies. *Bulletin of the American Meteorological Society*, 93(12), 1879–1900. <https://doi.org/10.1175/BAMS-D-11-00019.1>
- Stichting Climate Adaptation Services. (2023). *Klimaat-effectatlas*. Ministerie van Infrastructuur En Waterstaat.

- Thoubboron, K. (2021, July 28). *Solar Easements: What You Need To Know*. Energy Sage. <https://www.energysage.com/solar/what-is-a-solar-easement/>
- UNDP. (2000). *World Energy Assessment and the Challenge of Sustainability: Energy*.
- US DOE. (n.d.). *Solar Rooftop Potential | Department of Energy*. Retrieved June 12, 2024, from <https://www.energy.gov/eere/solar/solar-rooftop-potential>
- van Daalen, K. R., Romanello, M., Rocklöv, J., Semenza, J. C., Tonne, C., Markandya, A., Dasandi, N., Jankin, S., Achebak, H., Ballester, J., Bechara, H., Callaghan, M. W., Chambers, J., Dasgupta, S., Drummond, P., Farooq, Z., Gasparyan, O., Gonzalez-Reviriego, N., Hamilton, I., ... Lowe, R. (2022). The 2022 Europe report of the Lancet Countdown on health and climate change: towards a climate resilient future. *The Lancet Public Health*, 7(11), e942–e965. [https://doi.org/10.1016/S2468-2667\(22\)00197-9](https://doi.org/10.1016/S2468-2667(22)00197-9)
- van der Hoeven, F., Wandl, A., Vaissier, N., & de Deckere, M. (2019). *The Hague heat - Mapping The Hague's Urban Heat Island*.
- Van Hove, L. W. A., Steeneveld, G. J., Jacobs, C. M. J., Heusinkveld, B. G., Elbers, J. A., Moors, E. J., & Holtslag, A. A. M. (2011). *Assessment based on a literature review, recent meteorological observations and datasets provided by bobby meteorologists Exploring the Urban Heat Island Intensity of Dutch cities*. www.alterra.wur.nl/uk
- van Oostrom, C. (2022). *Here's how the construction industry can reach net-zero | World Economic Forum*. World Economic Forum. <https://www.weforum.org/agenda/2022/09/construction-industry-zero-emissions/>
- Xu, X., Yin, C., Wang, W., Xu, N., Hong, T., & Li, Q. (2019). Revealing Urban Morphology and Outdoor Comfort through Genetic Algorithm-Driven Urban Block Design in Dry and Hot Regions of China. *Sustainability*, 11(13), 3683. <https://doi.org/10.3390/su11133683>
- Yorulmaz, T. E. (2023, June 23). *Rooftop Solar Energy Potential Assessment using GIS and Photogrammetry: Case Study of Karaman Province/Turkiye*. Medium. <https://medium.com/@taremyor/rooftop-solar-potential-assessment-using-gis-and-photogrammetry-case-study-of-karaman-turkiye-f179494c671c>
- Zhou, Y., Wilmink, D., Zeman, M., Isabella, O., & Ziar, H. (2023). A geographic information system-based large scale visibility assessment tool for multi-criteria photovoltaic planning on urban building roofs. *Renewable and Sustainable Energy Reviews*, 188. <https://doi.org/10.1016/j.rser.2023.113885>
- Zhou, Y., Zhuang, Z., Yang, F., Yu, Y., & Xie, X. (2017). Urban morphology on heat island and building energy consumption. *Procedia Engineering*, 205, 2401–2406. <https://doi.org/10.1016/j.proeng.2017.09.862>

8. APPENDIX

8.1. Organising and documenting research data

Folder structure and naming conventions

The folders are numbered and have a searchable name. They are saved as per the stage of the process, i.e., if it is raw acquired files, processed file, analysis, or derived results. Reports and presentations are saved separately in separate folders.

A shortened version of file hierarchy is as follows:

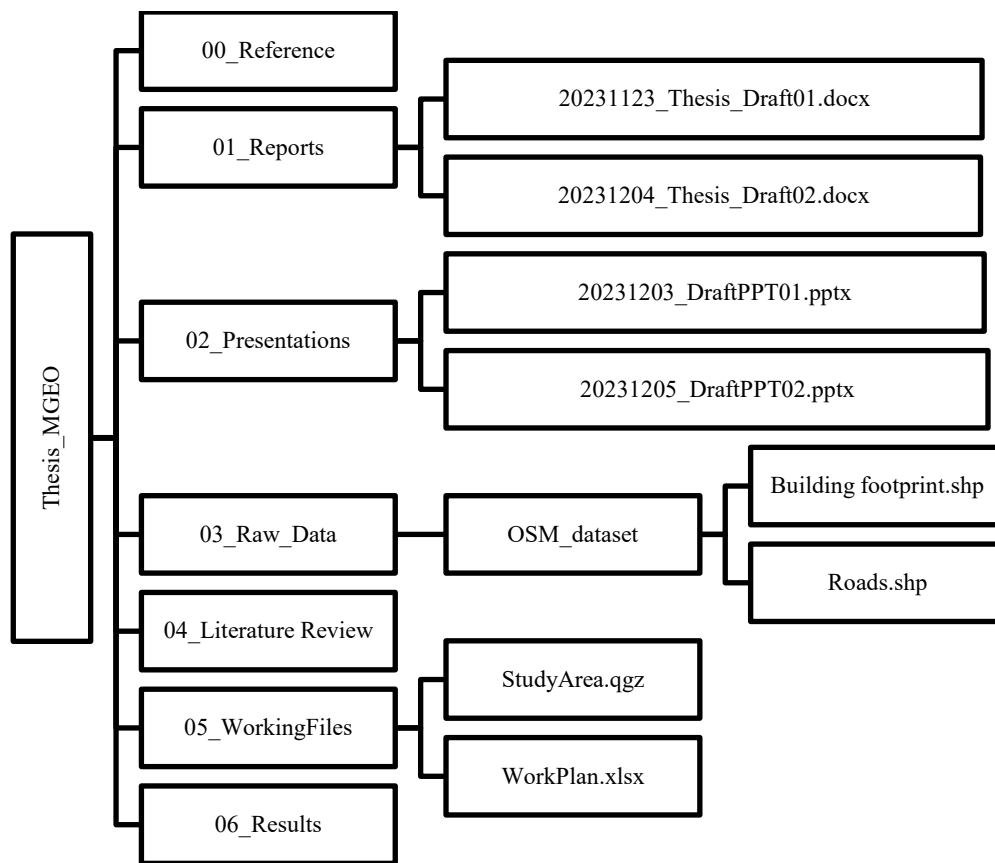


Figure 36 - Folder Structure

- For naming files of results, the date of creation is used, followed by a searchable name and year of study, and the version of the data. For example: 20231203_DraftPPT01.pptx
- Version control is done by adding suffixes. For code, Git versions will be used.
- Metadata standards will be as per ISO 19115.
- Files are to be stored locally as of now, with regular backups on a hard drive. Final files to be uploaded to ITC server as instructed.

8.2. Detailed step-by-step workflow – Pre-processing on CloudCompare

- Download AHN-4 dataset from PDOK. Download .LAZ from PDOK.

- Import to CloudCompare to Inspect the LIDAR dataset. The data is already filtered into various categories such as Ground, Building, Noise and so on.
- Filter using Scalar value for Ground alone, and for Ground+buildings. This gives us the basis for creating a DEM using Ground points, and DSM using Ground+building points.
- The area can be cropped using in-built functions in Cloud Compare.
- Process/crop and save as .las using CloudCompare

8.2.1. Lidar Acquisition

AHN-4 LIDAR dataset is downloaded as a compressed .laz file from PDOK/Geotiles.nl. Using the interactive tile map, the required tile of any part of Netherlands can be chosen. The tile used here is 34FN2_12 and is a tile of the buurt of Twekkelerveld in Enschede.

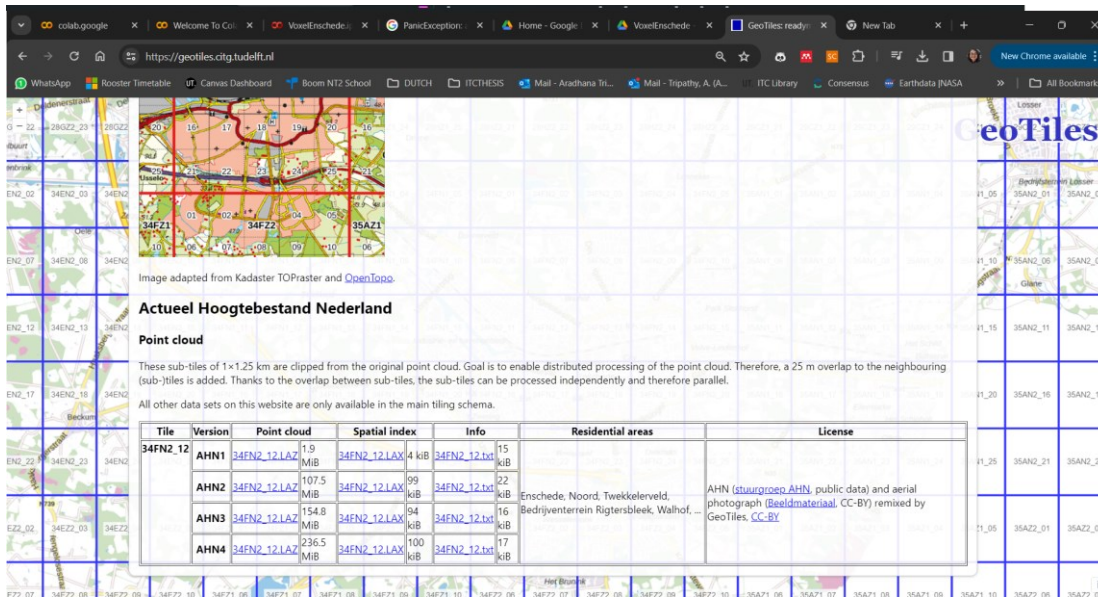


Figure 37 - Tile selection on Geotiles website

8.2.2. Inspect data in CloudCompare

The downloaded point cloud can be visualized easily in the software CloudCompare, which is designed to handle point clouds. Click File>Open>'Yourfile.laz' – navigate to your saved file.

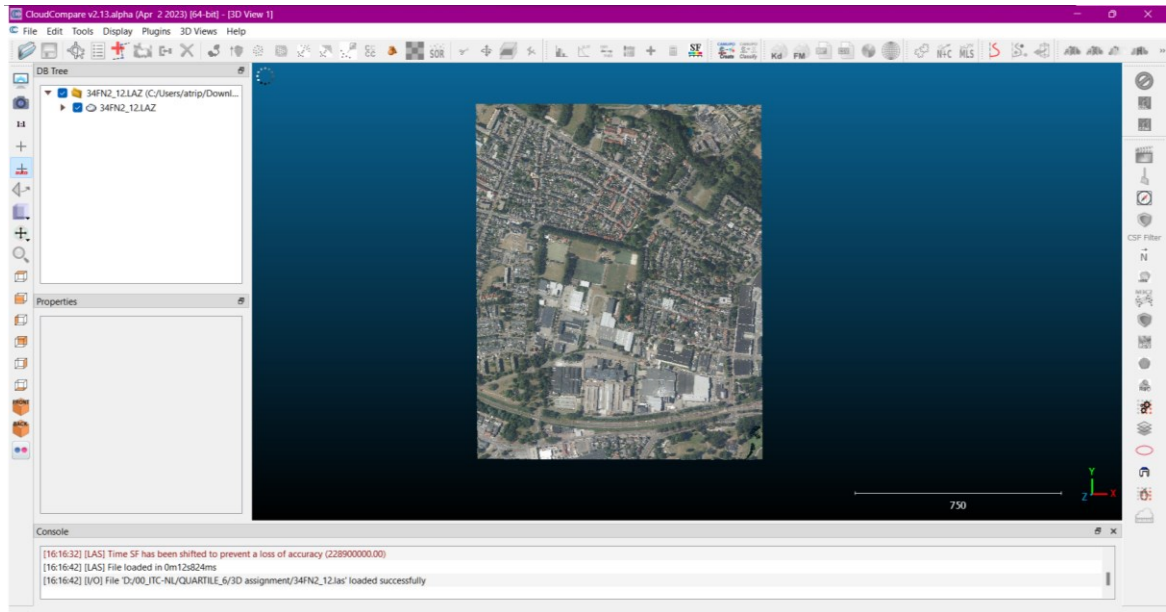


Figure 38 - Visualising point cloud tile on CloudCompare

Zoom into area of interest in the north of the tile, which is composed of residential zones. The tile has height information stored in the points, and the colour is taken from the superimposed imagery.

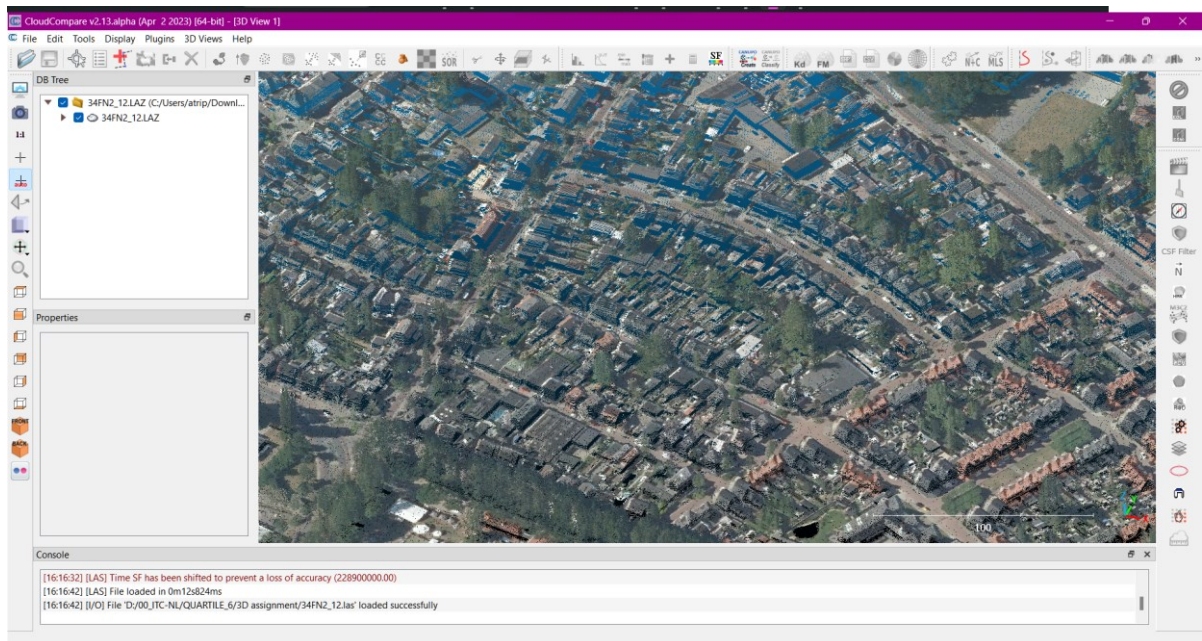


Figure 39 - Zooming into model on CloudCompare

Convert file to .las format for further processing by using LAS Save options, as .las is easier to work with in other software. Keep as options as they are and retain the original scale.

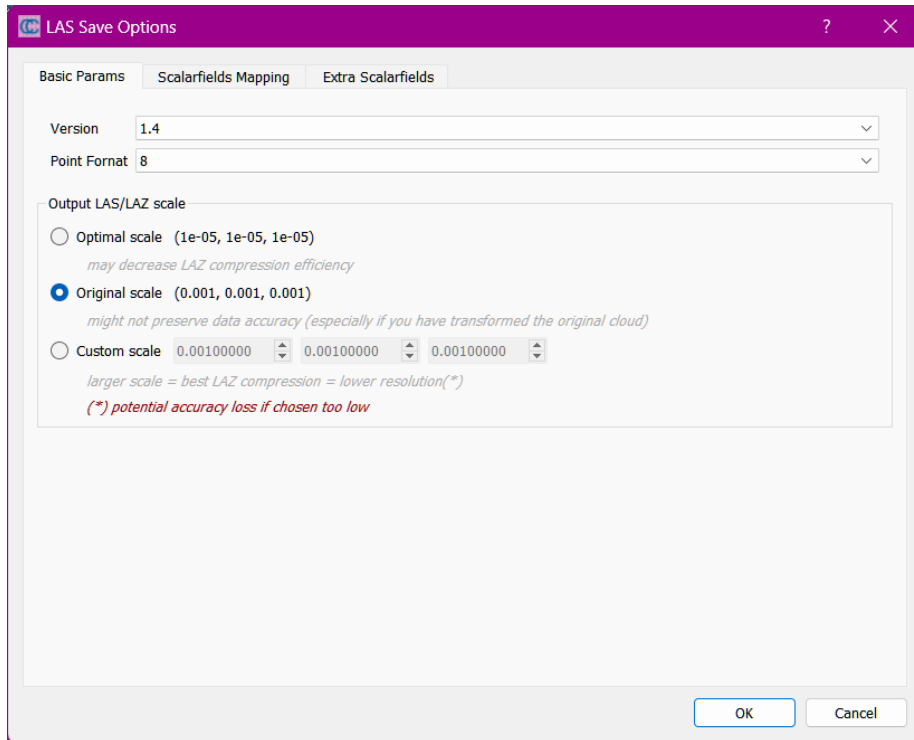


Figure 40 - Convert to .las format and retain scale

8.2.3. Segment/Isolate building information

As the tile is quite large, and bigger than the area of Interest, 'SegmentIn' command is used to cut out the segment of interest. This divides the .las file into two different files. For the rest of the project, we will model with the smaller residential zone.

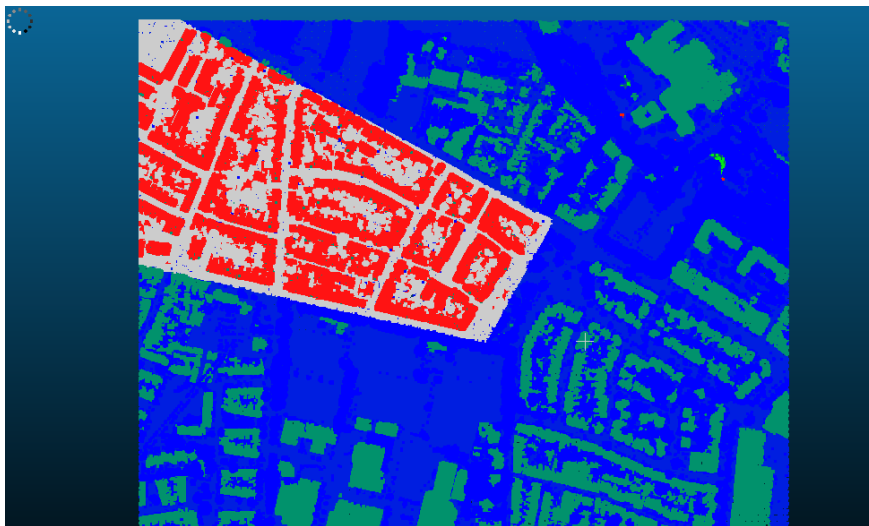


Figure 41 - Selecting part of point cloud for further modelling

The AHN-4 data already has values given to segmented clouds in the Scalar Value field. This means it has already been segmented and classified and does not need to be classified again.

Visible	Name	Code	Color	Count
<input checked="" type="checkbox"/>	Misc Permanent	82		0
<input checked="" type="checkbox"/>	Not classified	0		0
<input checked="" type="checkbox"/>	Overlap	12		0
<input checked="" type="checkbox"/>	Model Keypoint	8		0
<input checked="" type="checkbox"/>	Unclassified	1		774793
<input checked="" type="checkbox"/>	Substation	75		0
<input checked="" type="checkbox"/>	Structure Top Points	67		0
<input checked="" type="checkbox"/>	Transmission Tower	15		0
<input checked="" type="checkbox"/>	Ground	2		1330811
<input checked="" type="checkbox"/>	Building	6		0
<input checked="" type="checkbox"/>	Rail	10		0
<input checked="" type="checkbox"/>	Low vegetation	3		0
<input checked="" type="checkbox"/>	Shield Attachment Points	65		0
<input checked="" type="checkbox"/>	Road surface	11		0
<input checked="" type="checkbox"/>	Conductor Attachment Points	64		0
<input checked="" type="checkbox"/>	Structure Bottom Points	68		0
<input checked="" type="checkbox"/>	Misc Fences	83		0

Input Class: All Points Output Class: Building

Figure 42 - Filtering by Scalar Value of layers in CC – this is for the layer which only contains the ground and unclassified points.

Using Scalar Field, one can clearly see ground points, trees, and buildings in the visualization.

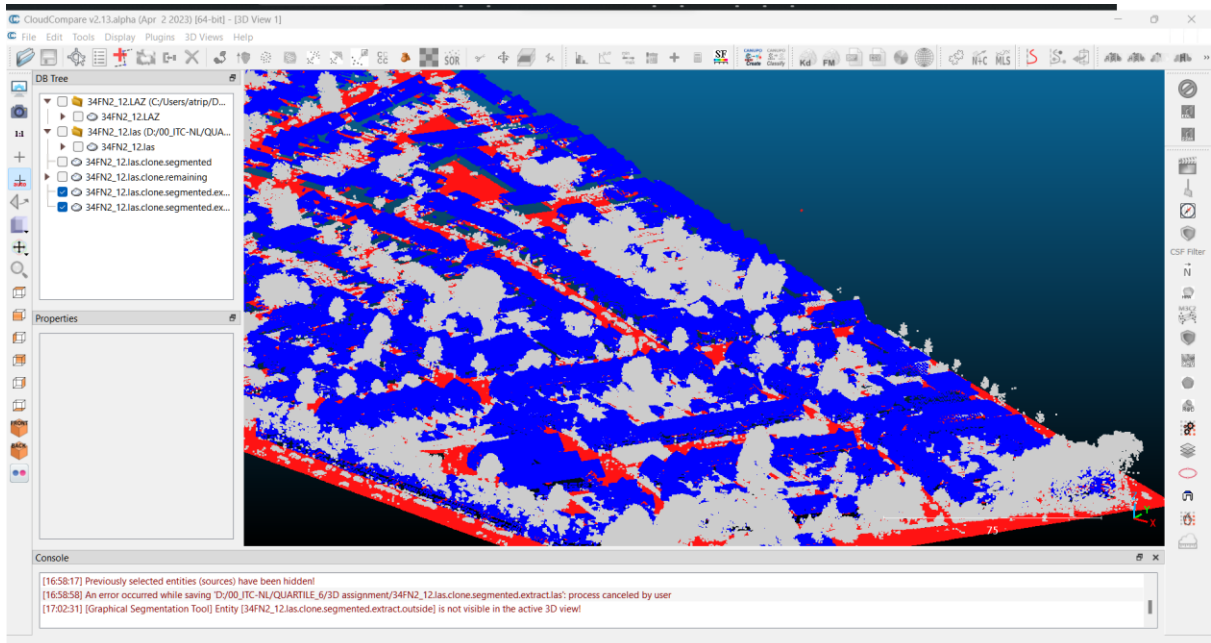


Figure 43 - Visualising scalar fields in CC

The building code is 6. Using this value, I do Edit>Scalar fields> Filter by value, in range 6 to 6 to only extract buildings. As can be seen in the figure below using the RGB colours, only the building data points have been removed out into a different .las file.

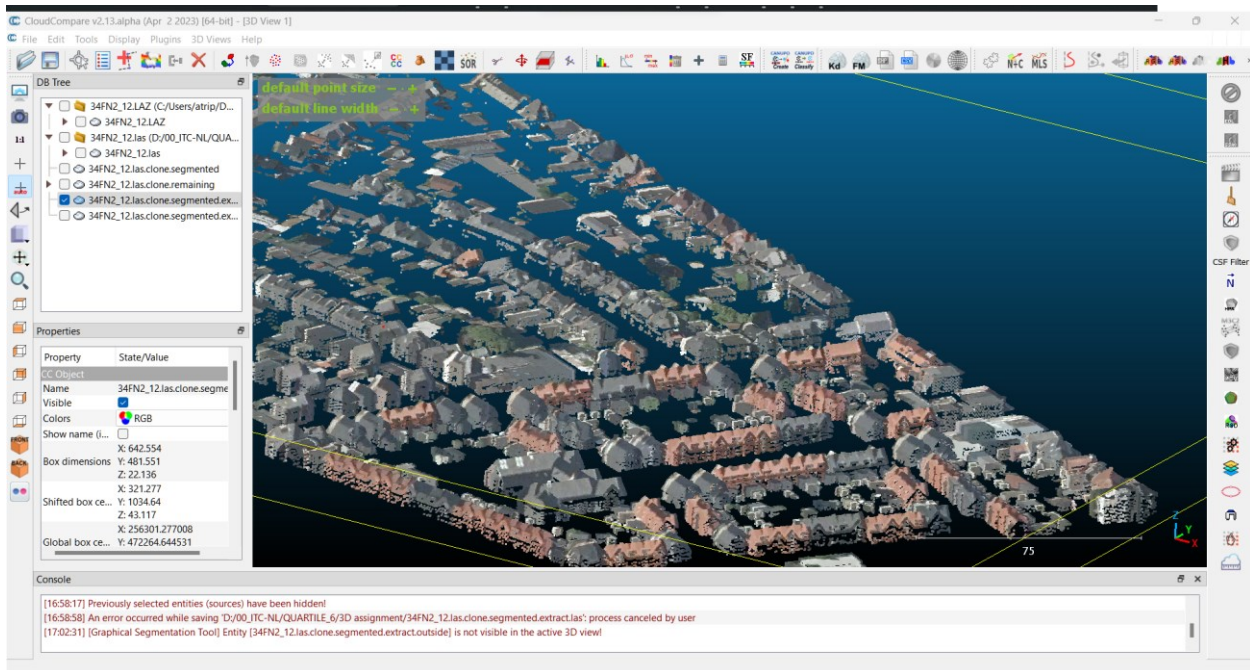


Figure 44 - Separating and only visualising building data points

8.2.4. Open in QGIS – LASTools

Download and install from net to c/lastools. Then install plugin. Check settings to see if the directory of the plugin is set to c/lastools or it will not work – also will fail.

8.2.5. Split to 1mil point tiles using lastools

Lastools is a licensed software – cannot process more than 1.5mil points at a time. Split using LASSplit to make it manageable.

https://www.youtube.com/watch?v=9LUuMYzwjfl&ab_channel=HansvanderKwast

In addition, can also use code used in the Enschede Workbench to convert Las to 3d array to DEM. Takes 1.5 hours on a 1.7mil point las file for 0.5m DEM cell size.

8.2.6. Convert to DEM using las2dem folder

Save output as tif, using smaller tile size of 0.25m. Save to a new DEM folder. This is being done with the full segmented LAS file – will give DSM.

Add the 4 DEM tif files to the correct projection RDNew QGIS file. Build virtual raster using Raster>Misc>Build Virtual raster

8.3. Detailed step-by-step workflow – Estimating Solar potential and savings per rooftop

8.3.1. Install UMEP in QGIS

- Install using manage plugins.
- UMEP for processing also requires installation through OSGeo4W shell. Use method on the UMEP GitHub for working with shell installations.
- Download weather data from EU-RJC TMY yearly weather data. Csv and EPW file for further work.
- https://re.jrc.ec.europa.eu/pvg_tools/en/#TMY

8.3.2. Calculate Slope and Aspect – Raster Analysis

- Using Raster Analysis, calculate Slope and Aspect keeping angle values – 0-90, 1-360 etc.
- Reclassify – find out the correct way to range the reclass for N,S,E,W.
- Slope classes – 0-25 (can be managed), 25-60 (ideal), 60+ (unsuitable). Filter the rasters using

(("DEM@1" > 0) * "DEMr@1") on Raster Calculator. The syntax is different from how calculations are done in ArcGIS.

- Remove noise using the Sieve tool – fill patches and gaps, remove small issues – check.

8.3.3. Building footprints

- Building footprints can be processed from OSM or from top10NL (PDOK) (more accurate/acceptable)
- Filter to remove polygons less than 15 sqm which is unsuitable for solar panels and is thus unusable in this analysis.
- Clip the Aspect and Slope Raster to the building shp file.
- Polygonise tool to make rasters into DEM shp.
- Intersect the clipped slope and raster files to get common roof areas sharing single values of slope and aspect respectively.

8.3.4. Buffering/gap filling

Figure out post-processing – simplify/regularize the borders to get info on usable roof planes.

8.3.5. Zonal statistics

Transfer value of aspect and slope to the polygons using zonal stats? – check – mean value using circular statistics for aspect. Regular arithmetic for slope.

8.3.6. UMEP for processing setup

UMEP for processing includes python dependencies. There may be errors in installation saying certain packages or modules are not available. In that case, open the OSGeo4WSHELL from the start menu, and use pip install command to install it. In my case, jaydebeapi was missing. Another alternative in case you cannot find out why an error is occurring, is to ask in the GitHub Issues page.

```

OSGeo4W Shell
run o-help for a list of available commands
C:\Program Files\QGIS 3.22.9>python -m pip install jaydebeapi
Defaulting to user installation because normal site-packages is not writeable
Collecting jaydebeapi
  Using cached JayDeBeApi-1.2.3-py3-none-any.whl (26 kB)
Collecting JPype1 (from jaydebeapi)
  Using cached JPype1-1.5.0-cp39-cp39-win_amd64.whl.metadata (5.0 kB)
Requirement already satisfied: packaging in c:\users\atrip\appdata\roaming\python\python39\site-packages (from JPype1->jaydebeapi) (23.2)
Downloading JPype1-1.5.0-cp39-cp39-win_amd64.whl (351 kB)
  351.6/351.6 kB 4.4 MB/s eta 0:00:00
Installing collected packages: JPype1, jaydebeapi
Successfully installed JPype1-1.5.0 jaydebeapi-1.2.3
C:\Program Files\QGIS 3.22.9>

```

Figure 45 - Install necessary modules

https://umep-docs.readthedocs.io/en/latest/Getting_Started.html#adding-missing-python-libraries-and-other-osgeo-functionalities

8.3.7. Calculate Wall Height and Wall Aspect (UMEP)

This is done as pre-processing input for shadow generation, accounting for the effect of vertical walls and their aspect on casting shadows.

- Go to UMEP Preprocessor>Urban Geometry>Wall Height and Aspect
- Input the DSM as Ground and Building DSM. Do not enter vegetation canopy.
- Save both Wall aspect and wall height files to disk.

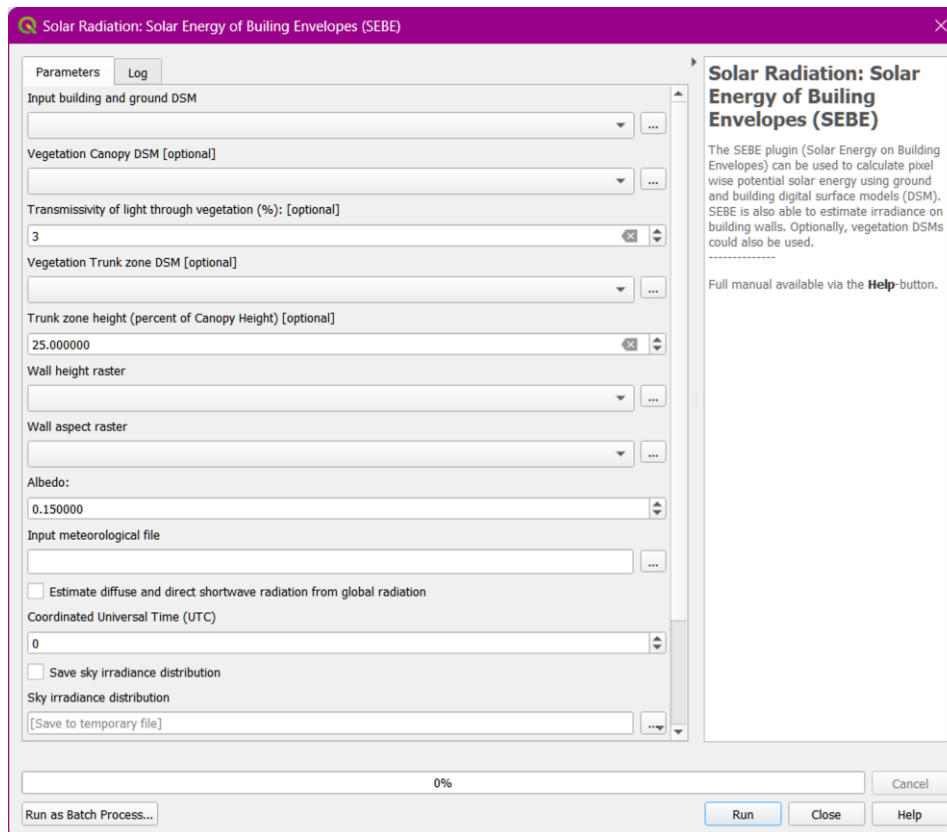
8.3.8. Shadow Generation

- UMEP for processing has a daily shadow generation function that can allow for creating shadow patterns every 30 mins or as decided.
- Using that function, shadows are generated for different months/important days like the solstices and equinoxes.
- Can also generate average shadow for the day.
- Importance of seasons in shading – summer exposure more important than winter – check citation.
- Create binary shadow rasters – suitable and unsuitable by filtering for value = maybe minimum 60% exposure? – trial and error. Using Raster calculator on the Aggregated shadow, enter the expression: ("AggShadow_Jun21@1" > 0.6)*1 + ("AggShadow_Jun21@1" <= 0.6)*0
- Intersect with roof plane – zonal statistics to filter out highly shaded rooftops – check process. Calculate shadow mean per polygon. Using binary classification per cell, can see what % receives sunlight.

8.3.9. Solar simulation using UMEP

Convert EPW file to .txt using Meteorological pre-processor in UMEP.

Input needs DSM+buildings and EPW weather file (converted to .txt) – real data value.



Once the raster of kWh is done, filter that to suitability using the expression: ("IRR@1" >= 900) * "IRR@1" + ("IRR" < 900) * 0 in raster calculator, to only isolate suitable cells.

8.3.10. Shadow x Energy Raster

The shadow raster at 60% is binary, which means the cells receiving sun at 60% or more of the day are classified a 1, the rest as 0. When multiplied with the energy filtered raster (at 900kWh and above), it only shows those cells which are above 900kWh and also receiving sun without shadow 60% of the time.

8.3.11. Filtering cells at 950, with those below at null value

This is done because Region Grouping cannot be done when cells have different values. It has to be converted to a 1-0 binary raster to allow for clumping and vectorizing to filter by area.

- **Create Mask Raster:** Use the "Raster Calculator" tool to create a mask raster where cells with values above 900 are assigned a value of 1, and all other cells are assigned a value of 0. This mask will identify the cells of interest.

("Solar irradiation@1" > 900) * 1

- **Polygonize Mask Raster:** Use the "Raster pixels to polygons" tool to convert the mask raster into a polygon layer. This will create polygons representing the contiguous areas of cells with values above 950.
- **Intersect with Overlaying Polygons:** Use the "Intersection" tool to overlay the polygons obtained from step 2 with your original polygon layer. This will ensure that you retain only the portions of polygons that intersect with the areas where your raster has values above 900.



Map 31 - Suitable cell filtration using Raster Calculator

8.3.12. Contiguous group identification

Using `r.clump` in GRASS plugin, cluster all contiguous pixels



Map 32 - identifying contiguous clusters of suitable cells

Vectorize these pixels, calculate area by Field Calculator (`$area`). This will be calculated in sqm.

It takes 1.6sqm to place a single panel. We take a round figure of 2sqm to place one singular panel as the minimum.

Using Select by expression (`Area ≥ 2`), select desired polygons, and save selected features as new layer.



Figure 46 - Converting contiguous patches to vector

Using these new clusters, Clip the ShadowXEnergyabove950 Raster, to get final raster output of clustered rooftop cells that receive low shadow and high irradiation above 950kWh per annum.



Figure 47 - IRR value of suitable cells

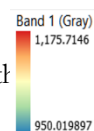
This is the final raster output of filtered cells that will be used for Zonal Statistics

8.3.13. Zonal Statistics - Transfer suitable area to Shp

Calculate Slope of roof, as that is needed to calculate the actual roof surface area th

Zonal statistics – mean value of pixel to polygon from top10NL

Also do count of cells within each pixel, mean and median values.



le.

8.3.14. Electricity Output Calculation:

Using global formula

$$E = A \cdot r \cdot H \cdot PR$$

E = Energy (kWh)

A = Total solar panel Area (m²)

r = solar panel yield or efficiency (%)

H = Annual average solar radiation on tilted panels (shadings not included)

PR = Performance ratio, coefficient for losses (between 0.5 and 0.9, default value 0.75)

Here, A is calculated in Field calculator as Area = count0.50.5 (as the cell size is 0.5m)

H is the average annual solar rad from UMEP - taken here as the median kWh received by the roof.

R is assumed at 14%

PR is assumed at default value 0.75 - solar module efficiency, assumed at 14% because PVGIS uses 14% for Crystalline Silicone modules.

8.3.15. Price calculation

0.35 EUR per kWh. Source: <https://www.overstappen.nl/energie/compare-energy/energy-prices-netherlands/#:~:text=The>

Using field calculator, calculate new field of Yield per Rooftop (Elec_Calc) = Area*mean0.75*0.14



Figure 48 - Estimating Energy production per rooftop - in kWh.

Given that 1kWh of energy is 35 cents, final savings estimate can be made using Field Calculator.



Figure 49 - Estimating Euro value of the estimated energy (legend in Euros)

These values are the maximum possible savings in EUR.

In this Area:

- 14448.250 sqm is highly suitable rooftop area, out of a total of 49168sqm (calculated from Gebouw .dbf layer).
- EUR 541936.00 is the MAX amount monetary savings predicted.
- 1548377.00 kWh is the MAX energy output predicted.

This is calculated from the .dbf of the Zonal Statistics .shp file on Excel.

8.3.16. Issues with UMEP for tif

When tif is loaded, save again as a geotiff by exporting it. Otherwise SEBE runs into projection errors and does not run

Formula to keep only cells with raster values over 900, after shadowxIrrX contig

This converts everything over 900 to 1, and under 900 to 0: (makes a binary)

`(("shadowxIrrXcontig2@1">900)*1)+ (("shadowxIrrXcontig2@1"<900)*0)`

This keeps the values over 900 intact and deletes the rest:

`(("shadowxIrrXcontig2@1">900)* "shadowxIrrXcontig2@1">)+ (("shadowxIrrXcontig2@1"<900)*0)`

Formula for shadow binary:

`("Aggregatedshadow_SINGLE@1">0.6)*1 + ("Aggregatedshadow_SINGLE@1"<0.6)*0'`

Formula for roof irradiance filter raster:

```
("ROOFIRR@1" > 900)*"ROOFIRR@1" + ("ROOFIRR@1"<900)*0
```

Irradiance x shadow binary:

```
"Irradiance 900@1" * "Shadow Binary@1"
```

Followed by: GDAL>Clip raster by mask layer

Raster input: ShadowX Irr

Mask: Polygon Shp of contig Area

Output: cells that fall within accepted contig areas - ClippedMask

But here too, there are cells with 0 value. We want them deleted, or they interfere with the zonal stats

```
("Clipped (mask)@1" > 900) * "Clipped (mask)@1"+ ("Clipped (mask)@1"<= 900) * 0/0
```

This often does not work

Thus, now we convert this clip to binary 1 and 0 – Raster Calculator

```
("Clipped (mask)@1" >900)*1'
```

Polygonize raster to Vector

Attribute Table has DN values

Select and delete all values with 0 (Extract by attribute)

Clip ShadowXIRRXCContig with Value 1 shp

This will ONLY retain the pixels above 900

Now do Zonal Stats

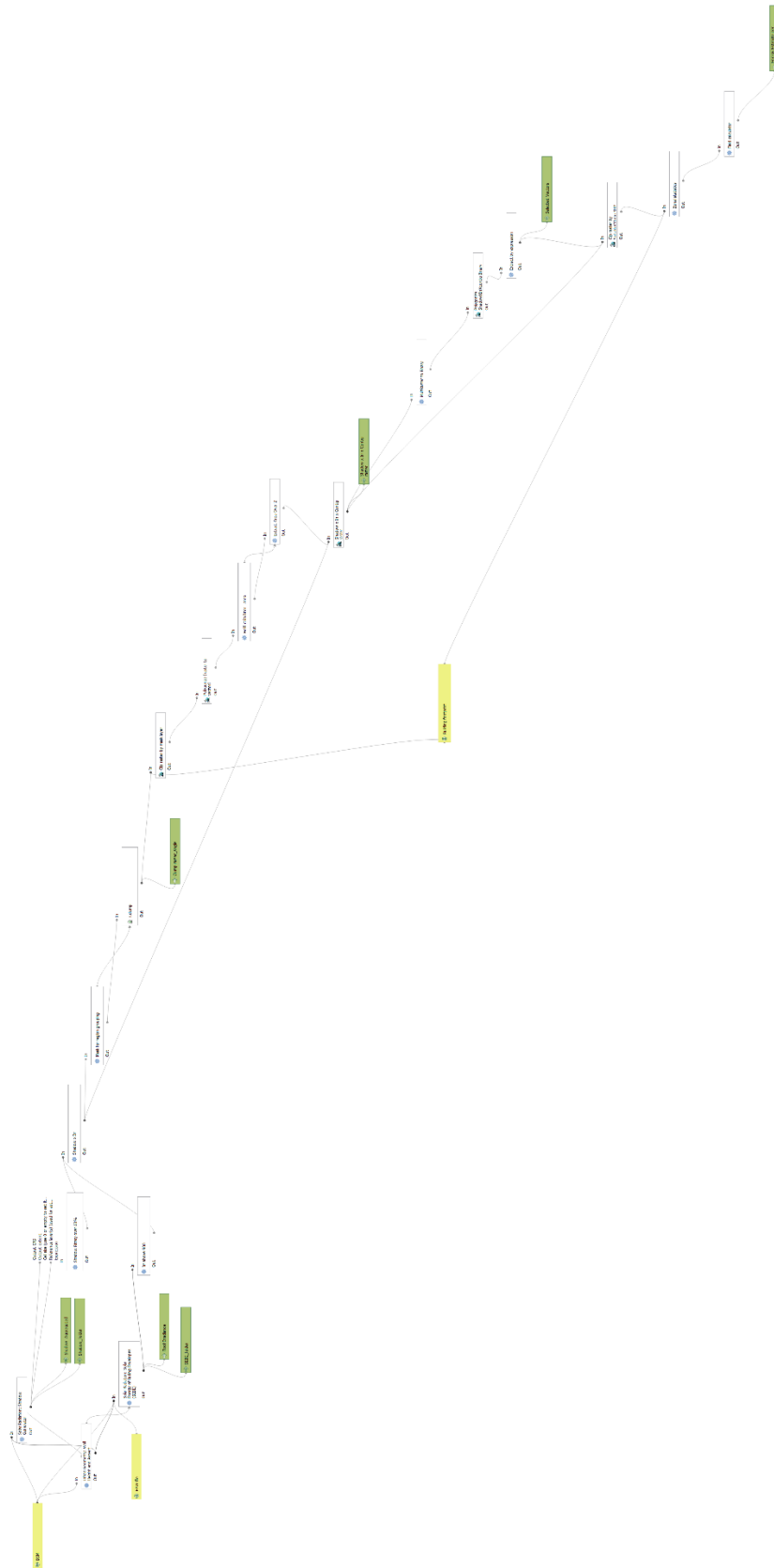


Figure 50 - The suitability filtering is made replicable and time-efficient using Graphic Modeller.

8.3.17. Python Script of Solar Model

```
"""
Model exported as python.
Name : Solar Graphic FINALMODEL
Group :
With QGIS : 32209
"""

from qgis.core import QgsProcessing
from qgis.core import QgsProcessingAlgorithm
from qgis.core import QgsProcessingMultiStepFeedback
from qgis.core import QgsProcessingParameterVectorLayer
from qgis.core import QgsProcessingParameterRasterLayer
from qgis.core import QgsProcessingParameterFile
from qgis.core import QgsProcessingParameterRasterDestination
from qgis.core import QgsProcessingParameterFeatureSink
from qgis.core import QgsProcessingParameterFolderDestination
from qgis.PyQt.QtCore import QDateTime
from qgis.PyQt.QtCore import QDateTime
import processing

class SolarGraphicFinalmodel(QgsProcessingAlgorithm):

    def initAlgorithm(self, config=None):
        self.addParameter(QgsProcessingParameterVectorLayer('buildingfootprint', 'Building footprint', defaultValue=None))
        self.addParameter(QgsProcessingParameterRasterLayer('dsm', 'DSM', defaultValue=None))
        self.addParameter(QgsProcessingParameterFile('epwfile', 'EPW file', behavior=QgsProcessingParameterFile.File, fileFilter='All Files (*.*)', defaultValue=None))
        self.addParameter(QgsProcessingParameterRasterDestination('ShadowXIrrXContigRaster', 'Shadow x Irr x Contig raster', createByDefault=True, defaultValue=None))
        self.addParameter(QgsProcessingParameterRasterDestination('ClumpRaster_single', 'Clump raster_single', createByDefault=True, defaultValue=None))
        self.addParameter(QgsProcessingParameterFeatureSink('SelectedVectors', 'Selected Vectors', type=QgsProcessing.TypeVectorAnyGeometry, createByDefault=True, defaultValue=None))
        self.addParameter(QgsProcessingParameterFeatureSink('EnergyEstimatePerBuilding', 'Energy Estimate per Building', type=QgsProcessing.TypeVectorAnyGeometry, createByDefault=True, supportsAppend=True, defaultValue=None))
```

```

        self.addParameter(QgsProcessingParameterRasterDestination('Shadow_aggr
egated', 'Shadow_Aggregated', optional=True, createByDefault=False,
defaultValue=None))
        self.addParameter(QgsProcessingParameterFolderDestination('Shadow_fold
er', 'Shadow_folder', createByDefault=True, defaultValue=None))
        self.addParameter(QgsProcessingParameterRasterDestination('RoofIrradia
nce', 'Roof Irradiance', optional=True, createByDefault=False,
defaultValue=None))
        self.addParameter(QgsProcessingParameterFolderDestination('Sebe_folder
', 'SEBE_folder', createByDefault=True, defaultValue=None))

    def processAlgorithm(self, parameters, context, model_feedback):
        # Use a multi-step feedback, so that individual child algorithm
progress reports are adjusted for the
        # overall progress through the model
        feedback = QgsProcessingMultiStepFeedback(19, model_feedback)
        results = {}
        outputs = {}

        # Urban Geometry: Wall Height and Aspect
        alg_params = {
            'INPUT': parameters['dsm'],
            'INPUT_LIMIT': 3,
            'OUTPUT_ASPECT': QgsProcessing.TEMPORARY_OUTPUT,
            'OUTPUT_HEIGHT': QgsProcessing.TEMPORARY_OUTPUT
        }
        outputs['UrbanGeometryWallHeightAndAspect'] =
processing.run('umep:Urban Geometry: Wall Height and Aspect', alg_params,
context=context, feedback=feedback, is_child_algorithm=True)

        feedback.setCurrentStep(1)
        if feedback.isCanceled():
            return {}

        # Solar Radiation: Solar Energy of Building Envelopes (SEBE)
        alg_params = {
            'ALBEDO': 0.15,
            'INPUTMET': parameters['epwfile'],
            'INPUT_ASPECT':
outputs['UrbanGeometryWallHeightAndAspect']['OUTPUT_ASPECT'],
            'INPUT_CDSM': None,
            'INPUT_DSM': parameters['dsm'],
            'INPUT_HEIGHT':
outputs['UrbanGeometryWallHeightAndAspect']['OUTPUT_HEIGHT'],
            'INPUT_TDSM': None,
            'INPUT_THEIGHT': 25,
            'ONLYGLOBAL': True,
            'SAVESKYIRR': False,

```

```

        'TRANS_VEG': 3,
        'UTC': 1,
        'IRR_FILE': QgsProcessing.TEMPORARY_OUTPUT,
        'OUTPUT_DIR': parameters['Sebe_folder'],
        'OUTPUT_ROOF': parameters['RoofIrradiance']
    }
    outputs['SolarRadiationSolarEnergyOfBuilingEnvelopesSebe'] =
processing.run('umep:Solar Radiation: Solar Energy of Builing Envelopes
(SEBE)', alg_params, context=context, feedback=feedback,
is_child_algorithm=True)
    results['RoofIrradiance'] =
outputs['SolarRadiationSolarEnergyOfBuilingEnvelopesSebe']['OUTPUT_ROOF']
    results['Sebe_folder'] =
outputs['SolarRadiationSolarEnergyOfBuilingEnvelopesSebe']['OUTPUT_DIR']

    feedback.setCurrentStep(2)
    if feedback.isCanceled():
        return {}

    # Irr above 900
    alg_params = {
        'CELLSIZE': 0,
        'CRS': 'ProjectCrs',
        'EXPRESSION': '("\Roof Irradiance\ from algorithm \Solar
Radiation: Solar Energy of Builing Envelopes (SEBE)\@1" >= 900)*"\Roof
Irradiance\ from algorithm \Solar Radiation: Solar Energy of Builing
Envelopes (SEBE)\@1" + ("\Roof Irradiance\ from algorithm \Solar
Radiation: Solar Energy of Builing Envelopes (SEBE)\@1" < 900)*0\n',
        'EXTENT':
outputs['SolarRadiationSolarEnergyOfBuilingEnvelopesSebe']['OUTPUT_ROOF'],
        'LAYERS':
outputs['SolarRadiationSolarEnergyOfBuilingEnvelopesSebe']['OUTPUT_ROOF'],
        'OUTPUT': QgsProcessing.TEMPORARY_OUTPUT
    }
    outputs['IrrAbove900'] = processing.run('qgis:rastercalculator',
alg_params, context=context, feedback=feedback, is_child_algorithm=True)

    feedback.setCurrentStep(3)
    if feedback.isCanceled():
        return {}

    # Solar Radiation: Shadow Generator
    alg_params = {
        'DATEINI': QDate(2024, 6, 27),
        'DST': False,
        'INPUT_ASPECT':
outputs['UrbanGeometryWallHeightAndAspect']['OUTPUT_ASPECT'],
        'INPUT_CDSM': None,

```

```

        'INPUT_DSM': parameters['dsm'],
        'INPUT_HEIGHT':
outputs['UrbanGeometryWallHeightAndAspect']['OUTPUT_HEIGHT'],
        'INPUT_TDSM': None,
        'INPUT_THEIGHT': 25,
        'ITERTIME': 60,
        'ONE_SHADOW': False,
        'TIMEINI': QTime(21, 59, 53),
        'TRANS_VEG': 3,
        'UTC': 1,
        'OUTPUT_DIR': parameters['Shadow_folder'],
        'OUTPUT_FILE': parameters['Shadow_aggregated']
    }
    outputs['SolarRadiationShadowGenerator'] = processing.run('umep:Solar
Radiation: Shadow Generator', alg_params, context=context, feedback=feedback,
is_child_algorithm=True)
    results['Shadow_aggregated'] =
outputs['SolarRadiationShadowGenerator']['OUTPUT_FILE']
    results['Shadow_folder'] =
outputs['SolarRadiationShadowGenerator']['OUTPUT_DIR']

    feedback.setCurrentStep(4)
    if feedback.isCanceled():
        return {}

    # Shadow Binary over 60%
    alg_params = {
        'CELLSIZE': 0.5,
        'CRS': 'ProjectCrs',
        'EXPRESSION': '("Shadow_Aggregated\' from algorithm \'Solar
Radiation: Shadow Generator\'@1" > 0.6) * 1 + ("Shadow_Aggregated\' from
algorithm \'Solar Radiation: Shadow Generator\'@1" < 0.6) * 0\n',
        'EXTENT': outputs['SolarRadiationShadowGenerator']['OUTPUT_FILE'],
        'LAYERS': outputs['SolarRadiationShadowGenerator']['OUTPUT_FILE'],
        'OUTPUT': QgsProcessing.TEMPORARY_OUTPUT
    }
    outputs['ShadowBinaryOver60'] =
processing.run('qgis:rastercalculator', alg_params, context=context,
feedback=feedback, is_child_algorithm=True)

    feedback.setCurrentStep(5)
    if feedback.isCanceled():
        return {}

    # Shadow x Irr
    alg_params = {
        'CELLSIZE': 0,
        'CRS': None,

```

```

        'EXPRESSION': '"\'Output\' from algorithm \'Shadow Binary over
60%\@1" * "\'Output\' from algorithm \'Irr above 900%\@1"',
        'EXTENT': None,
        'LAYERS':
[outputs['ShadowBinaryOver60']['OUTPUT'],outputs['IrrAbove900']['OUTPUT']],
        'OUTPUT': QgsProcessing.TEMPORARY_OUTPUT
    }
    outputs['ShadowXIrr'] = processing.run('qgis:rastercalculator',
alg_params, context=context, feedback=feedback, is_child_algorithm=True)

    feedback.setCurrentStep(6)
    if feedback.isCanceled():
        return {}

    # Mask for region grouping
    alg_params = {
        'CELLSIZE': 0,
        'CRS': None,
        'EXPRESSION': '("\'Output\' from algorithm \'Shadow x Irr%\@1" >
900) * 1',
        'EXTENT': None,
        'LAYERS': outputs['ShadowXIrr']['OUTPUT'],
        'OUTPUT': QgsProcessing.TEMPORARY_OUTPUT
    }
    outputs['MaskForRegionGrouping'] =
processing.run('qgis:rastercalculator', alg_params, context=context,
feedback=feedback, is_child_algorithm=True)

    feedback.setCurrentStep(7)
    if feedback.isCanceled():
        return {}

    # r.clump
    alg_params = {
        '-d': False,
        'GRASS_RASTER_FORMAT_META': '',
        'GRASS_RASTER_FORMAT_OPT': '',
        'GRASS_REGION_CELLSIZE_PARAMETER': 0,
        'GRASS_REGION_PARAMETER': None,
        'input': outputs['MaskForRegionGrouping']['OUTPUT'],
        'threshold': 0,
        'title': 'Coniguous patch r.clump',
        'output': parameters['ClumpRaster_single']
    }
    outputs['Rclump'] = processing.run('grass7:r.clump', alg_params,
context=context, feedback=feedback, is_child_algorithm=True)
    results['ClumpRaster_single'] = outputs['Rclump']['output']

```

```

feedback.setCurrentStep(8)
if feedback.isCanceled():
    return {}

# Clip raster by mask layer
alg_params = {
    'ALPHA_BAND': False,
    'CROP_TO_CUTLINE': True,
    'DATA_TYPE': 0, # Use Input Layer Data Type
    'EXTRA': '',
    'INPUT': outputs['Rclump']['output'],
    'KEEP_RESOLUTION': False,
    'MASK': parameters['buildingfootprint'],
    'MULTITHREADING': False,
    'NODATA': None,
    'OPTIONS': '',
    'SET_RESOLUTION': False,
    'SOURCE_CRS': 'ProjectCrs',
    'TARGET_CRS': 'ProjectCrs',
    'X_RESOLUTION': None,
    'Y_RESOLUTION': None,
    'OUTPUT': QgsProcessing.TEMPORARY_OUTPUT
}
outputs['ClipRasterByMaskLayer'] =
processing.run('gdal:cliprasterbymasklayer', alg_params, context=context,
feedback=feedback, is_child_algorithm=True)

feedback.setCurrentStep(9)
if feedback.isCanceled():
    return {}

# Polygonize (raster to vector)
alg_params = {
    'BAND': 1,
    'EIGHT_CONNECTEDNESS': False,
    'EXTRA': '',
    'FIELD': 'DN',
    'INPUT': outputs['ClipRasterByMaskLayer']['OUTPUT'],
    'OUTPUT': QgsProcessing.TEMPORARY_OUTPUT
}
outputs['PolygonizeRasterToVector'] =
processing.run('gdal:polygonize', alg_params, context=context,
feedback=feedback, is_child_algorithm=True)

feedback.setCurrentStep(10)
if feedback.isCanceled():
    return {}

```

```

# Field calculator - Area
alg_params = {
    'FIELD_LENGTH': 10,
    'FIELD_NAME': 'Area',
    'FIELD_PRECISION': 4,
    'FIELD_TYPE': 0, # Float
    'FORMULA': ' $area ',
    'INPUT': outputs['PolygonizeRasterToVector']['OUTPUT'],
    'OUTPUT': QgsProcessing.TEMPORARY_OUTPUT
}
outputs['FieldCalculatorArea'] =
processing.run('native:fieldcalculator', alg_params, context=context,
feedback=feedback, is_child_algorithm=True)

feedback.setCurrentStep(11)
if feedback.isCanceled():
    return {}

# Extract Area Over 2
alg_params = {
    'EXPRESSION': '"Area" > 2',
    'INPUT': outputs['FieldCalculatorArea']['OUTPUT'],
    'OUTPUT': QgsProcessing.TEMPORARY_OUTPUT
}
outputs['ExtractAreaOver2'] =
processing.run('native:extractbyexpression', alg_params, context=context,
feedback=feedback, is_child_algorithm=True)

feedback.setCurrentStep(12)
if feedback.isCanceled():
    return {}

# Shadow x Irr x Contig raster
alg_params = {
    'ALPHA_BAND': False,
    'CROP_TO_CUTLINE': True,
    'DATA_TYPE': 0, # Use Input Layer Data Type
    'EXTRA': '',
    'INPUT': outputs['ShadowXIrr']['OUTPUT'],
    'KEEP_RESOLUTION': True,
    'MASK': outputs['ExtractAreaOver2']['OUTPUT'],
    'MULTITHREADING': False,
    'NODATA': None,
    'OPTIONS': '',
    'SET_RESOLUTION': False,
    'SOURCE_CRS': 'ProjectCrs',
    'TARGET_CRS': 'ProjectCrs',
    'X_RESOLUTION': None,

```

```

        'Y_RESOLUTION': None,
        'OUTPUT': parameters['ShadowXIrrXContigRaster']
    }
    outputs['ShadowXIrrXContigRaster'] =
processing.run('gdal:cliprasterbymasklayer', alg_params, context=context,
feedback=feedback, is_child_algorithm=True)
    results['ShadowXIrrXContigRaster'] =
outputs['ShadowXIrrXContigRaster']['OUTPUT']

    feedback.setCurrentStep(13)
    if feedback.isCanceled():
        return {}

    # MultRaster to Binary
    alg_params = {
        'CELLSIZE': 0,
        'CRS': None,
        'EXPRESSION': '("\'Shadow x Irr x Contig raster\' from algorithm
\'Shadow x Irr x Contig raster\'@1" > 900)*1',
        'EXTENT':
'256056.500000000,256622.000000000,472024.545200000,472459.045200000
[EPSG:28992]',
        'LAYERS': outputs['ShadowXIrrXContigRaster']['OUTPUT'],
        'OUTPUT': QgsProcessing.TEMPORARY_OUTPUT
    }
    outputs['MultirasterToBinary'] =
processing.run('qgis:rastercalculator', alg_params, context=context,
feedback=feedback, is_child_algorithm=True)

    feedback.setCurrentStep(14)
    if feedback.isCanceled():
        return {}

    # Polygonize ShadowXIrrXcontig Binary
    alg_params = {
        'BAND': 1,
        'EIGHT_CONNECTEDNESS': False,
        'EXTRA': '',
        'FIELD': 'DN',
        'INPUT': outputs['MultirasterToBinary']['OUTPUT'],
        'OUTPUT': QgsProcessing.TEMPORARY_OUTPUT
    }
    outputs['PolygonizeShadowxirrxcontigBinary'] =
processing.run('gdal:polygonize', alg_params, context=context,
feedback=feedback, is_child_algorithm=True)

    feedback.setCurrentStep(15)
    if feedback.isCanceled():

```

```

        return {}

    # Extract by expression
    alg_params = {
        'EXPRESSION': '"DN">=1',
        'INPUT': outputs['PolygonizeShadowxirrxcontigBinary']['OUTPUT'],
        'OUTPUT': parameters['SelectedVectors']
    }
    outputs['ExtractByExpression'] =
processing.run('native:extractbyexpression', alg_params, context=context,
feedback=feedback, is_child_algorithm=True)
    results['SelectedVectors'] = outputs['ExtractByExpression']['OUTPUT']

    feedback.setCurrentStep(16)
    if feedback.isCanceled():
        return {}

    # Clip raster by SuitableContig SHP
    alg_params = {
        'ALPHA_BAND': False,
        'CROP_TO_OUTLINE': True,
        'DATA_TYPE': 0, # Use Input Layer Data Type
        'EXTRA': '',
        'INPUT': outputs['ShadowXirrXContigRaster']['OUTPUT'],
        'KEEP_RESOLUTION': False,
        'MASK': outputs['ExtractByExpression']['OUTPUT'],
        'MULTITHREADING': False,
        'NODATA': None,
        'OPTIONS': '',
        'SET_RESOLUTION': False,
        'SOURCE_CRS': 'ProjectCrs',
        'TARGET_CRS': 'ProjectCrs',
        'X_RESOLUTION': None,
        'Y_RESOLUTION': None,
        'OUTPUT': QgsProcessing.TEMPORARY_OUTPUT
    }
    outputs['ClipRasterBySuitablecontigShp'] =
processing.run('gdal:cliprasterbymasklayer', alg_params, context=context,
feedback=feedback, is_child_algorithm=True)

    feedback.setCurrentStep(17)
    if feedback.isCanceled():
        return {}

    # Zonal statistics
    alg_params = {
        'COLUMN_PREFIX': '_',
        'INPUT': parameters['buildingfootprint'],

```

```

        'INPUT_RASTER':
outputs['ClipRasterBySuitablecontigShp']['OUTPUT'],
        'RASTER_BAND': 1,
        'STATISTICS': [0,2,3], # Count,Mean,Median
        'OUTPUT': QgsProcessing.TEMPORARY_OUTPUT
    }
    outputs['ZonalStatistics'] =
processing.run('native:zonalstatisticsfb', alg_params, context=context,
feedback=feedback, is_child_algorithm=True)

    feedback.setCurrentStep(18)
    if feedback.isCanceled():
        return {}

    # Field calculator
    alg_params = {
        'FIELD_LENGTH': 10,
        'FIELD_NAME': 'EnergyEstimate',
        'FIELD_PRECISION': 0,
        'FIELD_TYPE': 0, # Float
        'FORMULA': '_count * 0.5 * 0.5 *_mean *0.75* 0.14',
        'INPUT': outputs['ZonalStatistics']['OUTPUT'],
        'OUTPUT': parameters['EnergyEstimatePerBuilding']
    }
    outputs['FieldCalculator'] = processing.run('native:fieldcalculator',
alg_params, context=context, feedback=feedback, is_child_algorithm=True)
    results['EnergyEstimatePerBuilding'] =
outputs['FieldCalculator']['OUTPUT']
    return results

    def name(self):
        return 'Solar Graphic FINALMODEL'

    def displayName(self):
        return 'Solar Graphic FINALMODEL'

    def group(self):
        return ''

    def groupId(self):
        return ''

    def createInstance(self):
        return SolarGraphicFinalmodel()

```

8.4. Model for PET estimation

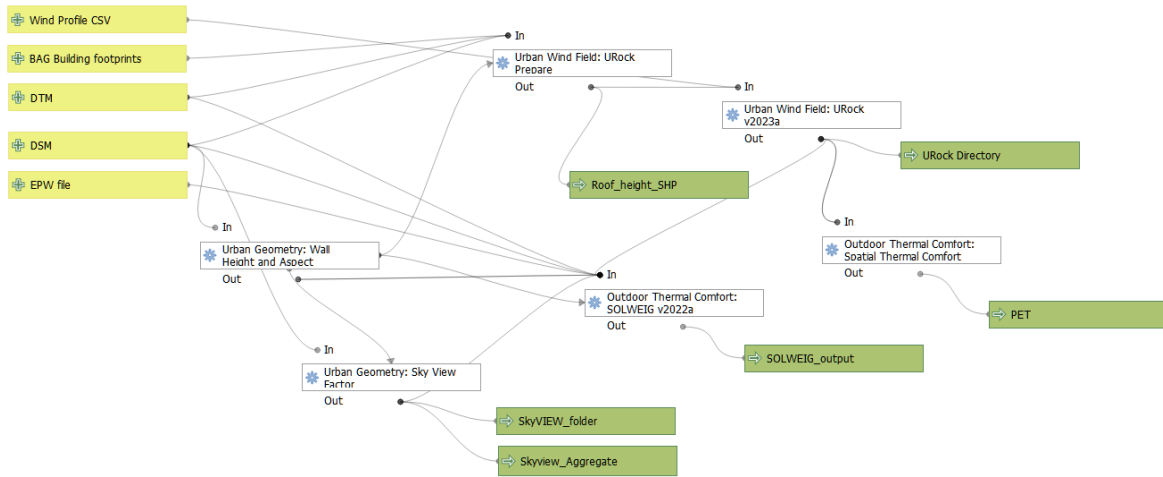


Figure 51 - Graphic modeller diagram of the PET model

8.4.1. Code for the PET model

```

"""
Model exported as python.
Name : PET MODEL
Group :
With QGIS : 32209
"""

from qgis.core import QgsProcessing
from qgis.core import QgsProcessingAlgorithm
from qgis.core import QgsProcessingMultiStepFeedback
from qgis.core import QgsProcessingParameterVectorLayer
from qgis.core import QgsProcessingParameterRasterLayer
from qgis.core import QgsProcessingParameterFile
from qgis.core import QgsProcessingParameterFolderDestination
from qgis.core import QgsProcessingParameterRasterDestination
from qgis.core import QgsProcessingParameterVectorDestination
import processing

class PetModel(QgsProcessingAlgorithm):

    def initAlgorithm(self, config=None):
        self.addParameter(QgsProcessingParameterVectorLayer('bagbuildingfootpr
ints', 'BAG Building footprints', defaultValue=None))
        self.addParameter(QgsProcessingParameterRasterLayer('dsm', 'DSM',
defaultValue=None))
        self.addParameter(QgsProcessingParameterRasterLayer('dtm', 'DTM',
defaultValue=None))

```

```

        self.addParameter(QgsProcessingParameterFile('windprofilecsv', 'Wind
Profile CSV', behavior=QgsProcessingParameterFile.File, fileFilter='All Files
(*.*)', defaultValue=None))
        self.addParameter(QgsProcessingParameterFile('epwfile', 'EPW file',
behavior=QgsProcessingParameterFile.File, fileFilter='All Files (*.*)',
defaultValue=None))
        self.addParameter(QgsProcessingParameterFolderDestination('Solweig_out
put', 'SOLWEIG_output', createByDefault=True, defaultValue=None))
        self.addParameter(QgsProcessingParameterRasterDestination('Pet',
'PET', createByDefault=True, defaultValue=None))
        self.addParameter(QgsProcessingParameterFolderDestination('Skyview_fol
der', 'SkyVIEW_folder', createByDefault=True, defaultValue=None))
        self.addParameter(QgsProcessingParameterRasterDestination('Skyview_agg
regate', 'Skyview_Aggregate', createByDefault=True, defaultValue=None))
        self.addParameter(QgsProcessingParameterVectorDestination('Roof_height
_shp', 'Roof_height_SHP', type=QgsProcessing.TypeVectorAnyGeometry,
createByDefault=True, defaultValue=None))
        self.addParameter(QgsProcessingParameterFolderDestination('UrockDirect
ory', 'URock Directory', createByDefault=True, defaultValue=None))

    def processAlgorithm(self, parameters, context, model_feedback):
        # Use a multi-step feedback, so that individual child algorithm
progress reports are adjusted for the
        # overall progress through the model
        feedback = QgsProcessingMultiStepFeedback(6, model_feedback)
        results = {}
        outputs = {}

        # Urban Geometry: Wall Height and Aspect
        alg_params = {
            'INPUT': parameters['dsm'],
            'INPUT_LIMIT': 3,
            'OUTPUT_ASPECT': QgsProcessing.TEMPORARY_OUTPUT,
            'OUTPUT_HEIGHT': QgsProcessing.TEMPORARY_OUTPUT
        }
        outputs['UrbanGeometryWallHeightAndAspect'] =
processing.run('umep:Urban Geometry: Wall Height and Aspect', alg_params,
context=context, feedback=feedback, is_child_algorithm=True)

        feedback.setCurrentStep(1)
        if feedback.isCanceled():
            return {}

        # Urban Wind Field: URock Prepare
        alg_params = {
            'HEIGHT_VEG_FIELD': '',
            'INPUT_BUILD_DEM': parameters['dtm'],
            'INPUT_BUILD_DSM': parameters['dsm'],

```

```

        'INPUT_BUILD_FOOTPRINT': parameters['bagbuildingfootprints'],
        'INPUT_VEG_CDSM': None,
        'INPUT_VEG_POINTS': None,
        'OUTPUT_BUILD_HEIGHT_FIELD': 'ROOF_HEIGHT',
        'OUTPUT_VEG_HEIGHT_FIELD': 'VEG_HEIGHT',
        'RADIUS_VEG_FIELD': '',
        'VEGETATION_ASPECT': '0.75',
        'BUILDINGS_WITH_HEIGHT': parameters['Roof_height_shp'],
        'VEGETATION_WITH_HEIGHT': QgsProcessing.TEMPORARY_OUTPUT
    }
    outputs['UrbanWindFieldUrockPrepare'] = processing.run('umep:Urban
Wind Field: URock Prepare', alg_params, context=context, feedback=feedback,
is_child_algorithm=True)
    results['Roof_height_shp'] =
outputs['UrbanWindFieldUrockPrepare']['BUILDINGS_WITH_HEIGHT']

    feedback.setCurrentStep(2)
    if feedback.isCanceled():
        return {}

    # Urban Geometry: Sky View Factor
    alg_params = {
        'ANISO': True,
        'INPUT_CDSM': None,
        'INPUT_DSM': parameters['dsm'],
        'INPUT_TDSM': None,
        'INPUT_THEIGHT': 25,
        'TRANS_VEG': 3,
        'OUTPUT_DIR': parameters['Skyview_folder'],
        'OUTPUT_FILE': parameters['Skyview_aggregate']
    }
    outputs['UrbanGeometrySkyViewFactor'] = processing.run('umep:Urban
Geometry: Sky View Factor', alg_params, context=context, feedback=feedback,
is_child_algorithm=True)
    results['Skyview_folder'] =
outputs['UrbanGeometrySkyViewFactor']['OUTPUT_DIR']
    results['Skyview_aggregate'] =
outputs['UrbanGeometrySkyViewFactor']['OUTPUT_FILE']

    feedback.setCurrentStep(3)
    if feedback.isCanceled():
        return {}

    # Urban Wind Field: URock v2023a
    alg_params = {
        'ATTENUATION_FIELD': '',
        'BUILDINGS':
outputs['UrbanWindFieldUrockPrepare']['BUILDINGS_WITH_HEIGHT'],

```

```

        'HEIGHT_FIELD_BUILD': '',
        'HORIZONTAL_RESOLUTION': 1,
        'INPUT_PROFILE_FILE': parameters['windprofilecsv'],
        'INPUT_PROFILE_TYPE': 1, # urban
        'INPUT_WIND_DIRECTION': 45,
        'INPUT_WIND_HEIGHT': 10,
        'INPUT_WIND_SPEED': 2,
        'LOAD_OUTPUT': True,
        'OUTPUT_FILENAME': 'urock_output',
        'RASTER_OUTPUT': None,
        'SAVE_NETCDF': True,
        'SAVE_RASTER': True,
        'SAVE_VECTOR': True,
        'VEGETATION': None,
        'VEGETATION_CROWN_BASE_HEIGHT': '',
        'VEGETATION_CROWN_TOP_HEIGHT': '',
        'VERTICAL_RESOLUTION': 1,
        'WIND_HEIGHT': '1.5',
        'UROCK_OUTPUT': parameters['UrockDirectory']
    }
    outputs['UrbanWindFieldUrockV2023a'] = processing.run('umep:Urban Wind
Field: URock', alg_params, context=context, feedback=feedback,
is_child_algorithm=True)
    results['UrockDirectory'] =
outputs['UrbanWindFieldUrockV2023a']['UROCK_OUTPUT']

    feedback.setCurrentStep(4)
    if feedback.isCanceled():
        return {}

    # Outdoor Thermal Comfort: SOLWEIG v2022a
    alg_params = {
        'ABS_L': 0.95,
        'ABS_S': 0.7,
        'ACTIVITY': 80,
        'AGE': 35,
        'ALBEDO_GROUND': 0.15,
        'ALBEDO_WALLS': 0.2,
        'CLO': 0.9,
        'CONIFER_TREES': False,
        'CYL': True,
        'EMIS_GROUND': 0.95,
        'EMIS_WALLS': 0.9,
        'HEIGHT': 180,
        'INPUTMET': parameters['epwfile'],
        'INPUT_ANISO':
outputs['UrbanWindFieldUrockV2023a']['UROCK_OUTPUT'],

```

```

        'INPUT_ASPECT':
outputs['UrbanGeometryWallHeightAndAspect']['OUTPUT_ASPECT'],
        'INPUT_CDSM': None,
        'INPUT_DEM': parameters['dtm'],
        'INPUT_DSM': parameters['dsm'],
        'INPUT_HEIGHT':
outputs['UrbanGeometryWallHeightAndAspect']['OUTPUT_HEIGHT'],
        'INPUT_LC': None,
        'INPUT_SVF': outputs['UrbanGeometrySkyViewFactor']['OUTPUT_DIR'],
        'INPUT_TDSM': None,
        'INPUT_THEIGHT': 25,
        'LEAF_END': 300,
        'LEAF_START': 97,
        'ONLYGLOBAL': True,
        'OUTPUT_KDOWN': True,
        'OUTPUT_KUP': True,
        'OUTPUT_LDOWN': True,
        'OUTPUT_LUP': True,
        'OUTPUT_SH': True,
        'OUTPUT_TMRT': True,
        'OUTPUT_TREEPLANTER': True,
        'POI_FIELD': '',
        'POI_FILE': None,
        'POSTURE': 0, # Standing
        'SAVE_BUILD': False,
        'SENSOR_HEIGHT': 10,
        'SEX': 0, # Male
        'TRANS_VEG': 3,
        'USE_LC_BUILD': False,
        'UTC': 1,
        'WEIGHT': 75,
        'OUTPUT_DIR': parameters['Solweig_output']
    }
    outputs['OutdoorThermalComfortSolweigV2022a'] =
processing.run('umep:Outdoor Thermal Comfort: SOLWEIG', alg_params,
context=context, feedback=feedback, is_child_algorithm=True)
    results['Solweig_output'] =
outputs['OutdoorThermalComfortSolweigV2022a']['OUTPUT_DIR']

    feedback.setCurrentStep(5)
    if feedback.isCanceled():
        return {}

    # Outdoor Thermal Comfort: Spatial Thermal Comfort
    alg_params = {
        'ACTIVITY': 80,
        'AGE': 35,
        'CLO': 0.9,

```

```

        'COMFA': False,
        'HEIGHT': 180,
        'SEX': 0, # Male
        'TC_TYPE': 0, # Physiological Equivalent Temperature (PET)
        'TMRT_MAP': outputs['UrbanWindFieldUrockV2023a']['UROCK_OUTPUT'],
        'UROCK_MAP': outputs['UrbanWindFieldUrockV2023a']['UROCK_OUTPUT'],
        'WEIGHT': 75,
        'TC_OUT': parameters['Pet']
    }
    outputs['OutdoorThermalComfortSpatialThermalComfort'] =
processing.run('umep:Outdoor Thermal Comfort: Spatial Thermal Comfort',
alg_params, context=context, feedback=feedback, is_child_algorithm=True)
    results['Pet'] =
outputs['OutdoorThermalComfortSpatialThermalComfort']['TC_OUT']
    return results

def name(self):
    return 'PET MODEL'

def displayName(self):
    return 'PET MODEL'

def group(self):
    return ''

def groupId(self):
    return ''

def createInstance(self):
    return PetModel()

```

8.5. Detailed step-by-step workflow – Using 3DBAG to modify urban form in Blender

8.5.1. Exporting

Selecting z as up and Y as forward direction in Blender.

8.5.2. Cloud Compare

Bring in both the ground cloud and the building .obj

Convert .obj to point cloud by Edit>Mesh? Sample points – at 10 per cu.m.

Move the the point clouds to the right locations by using the translate tool (Translate/Rotate). Select what direction you want movement and move forward/backward.

Once aligned, Merge the point clouds by Edit> Merge

Then convert to 2D raster

8.6. Joining Solar Radiation final shp values to 3D model

The 3D BAG pand and the 2d shapefiles have the same IDs.

8.6.1. Blender scripting

Open Blender Scripting console. Load the .obj scenario model already to Blender. Paste this code to see the names of the models:

```
import bpy

# Print the names of all objects in the scene
for obj in bpy.data.objects:
    print (obj.name)
```

Go to the Window menu at the top of Blender. Select Toggle System Console. This will open a separate console window where you can see the output. This list of names should match the key value column in Excel.

To match the names, create the names in Excel using CONCATENATE function. Move this column to the 1st position so it is read as row[0] by the script later.

Next, open another Blender script text file. The following code works if your collection of buildings is already loaded into Blender. Copy Paste this given code and change the locations/directory of the saved files:

```
import bpy
import csv

# Path to the CSV file
csv_path = r"D:\00_ITC-NL\THESIS\17_CLEAN PROCESS FILES\02_SINGLE\3D model and
data joining\Energy estimate_single.csv"

# Step 1: Read the CSV file and extract necessary columns
data = {}
with open (csv_path, newline='') as csvfile:
    csvreader = csv.reader (csvfile)
    header = next (csvreader) # Skip header row if there is one
    for row in csvreader:
        # Assuming the first column is the model name and columns 2, 3, 4, 5
        # are the ones we need
        model_name = row[0]
        custom_props = {
            "TotalArea": row[9], # Column 10
            "CellCount": row[10], # Column 11
            "MedianVal": row[12], # Column 13
            "EnergyEst": row[13], # Column 14
            "UsableArea": row [14], #Column 15
            "UsedAreaPerc": row [15] #Column 16
        }
        data[model_name] = custom_props
```

```

# Step 2: Assign custom properties to the already loaded models
for model_name, props in data.items ():
    # Find the object by name
    obj = bpy.data.objects.get (model_name)

    if obj:
        # Set the custom properties
        for prop_name, value in props.items ():
            obj[prop_name] = value
    else:
        print (f"Object {model_name} not found in the scene")

# Save the Blender file to preserve changes
bpy.ops.wm.save_mainfile (filepath=r"D:\00_ITC-NL\THESIS\17_CLEAN PROCESS
FILES\02_SINGLE\3D model and data joining\ENRICHED_SINGLE.blend")

# Note: Ensure the CSV file path is correct and adapt the file handling as per
your requirements.

```

This creates a new Blender file where the data is transferred into custom properties of the model.

8.6.2. Convert to .gltf to visualise later as maptile

If you prefer to do this manually, you can follow these steps:

- Open Blender and ensure your model is loaded with custom properties assigned.
- Select the Model you want to export.
- Go to File > Export > glTF 2.0 (.glb/.gltf).
- In the export options, set the desired format (GLB for binary, GLTF for JSON + separate resources).
- Check the Include and Transform options as needed (e.g., to apply transformations).
- Specify the file path and click Export.

This will create a .gltf or .glb file that includes your model along with the custom properties.

8.7. Script to view 3d Model and 2D raster using Cesium JS

In this code, replace asset ID as uploaded on Cesium Assets, and the access token as per your individual access token.

```

<!DOCTYPE html>
<html lang="en">
<head>
  <meta charset="utf-8">
  <!-- Include the CesiumJS JavaScript and CSS files -->
  <script
src="https://cesium.com/downloads/cesiumjs/releases/1.117/Build/Cesium/Cesium.
js"></script>

```

```

<link
href="https://cesium.com/downloads/cesiumjs/releases/1.117/Build/Cesium/Widgets/widgets.css" rel="stylesheet">
<script
src="https://cdnjs.cloudflare.com/ajax/libs/PapaParse/5.3.0/papaparse.min.js">
</script>
<script src="Assets/script.js">
</script>

</head>
<body>
<div id="cesiumContainer"></div>
<script type="module">
  // Your access token can be found at: https://ion.cesium.com/tokens.
  // This is the default access token from your ion account

  Cesium.Ion.defaultAccessToken =
'eyJhbGciOiJIUzI1NiIsInR5cCI6IkpXVCJ9.eyJqdGkiOiJiZDAyZTYzYi1mMTY0LTQxMDctYmZiMi03MjA2YTJjOGUxNzUiLCJpZCI6MjAxNjEyLCJpYXQiOiJlE3MTAzMzE1NzB9.4wOkzeP1jje11UpBC6NsQwe5RS1s9-3G0MfzWMtQr2Y';

  // Initialize the Cesium Viewer in the HTML element with the
  `cesiumContainer` ID.
  const viewer = new Cesium.Viewer('cesiumContainer', {
    terrain: Cesium.Terrain.fromWorldTerrain(),
  });

  // Fly the camera to site
  viewer.camera.flyTo({
    destination: Cesium.Cartesian3.fromDegrees(6.86969, 52.22053, 300),
    orientation: {
      heading: Cesium.Math.toRadians(0.0),
      pitch: Cesium.Math.toRadians(-25.0),
    }
  });

  // Grant CesiumJS access to your ion assets
  Cesium.Ion.defaultAccessToken =
"eyJhbGciOiJIUzI1NiIsInR5cCI6IkpXVCJ9.eyJqdGkiOiJiZDAyZTYzYi1mMTY0LTQxMDctYmZiMi03MjA2YTJjOGUxNzUiLCJpZCI6MjAxNjEyLCJpYXQiOiJlE3MTAzMzE1NzB9.4wOkzeP1jje11UpBC6NsQwe5RS1s9-3G0MfzWMtQr2Y";

  try {
    const tileset = await Cesium.Cesium3DTileset.fromIonAssetId(2601760);
    viewer.scene.primitives.add(tileset);
    await viewer.zoomTo(tileset);
  }
}

```

```

// Apply the default style if it exists
const extras = tileset.asset.extras;
if (
  Cesium.defined(extras) &&
  Cesium.defined(extras.ion) &&
  Cesium.defined(extras.ion.defaultStyle)
) {
  tileset.style = new Cesium.Cesium3DTileStyle(extras.ion.defaultStyle);
}
} catch (error) {
  console.log(error);
}

//Add 2D raster

try {
  const imageryLayer = viewer.imageryLayers.addImageryProvider(
    await Cesium.IonImageryProvider.fromAssetId(2630168),
  );
  await viewer.zoomTo(imageryLayer);
} catch (error) {
  console.log(error);
}

</script>
</div>
</body>
</html>

```

8.8. Code to analyse the results

8.8.1. KL Divergence

```

%pip install scipy
import pandas as pd
import numpy as np
import matplotlib.pyplot as plt
from scipy.stats import entropy
# Paths to the .csv files
file_path1 = 'Original_Jun_EE.csv'
file_path2 = 'Single_jun_EE.csv'
file_path3 = 'multiple_Jun_EE.csv'
key_col = 'feature_id' # Column name for the key
value_col = 'EnergyEsti' # Column name for the values
# Function to read and preprocess datasets

```

```

def read_and_preprocess(file_path, key_col, value_col):
    df = pd.read_csv(file_path)
    df = df[[key_col, value_col]]
    # Normalize to get probability distribution
    df[value_col] = df[value_col] / df[value_col].sum()
    return df
# Read and preprocess datasets
df1 = read_and_preprocess(file_path1, key_col, value_col)
df2 = read_and_preprocess(file_path2, key_col, value_col)
df3 = read_and_preprocess(file_path3, key_col, value_col)

# Function to calculate KL divergence using scipy for original and Single
def calculate_kl_divergence(df1, df2, key_col, value_col):
    merged_df = pd.merge(df1, df2, on=key_col, suffixes=('_P', '_Q'))

    # Handle cases where probabilities are zero or NaN
    merged_df = merged_df.replace(0, np.finfo(float).eps) # Replace 0 with a
small epsilon
    merged_df = merged_df.dropna() # Drop rows with NaN values

    kl_divergence = entropy(merged_df[f'{value_col}_P'],
merged_df[f'{value_col}_Q'])
    return kl_divergence, merged_df

# Calculate KL divergence
kl_divergence, merged_df = calculate_kl_divergence(df1, df3, key_col,
value_col)
print(f'KL Divergence: {kl_divergence}')

```

repeat for other combinations of datasets.

Visualise the distributions:

```

%pip install seaborn
import matplotlib.pyplot as plt
import seaborn as sns

column_name = 'EnergyEsti'

# Using seaborn to plot the distribution
sns.histplot(df1[column_name], kde=True)
plt.title(f'Distribution of Energy Estimate in case A')
plt.xlabel('Energy Estimate in kWh/sqm')
plt.ylabel('Frequency')
plt.show()

#repeat for different distributions

```

```

#read the distribution together
column_name = 'EnergyEsti'

# Plotting the distributions
plt.figure(figsize=(10, 6))

sns.histplot(df1[column_name], kde=True, color='blue', label='Case A',
stat='probability', bins=30)
sns.histplot(df2[column_name], kde=True, color='red', label='Case B',
stat='probability', bins=30)
sns.histplot(df3[column_name], kde=True, color='yellow', label='Case C',
stat='probability', bins=30)

plt.legend()
plt.title('Overlay of three Distributions')
plt.xlabel('Value')
plt.ylabel('Density')
plt.show()

#draw the 95percentile distribution

column_name = 'EnergyEsti'
# Check and handle NaN/Inf values in each DataFrame
for df in [df1, df2, df3]:
    df[column_name].fillna(0, inplace=True)
    df[column_name].replace([np.inf, -np.inf], 0, inplace=True)

# Calculate mean and 95% percentiles for all datasets
means = [df[column_name].mean() for df in [df1, df2, df3]]
percentiles = [np.percentile(df[column_name], [2.5, 97.5]) for df in [df1,
df2, df3]]

# Determine common x-axis limits based on all percentiles
x_min = min([p[0] for p in percentiles])
x_max = max([p[1] for p in percentiles])

# Plotting the distributions side by side
plt.figure(figsize=(18, 6)) # Adjust figsize as needed

# Plot for Case A
plt.subplot(1, 3, 1)
sns.histplot(df1[column_name], kde=True, color='blue', label='Case A',
stat='probability', bins=100)
plt.axvline(means[0], color='blue', linestyle='dashed', linewidth=2,
label=f'Mean: {means[0]:.2f}')
plt.fill_betweenx([0, plt.ylim()[1]], percentiles[0][0], percentiles[0][1],
color='blue', alpha=0.2)

```

```

plt.legend()
plt.title('Case A Distribution')
plt.xlabel('Value')
plt.ylabel('Probability')
plt.xlim(x_min, x_max)

# Plot for Case B
plt.subplot(1, 3, 2)
sns.histplot(df2[column_name], kde=True, color='red', label='Case B',
stat='probability', bins=100)
plt.axvline(means[1], color='red', linestyle='dashed', linewidth=2,
label=f'Mean: {means[1]:.2f}')
plt.fill_betweenx([0, plt.ylim()[1]], percentiles[1][0], percentiles[1][1],
color='red', alpha=0.2)
plt.legend()
plt.title('Case B Distribution')
plt.xlabel('Value')
plt.ylabel('Probability')
plt.xlim(x_min, x_max)

# Plot for Case C
plt.subplot(1, 3, 3)
sns.histplot(df3[column_name], kde=True, color='green', label='Case C',
stat='probability', bins=200)
plt.axvline(means[2], color='green', linestyle='dashed', linewidth=2,
label=f'Mean: {means[2]:.2f}')
plt.fill_betweenx([0, plt.ylim()[1]], percentiles[2][0], percentiles[2][1],
color='green', alpha=0.2)
plt.legend()
plt.title('Case C Distribution')
plt.xlabel('Value')
plt.ylabel('Probability')
plt.xlim(x_min, x_max)

# Adjust layout and show plot
plt.tight_layout()
plt.suptitle('Overlay of three Distributions with Mean  $\pm$ 95% Range', y=1.05)
plt.show()

```

8.8.2. Raster Statistics

```

import rasterio
import numpy as np
import seaborn as sns
import matplotlib.pyplot as plt

```

```
raster_files = ['Pet_Original.tif', 'PET ESTIMATE_SINGLE_FINAL.tif',
               'PET_multiple_new.tif']

# Process each raster file to get the valid raster values
raster_values_list = [valid_raster_values, valid_raster_values2,
                     valid_raster_values3]

# Plot the distributions
plt.figure(figsize=(10, 6))

# Define labels for each distribution
labels = ['Case A', 'Case B', 'Case C']

# Plot each distribution
for raster_values, label in zip(raster_values_list, labels):
    sns.histplot(raster_values, kde=True, bins=50, label=label)

plt.title('Distribution of Raster values of PET estimation (excluding
nodata)')
plt.xlabel('Temperature Estimate')
plt.ylabel('Frequency')
plt.legend()
plt.show()
```